State of Oregon
Oregon Department of Geology and Mineral Industries
Ruarri Day-Stirrat, State Geologist

OPEN-FILE REPORT O-22-07

UMPQUA RIVER TSUNAMI MODELING: TOWARD IMPROVED MARITIME PLANNING RESPONSE

by Jonathan C. Allan[1], Joseph Zhang[2], Fletcher E. O'Brien[3], and Laura Gabel[1]

2022

[1]Oregon Department of Geology and Mineral Industries, Coastal Field Office, P.O. Box 1033, Newport, OR 97365
[2]Virginia Institute of Marine Science, College of William & Mary, Center for Coastal Resource Management, 1375 Greate Road, Gloucester Point, VA 23062
[3]Oregon Department of Geology and Mineral Industries, 800 NE Oregon Street, Suite 965, Portland, OR 97232

DISCLAIMER

This product is for informational purposes and may not have been prepared for or be suitable for legal, engineering, or surveying purposes. Users of this information should review or consult the primary data and information sources to ascertain the usability of the information. This publication cannot substitute for site-specific investigations by qualified practitioners. Site-specific data may give results that differ from the results shown in the publication.

WHAT'S IN THIS REPORT?

This study evaluates new tsunami modeling results completed for both distant and local tsunamis for the Umpqua River estuary. The goal is to examine the interaction of tsunamis with fluctuating (dynamic) tides (as opposed to modeling using a fixed tidal elevation such as mean higher high water), average riverine flow, and friction to provide an improved understanding of tsunami effects along the river and in the Ports of Winchester Bay and Reedsport. These data are then used to develop maritime tsunami guidance to assist all vessels operating offshore of the mouth of the Umpqua River and within the estuary.

Cover photo: View looking northwest over Winchester Bay, Umpqua River estuary, and navigation channel. Photo taken by J. Allan, August 2009

Oregon Department of Geology and Mineral Industries Open-File Report O-22-07
Published in conformance with ORS 516.030

DOGAMI Administrative Offices
800 NE Oregon Street, Suite 965
Portland, OR 97232
Telephone (971) 673-1555
https://www.oregongeology.org/
https://www.oregon.gov/DOGAMI/

TABLE OF CONTENTS

LIST OF FIGURES

LIST OF TABLES

EXECUTIVE SUMMARY

Distant tsunamis affecting the West Coast of the United States over the past two decades have resulted in significant damage to ports and harbors as well as to recreational and commercial vessels attempting to escape the tsunami. Although local tsunamis will strike the coast within minutes after the start of earthquake shaking, providing little time to evacuate, distant tsunamis are expected to arrive some four to 12 hours after the event, providing time to respond. This study evaluates new tsunami modeling results completed for both distant and local tsunamis impacting the Umpqua Estuary, including the towns of Winchester Bay and Reedsport. Previous tsunami modeling used a fixed tide level — defined as mean higher high water (MHHW) — and no river flow or friction. The purpose of this study is to examine the interaction of local and distant tsunamis with dynamic tides (as opposed to a fixed tidal elevation such as MHHW), average river flow, and frictional effects to provide an improved understanding of tsunami effects on maritime operations offshore the Umpqua River and within the estuary. This was accomplished by evaluating a suite of tsunami simulations (15 in total) for the Umpqua Estuary focused on two distant earthquake scenarios — the 1964 Anchorage, Alaska (AK64), earthquake and a maximum-considered eastern Aleutian Island (AKMax) earthquake — and two local Cascadia Subduction Zone (CSZ) scenarios — Large1 (L1) and Extra-extra-large1 (XXL1).

Our modeling indicates that for a maximum-considered eastern Aleutian Island (AKMax) earthquake, the tsunami would arrive at the river mouth ~3 hours, 50 minutes after the start of the earthquake. The tsunami takes an additional 8 minutes to travel from the estuary mouth to Winchester Bay, and ~36 minutes to reach the town of Reedsport. Total travel time to Reedsport is 4 hours, 26 minutes. The largest tsunami waves are concentrated at the estuary mouth, where the AKMax tsunami reaches ~3.8 m (19 ft) in height. Water levels remain high between the mouth (river mile; RM-1) and Winchester Bay (RM1), before decreasing substantially upriver toward The Point (RM7). These changes are due to a combination of factors including bathymetric shallowing that effectively disperses much of the energy and morphological controls such as the shape and width of the estuary. The strongest currents are observed at the estuary mouth, whereas much of the lower estuary (RM-1 to RM4) would be affected by currents >2.0 m/s (>4 knots). These currents can cause damage to marina facilities such as those located in Winchester Bay, and vessels that may be moored in the marina. In contrast, our simulations indicate that a distant tsunami is unlikely to have an adverse effect on vessels and port facilities at Reedsport. This is because the distant tsunami loses significant energy by the time it reaches Reedsport.

For a distant tsunami, we recommend two maritime evacuation options:

1) Offshore: ***Seaward of the Umpqua River mouth, proceed to a staging area located ~1.8 km (1 nm) west of the mouth, where water depths are greater than 18 m (10 fathoms; 60 ft).*** Dangerous currents > 2.6 m/s (5 knots) are expected to occur at depths shallower than 18 m (10 fathoms; 60 ft). Offshore maritime evacuation may be feasible for some vessels operating out of Winchester Bay, or in the navigation channel downstream of The Point (RM7). Vessel operators need to assess if there is sufficient time to reach the staging area ahead of the tsunami.
2) Upriver: Vessels upriver of The Point (RM7) may choose to evacuate upriver toward Reedsport, where the tsunami currents drop off significantly.

For a maximum-considered locally generated CSZ tsunami, we find that the tsunami reaches the estuary mouth within minutes following the earthquake. The tsunami reaches Winchester Bay in ~21 minutes (peak wave at 25 minutes) and will reach Reedsport ~42 minutes after the start of earthquake shaking. Maximum water levels exceeding 14 m (46 ft) are observed at the estuary mouth, decreasing to ~10 to 12 m (~33 to 39 ft) in the navigation channel between RM2 and RM3. Extreme currents exceeding

6 m/s (12 knots) will be experienced in the lower estuary between RM-1 and RM4. Damage to Winchester Bay is expected to be devastating. Although modeling of the L1 Cascadia scenario indicates smaller tsunami waves throughout the Umpqua Estuary when compared to XXL1, the effects from an L1 event will remain damaging for infrastructure located in the tsunami inundation zone.

Due to the speed at which a CSZ tsunami reaches the Umpqua River, ***there is insufficient time for mariners in Winchester Bay to respond to this event other than to evacuate by foot to high ground***. Vessels operating on the ocean west of the mouth should immediately evacuate toward deeper water. ***We recommend an Umpqua River maritime evacuation zone for a local tsunami hazard beginning at water depths of ~118 m (65 fathoms) and extending westward to depths > 182 m (100 fathoms).*** Mariners should prepare to remain offshore for potentially days as the estuary is unlikely to be navigable following a CSZ tsunami. As a result, plans to evacuate to potentially safe ports located south of Cape Mendocino on the California coast should be developed. For vessels in the Umpqua Estuary, the only course of action is to head vessels toward the nearest point of high ground and evacuate uphill out of the tsunami inundation zone. No time can be spared in parking the boat at a designated site; the priority must be reaching high ground on foot.

1.0 INTRODUCTION

The objective of this study is to evaluate new modeling results completed for both distant and local tsunamis in the Umpqua River estuary, Douglas County, Oregon (**Figure 1**). The goal is to provide an improved understanding of tsunamis and their effect on maritime traffic operating offshore the mouth of the Umpqua River, within the estuary, and upriver toward the Port of Reedsport (**Figure 1**).

Figure 1. Location map of the Umpqua River Estuary showing key place names and model domain.

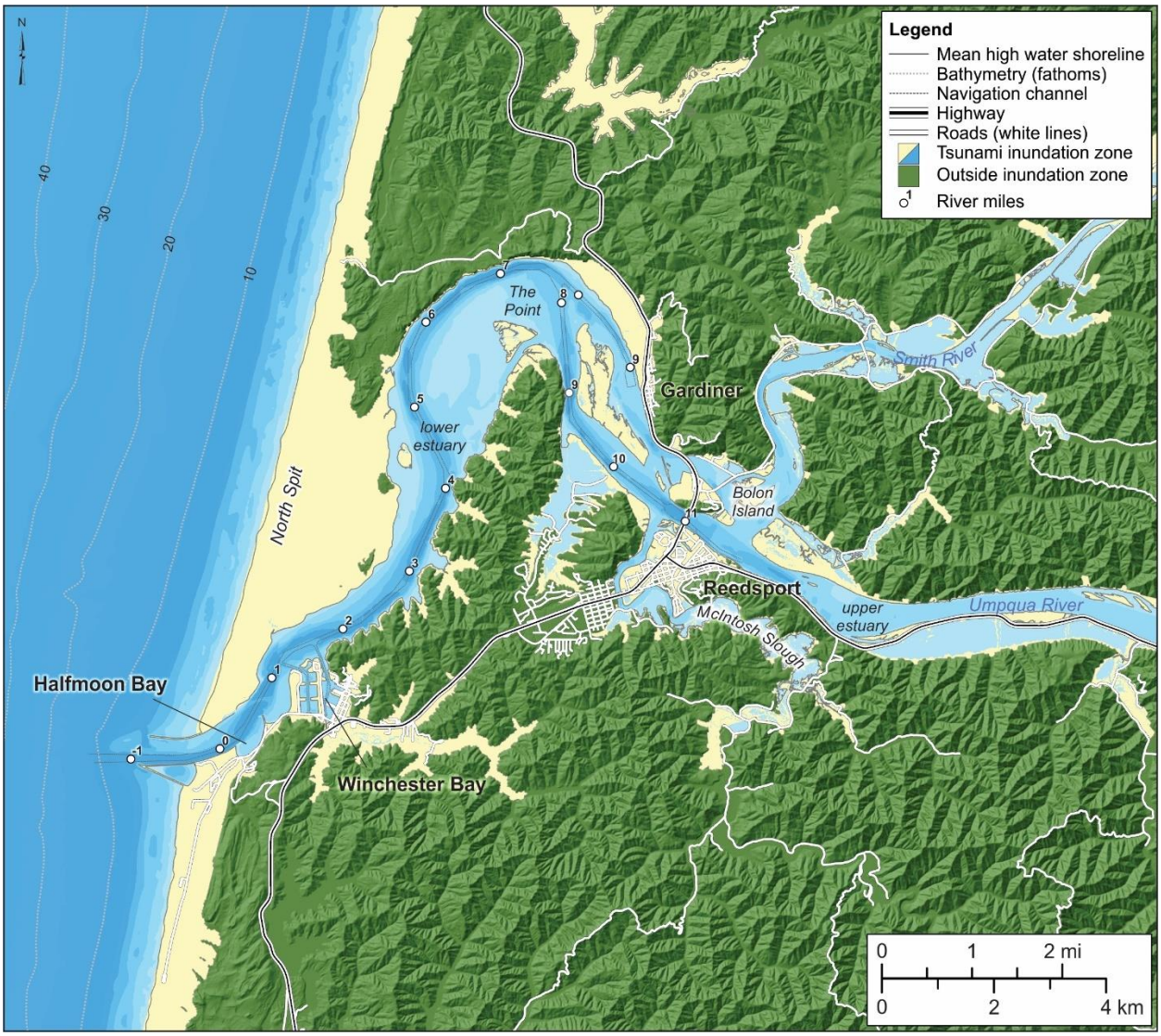

The coast of Oregon and its many estuaries are exposed to significant risk from tsunamis generated locally due to great (~ Mw 8–9) earthquakes on the Cascadia Subduction Zone (CSZ; Atwater and others, 1995; Satake and others, 2003; Witter and others, 2003; Atwater and others, 2005; Nelson and others, 2006; Priest and others, 2009; Witter and others, 2012), as well as from distant tsunamis generated elsewhere in the Pacific Basin (Allan and others, 2018a). Full-margin ruptures on the CSZ that trigger tsunamis are estimated to occur on the order of 480 to 505 years, with partial ruptures on the southern Oregon coast occurring more frequently (~220 years; Goldfinger and others, 2017). Conversely, similar

magnitude events from distant sources have historically had only a modest impact on the Oregon coast, but they occur much more frequently than local tsunamis (Lander and others, 1993; Priest and others, 2009). Although local tsunamis will strike the coast within minutes after the start of earthquake shaking, allowing little response time to evacuate, distant tsunamis are expected to arrive some four to 12 hours after the event, providing more time to respond. These differences are important not just for land-based tsunami evacuation but also for maritime evacuation for vessels operating offshore and potentially within ports and harbors.

The Umpqua River estuary is the third largest estuary on the Oregon coast (after the Columbia River and Coos estuaries) and boasts large recreational and commercial fishing fleets. The estuary is a drowned river valley, formed from sea-level rise during the last 10,000 years (O'Connor and others, 2009). The entrance to the estuary is flanked by jetties, and in the estuary the dredged main channel connects to several shallower tributaries (**Figure 1**). The navigation channel is ~11 m (36 ft) deep at the mouth and decreases to ~6 m (20 ft) in the channel. From its mouth, the river extends some 10.6 km (6.6 mi) upriver to the town of Reedsport. The river experiences highly variable seasonal river flows that ranges from an average of 30 m^3/s (1060 ft^3/s) in summer to 400 m^3/s (14,100 ft^3/s) in winter, whereas peak floods may reach 1400 m^3/s (49,400 ft^3/s). The estuary is tidally influenced from the mouth to 43 km (27 mi) upriver (O'Connor and others, 2009), and experiences a mesotidal range — mean tidal range of ~1.6 m (5.3 ft). Overall, the river may be broadly divided into three zones:

- A wave- and current-dominated entrance that includes Winchester Bay (**Figure 1**)
- The tidal estuary, which extends upriver to ~Mill Creek, 19 km (12 mi) upriver from Reedsport. We arbitrarily define an upper and lower estuary region, with the division occurring at The Point
- The freshwater dominated riverine portion upriver of Mill Creek.

Maritime traffic to and from the Pacific Ocean, Winchester Bay, and farther upriver to the Port of Reedsport (**Figure 1**) is predominantly a combination of commercial and recreational fishing boats. Because both Winchester Bay and Reedsport ports and harbors are in a tsunami inundation zone, they are potentially at risk of damage and destruction by both local and distant tsunamis. Importantly, although there is time for maritime operators to respond to a distant tsunami event, there is little time to respond for a local tsunami event. Determining where maritime safety zones may be found offshore the Umpqua Estuary is an important objective of this study.

To facilitate this work, new tsunami modeling has been completed for the Umpqua Estuary, extending from offshore of the coast, upriver to approximately Mill Creek. The specific tasks associated with this modeling included the following:

1) Quality assessment modeling of the 1964 Alaska tsunami to compare model results with dynamic (varying) tides versus a fixed (e.g., MHHW) tidal elevation
2) New tsunami modeling based on three specific scenarios drawn from Priest and others (2013):
    a. AKMax (maximum-considered distant tsunami event), based on an eastern Aleutian Island earthquake
    b. Large1 (L1), which has an estimated recurrence interval of ~2,500–3,333 years
    c. Extra-extra-large1 (XXL1), which has an estimated recurrence interval of >5,000 years (used by the state of Oregon to model its tsunami evacuation zone)

    Each of these scenarios was used to evaluate the sensitivity of peak tsunami currents, maximum water levels, vorticity, and minimum water depths to various tidal effects and average riverine flows for different parts of the estuary. These data provide important insights into the role of

dynamic tides and riverine flows in modifying tsunami waves. In addition, these data have been used to refine our understanding of timing of tsunamis at various points in the estuary system

3) Produce this technical report documenting the overall modeling approach and results, as well as key information that can be incorporated into needed maritime guidance information (e.g., Allan, 2020).

2.0 METHODS

2.1 Background

Between 2009 and 2013, the Oregon Department of Geology and Mineral Industries (DOGAMI) initiated a comprehensive effort to model and map tsunami inundation zones for the entire Oregon coast (Priest and others, 2010; Witter and others, 2011; Priest and others, 2013; Witter and others, 2013). Modeling of possible earthquake scenarios settled on two Gulf of Alaska distant source scenarios and five locally generated earthquake scenarios occurring on the CSZ. The local earthquake source parameters were guided by data that describe the geometry and tectonic behavior of the CSZ (Mitchell and others, 1994; Hyndman and Wang, 1995; McCrory and others, 2004; McCaffrey and others, 2007) and by knowledge of the size and frequency of earthquakes identified from offshore turbidite records that are inferred to record the occurrence of 42 tsunamigenic CSZ earthquakes over the last 10,000 years (Goldfinger and others, 2012). Here we briefly define the characteristics of the various earthquake source parameters before describing the hydrodynamic model used to simulate tsunami inundation.

2.1.1 Distant earthquake sources

Over the past 160 years, 29 distant (far-field) earthquake events have produced transoceanic tsunamis that struck the Oregon coast (Allan and others, 2018a). The majority (19) of the tsunamis were small, with a maximum water level heights of < 0.2 m (0.7 ft), which resulted in little to no impact on ports and harbors along the Oregon coast. Five events produced water level heights in the range of 0.2 to 0.6 m (0.7 to 2 ft), and the remaining five generated maximum water level heights exceeding 0.6 m (2 ft; NGDC, 2017). The latter five occurred in:

- 1873, from Northern California
- 1946, from Unimak, Alaska
- 1960, from Chile
- 1964, from the Gulf of Alaska
- 2011, from Tōhoku, Japan

Of these, the 1964 Alaska tsunami produced the largest observed water levels, with estuarine water levels between ~2.5 and 3.7 m (8 and 12 ft; Schatz and others, 1964; Lander and others, 1993; Zhang and others, 2011). A few observations of higher wave heights were made at the open coast, proximal to beaches: ~5 m (16 ft) in northern Oregon at Cannon Beach (Witter, 2008) and Seaside (Tsunami Pilot Study Working Group, 2006, Appendix C; TPSWG), 1.7 m (5.6 ft) just north of the Umpqua River mouth (NGDC, 2022), and >3.7 m (12 ft) at Sunset Beach, near Coos Bay in southern Oregon (Zhang and others, 2011). The Alaska tsunami caused significant damage to infrastructure in the coastal communities of Seaside and Cannon Beach (Witter, 2008) and killed four people camping along Beverly Beach near Newport on the central Oregon coast; minor damage was reported for the Umpqua Estuary. Other notable water levels produced by distant tsunamis include 3.05 m (10 ft) in 1873 at Port Orford, 1.8 m (6 ft) in 1946 at Clatsop

Spit, and 1.5 m (5 ft) in 1960 at Seaside. Each of these previous events exceeded the effects of the March 11, 2011, Japan tsunami and, by inference, had greater potential to cause damage to ports and harbors along the Oregon coast.

The March 11, 2011, Japan earthquake provided scientists with the most comprehensive set of modern observations of a major tsunami. The magnitude (Mw) 9.0 earthquake took place 129 km (80 mi) offshore from the coast of Sendai, northeast Honshu, Japan (Mori and Takahashi, 2012), triggering a catastrophic tsunami that inundated the northeast coast of Japan within minutes, killing ~18,000 people (Mori and others, 2011; Suppasri and others, 2013). In addition to loss of life, over 28,000 boats (including 26 ships) and 319 ports were damaged or destroyed (Suppasri and others, 2013). Economic losses due to port closures were estimated at $3.4 billion *per day* (Wiśniewski and Wolski, 2012).

The 2011 tsunami propagated eastward across the Pacific Ocean, impacting coastal communities in Hawaii and along the west coast of the continental United States, including Oregon. Along the Oregon coast the tsunami was relatively small, reaching heights of ~0.7–3.4 m (2.3–11.2 ft) at tide gauges near the open coast (Allan and others, 2012). The nearest tide gauge to the Umpqua is the Coos Bay tide gauge, where the maximum tsunami wave reached 1.75 m (5.7 ft). At Yaquina Bay, the same event produced a 0.86 m (2.8 ft) tsunami. Damage in Oregon was entirely confined to harbors, including the ports of Depoe Bay, Coos Bay, and at Brookings; most ports were unaffected. Fortunately for Oregon, the tsunami impact was moderated because the highest waves arrived during a low tide (Allan and others, 2012). Had the tsunami arrived at high tide, the local impact could have been much worse. At Brookings, on the southern Oregon coast, 12 fishing vessels put to sea at about 6 am, prior to the arrival of the tsunami waves. However, the *Hilda*, a 220-ton fishing boat and the largest remaining in the harbor, broke loose under the forces of the wave-induced currents and sank several other boats as it washed around the harbor. The tsunami destroyed much of the commercial part of the harbor and about one-third of the sports basin. The total damage was estimated at about $10 million. At Crescent City in California, where offshore bathymetry amplifies all tsunami waves relative to the Oregon coast, the tsunami was 4.2 m (13.8 ft) high in the local harbor (Allan and others, 2012). The tsunami damaged the entire open-coast breakwater, destroyed all the docks in the Inner Boat Basin, and sank or damaged numerous vessels. The estimated damage within Crescent City harbor was ~$20 million (Wilson and others, 2013). Accordingly, even modest distant tsunamis such as the one in 2011 pose a risk to Oregon ports and harbors and to the safety of commercial and recreational fishermen who operate offshore.

For the purposes of our simulations of a distant tsunami affecting the Umpqua Estuary, Priest and others (2013) and Witter and others (2011) defined two far-field earthquake sources (Mw ~9.2) for maximum-considered tsunamis originating on the eastern part of the Alaska-Aleutian subduction zone. The first scenario, termed AK64, reflects the historical 1964 Prince William Sound earthquake, which produced the largest distant tsunami to reach the Oregon coast in the written historical record. Simulations of this event were used to provide quality control against known observations of water levels and tsunami wave runup identified along the Oregon coast, enabling validation of the hydrodynamic model, Semi-implicit Eulerian-Lagrangian Finite Element model (SELFE), used to simulate tsunami inundation (Priest and others, 2010).

A hypothetical maximum-considered event originating in the eastern part of the Alaska-Aleutian subduction zone was also simulated. This second scenario, termed AKMax, is identified as “Source 3” in Table 1 of González and others (2009); more detailed information describing the earthquake parameters is provided by TPSWG (2006). The AKMax fault model reflects a distributed slip source on 12 subfaults, with each subfault assigned an individual slip value of 15, 20, 25, or 30 m (49, 66, 82, or 98 ft). These extreme parameters result in maximum seafloor uplift that is nearly twice as large as the uplift produced

by the 1964 Prince William Sound earthquake estimated by Johnson and others (1996). Examination of the simulated tsunami amplitudes for this source indicates beams of high energy directed more efficiently toward the Oregon coast (González and others, 2009; Allan and others, 2018a), when compared with other Alaska-Aleutian subduction zone sources. Accordingly, the hypothetical eastern Alaska-Aleutian subduction zone scenario (AKMax) was used by the state of Oregon as the maximum-considered distant tsunami source for modeling a far-field tsunami for the Oregon coast.

2.1.2 Local earthquake sources

Guided by CSZ geometry and tectonic behavior (Mitchell and others, 1994; Hyndman and Wang, 1995; McCrory and others, 2004; McCaffrey and others, 2007), Priest and others (2010) and Witter and others (2013) described the range of plausible CSZ earthquake sources for the Oregon coast. These data were calibrated against coastal paleoseismic records that document the impacts of as many as 13 major subduction zone earthquakes and associated tsunamis over the past ~7,000 years (Witter and others, 2003; Kelsey and others, 2005; Witter and others, 2010). Recent studies of turbidite records within sediment cores collected in deep water at the heads of Cascadia submarine canyons provide evidence for at least 19 full-margin ruptures and accompanying tsunamis over the past ~10,200 years (Goldfinger and others, 2012, 2017). Peak fault slip was assumed to be approximately equal to the accumulated plate convergence between earthquakes (i.e., coupling ratio = 1.0). Variations in the time intervals between offshore turbidites were interpreted to be representative of variations in coseismic slip (Priest and others, 2010).

The local earthquake scenarios that were ultimately used to model tsunami inundation for the Oregon coast reflect a full-length rupture of the Cascadia megathrust and the corresponding surface deformation used for tsunami simulations (Witter and others, 2013). This was necessary because the primary purpose of that effort was to develop regional tsunami inundation maps. For the purposes of that effort, representative slip models were defined and tested, including those in which slip is partitioned to a hypothetical splay fault in the accretionary wedge and models that varied the up-dip limit of slip on the megathrust. Each tsunami scenario was then weighted using a logic tree, and the results summarized in maps depicting the percent confidence that the local CSZ tsunami will reach no farther inland than each inundation line. Inter-event time intervals inferred to separate 19 sandy turbidites (tsunami deposits) range from as little as ~110 years to as long as ~1,150 years (Table 1 from Witter and others, 2011). From these data, four time intervals (mean values rounded to the nearest quarter century) were defined as representative of four general earthquake scenarios, or size classes: small (S), medium (M), large (L), and extra-large (XL). Respectively, these events have a mean inter-event time of 300 years (range = ~110 to 480 years, 5 events), 525 years (range = ~310 to 660 years, 10 events), 800 years (range = ~680 to 1,000 years, three events), and 1,150 years (one event), rounded to 1,200 years. The mean inter-event time interval multiplied by the CSZ plate convergence rate at each latitude equals the peak slip deficit released in each scenario earthquake. Slip was tapered to zero up and down dip from the peak value (Priest and others, 2010). Slip was also reduced progressively from north to south on the CSZ to account for evidence in the paleoseismic record of increasing numbers of partial CSZ ruptures from north to south (Goldfinger and others, 2012; Witter and others, 2013). A fifth scenario, termed extra-extra-large (XXL1), simulated a maximum-considered tsunami, which would be used to guide evacuation planning (Witter and others, 2013). This last hypothetical scenario assumes 1,200 years of slip deficit release but without any reduction of slip from north to south. According to Witter and others (2013), these size classes correspond to approximate recurrence rates as follows: S, 1/2,000 yr; M, 1/1,000 yr; L, 1/3,333 yr; and XL, < 1/10,000 yr. Recurrence for the maximum-considered XXL1 event is not known.

2.2 Tsunami Simulation

Vertical components of seabed deformation from the earthquake ruptures were used to set up the initial water surface for tsunami simulations as well as the initial velocity, assuming a short (10 s) initial constant acceleration of the seafloor. Simulations of tsunami propagation and inundation used the hydrodynamic finite element model SCHISM (Semi-implicit Cross-scale Hydroscience Integrated System Model; schism.wiki; Zhang and others, 2016a), which is derived from the SELFE model (Zhang and Baptista, 2008; Priest and others, 2009; Zhang and others, 2011; Witter and others, 2012). Algorithms used to solve the Navier-Stokes equations in these models are computationally efficient and stable. SELFE passed all standard tsunami benchmark tests (Zhang and Baptista, 2008; Zhang and others, 2011) and closely reproduced observed inundation and flow depths of the 1964 Alaska tsunami in a trial at Cannon Beach (Priest and others, 2009). More recently, SCHISM successfully passed a suite of standardized tsunami current benchmark tests (Zhang and others, 2016b; Lynett and others, 2017), indicating that the original SELFE model results are acceptable for simulating tsunami currents used in maritime evacuation planning.

The unstructured finite element mesh used in our Umpqua River modeling was constructed by first compiling digital elevation models (DEMs) covering the model domain and then retrieving elevations at a series of points defining a triangular irregular network. The DEM for the tsunami simulations was developed from a combined bathymetric/topographic seamless digital surface model created by the National Center for Environmental Information (NCEI). The DEM comprises a variety of data sources, including existing National Oceanic and Atmospheric Administration (NOAA) bathymetric data, water-penetrating airborne lidar survey, and channel surveys from the U.S. Army Corps of Engineers (USACE) (Carignan and others, 2021). In areas of dry land, Carignan and others (2021) supplemented the bathymetric data with 2008–2015 terrestrial lidar data collected by DOGAMI and other agencies. The final product consists of 1/9 arc-second (~3 m; 10 ft) grid cells referenced to the North American Vertical Datum of 1988 (NAVD88).

The completed tsunami model domain is shown in **Figure 1** for the Umpqua Estuary (shown in pale yellow and blue) and extends ~40 km (25 mi) offshore; green area is outside of the local Cascadia tsunami zone. The size of the unstructured grid consisted of ~2.24 million nodes and ~4.5 million triangular elements in the horizontal dimension. The nominal resolution is ~6 m (20 ft) in the river channel and ~6–10 m (20–33 ft) on land in areas adjacent to the estuary and river channel. The DEM was further refined by adding finer-resolution detail in areas adjacent to the Umpqua River jetties, the breakwaters and port docks at the port of Winchester Bay, along the Reedsport wharf and along various levees.

We use only one layer in the vertical, so the model is effectively 2D depth averaged. This is consistent with the majority of existing tsunami inundation maritime modeling efforts presently being implemented; incorporation of fully 3D modeling is left for future study. Ideally, SCHISM 3D would provide better results, especially in terms of resolving the density-driven currents that are important (Burla and others, 2010). However, the effects of the density flow (on the order of 1 m/s; 1.9 knot) are arguably minor compared to those from the tsunami event (on the order of 5 m/s; 9.7 knot). Furthermore, a fully 3D model with the required very fine resolution needed for tsunami simulations is too costly at present.

Each simulation was run for 24 hours, providing sufficient time for the tsunami to run its course; the simulation time step is one second for distant and two seconds for local sources; the data output was

established at 40-second intervals. The model is fully parallelized with hybrid openMP[1] and MPI[2] and runs ~16 times faster[3] than real time on 700 Intel® Ivy Bridge cores using this higher-resolution grid.

The tsunami simulations were run using both static (i.e., fixed tidal elevation) and dynamic tides (tide elevation varies over time) and a mean river discharge. The complete suite of simulations performed is summarized in **Table 1**. For static tidal runs, we used MHHW determined at the South Beach tide gauge station (**Figure 2**) located at Newport, Oregon, which is 2.54 m (8.34 ft). For dynamic-tide runs, the tsunami was timed to arrive at the Umpqua River mouth at the following tide stages: flood, ebb, flood slack, and ebb slack (**Table 1; Figure 2**). Tidal forcing at the ocean boundary was calculated from the WEBTIDE package (http://www.bio.gc.ca/science/research-recherche/ocean/webtide/index-en.php). Umpqua River discharge information was derived from the U.S. Geological Survey (USGS) Umpqua River gauge near Elkton (#14321000). Based on evaluation of these data we focused on a single average river flow regime (**Figure 3**, **Table 1**). We chose not to simulate a high river flow regime for the Umpqua River after finding that its effect on tsunami propagation in the Coos estuary was generally similar to the average flow condition (Allan and others, 2020).

Table 1. Umpqua River simulated tsunami scenarios. See text for scenario definitions.

Group Number	Scenario	Tidal Phase*	Spring/ Neap	River Flow (m^3/sec) (Q)**	Bottom Friction***	Run Name
1	AK64	event	event	estimated	landscape	RUN03c-1964
2	XXL1	static (MHHW)	N/A	0	0	RUN01b-XXL1 ***(2012 grid)*** RUN01c-XXL1 ***(2021 grid)***
3	AKMax/L1/XXL1	dynamic (MSL), flood	spring	average	landscape	XXL1 = Run05a L1 = Run05a-L1 AKMax = Run05a-pmel01
4	AKMax/L1/XXL1	dynamic (MSL), ebb	spring	average	landscape	XXL1 = Run06a L1 = Run06a-L1 AKMax = Run06a-pmel01
5	AKMax/L1/XXL1	dynamic (MSL), flood slack	spring	average	landscape	XXL1 = Run07a L1 = Run07a-L1 AKMax = Run07a-pmel01
6	AKMax/L1/XXL1	dynamic (MSL), ebb slack	spring	average	landscape	XXL1 = Run08a L1 = Run08a-L1 AKMax = Run08a-pmel01

Notes: Static means a fixed tidal elevation, and dynamic means the tide varies over time. MSL is mean sea level.

*Heights of tidal datums above the mean lower low water (MLLW datum of the South Beach tide gauge located at Newport, Oregon. Mean higher high water (MHHW) = 2.543 m (8.34 ft); MSL = 1.358 m (4.46 ft); NAVD88 = 0.234 m (0.77 ft).

**Average spring "freshet" (spring thaw resulting from snowmelt) flows = May 2006 conditions.

***Nodal Manning-*n* coefficients are spatially assigned using land-cover definitions from the USGS National Land Cover Data for Oregon and Washington (see **Table 2**). For the ocean bottom we used Manning-*n* = 0.02.

[1] openMP: share memory parallelism (MP=multi-processing)

[2] MPI: message passing protocol (for distributed parallelism)

[3] 24/16=1.5 hours to finish one simulation day

Figure 2. Tidal stages defined for the South Beach tide gauge.

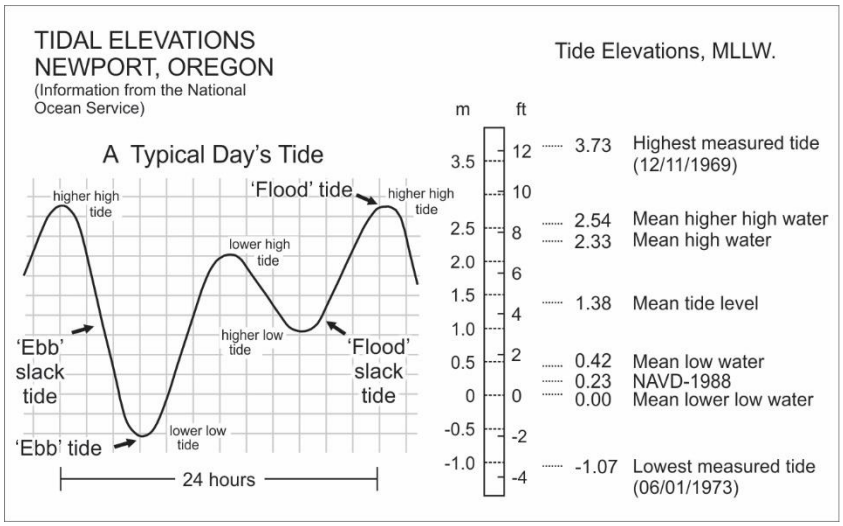

The bottom drag coefficient (*Cd*) or friction used in tsunami modeling is specified from Manning-*n*, which is a function of land-cover type (USACE, 2008). The Umpqua Estuary is characterized by a wide range of land-cover types, including open water, developed space, pastures, shrubs, wetlands, evergreen forest, and woodland, which are captured in the USGS 2011 National Land Cover Data (Homer and others, 2015). Values of Manning-*n* are estimated for each land-cover type based on published values provided by Bunya and others (2010) and provided in **Table 2.** This process is accomplished using a look-up table script that assigns the Manning-*n* value based on the local land-cover data. The spatial dataset of friction is then used in the model simulations. The friction generally increases landward, thus helping to dissipate the tsunami wave energy. For the subaqueous portion of the DEM, we used Manning-*n* = 0.02.

Figure 3. Time history of Umpqua River discharge measured at the Elkton River USGS gauge, 1905–2021. Faint black line defines the complete time history of river discharge, solid blue is the peak flood in 1964. Purple line represents the mean flow used in our tsunami simulations.

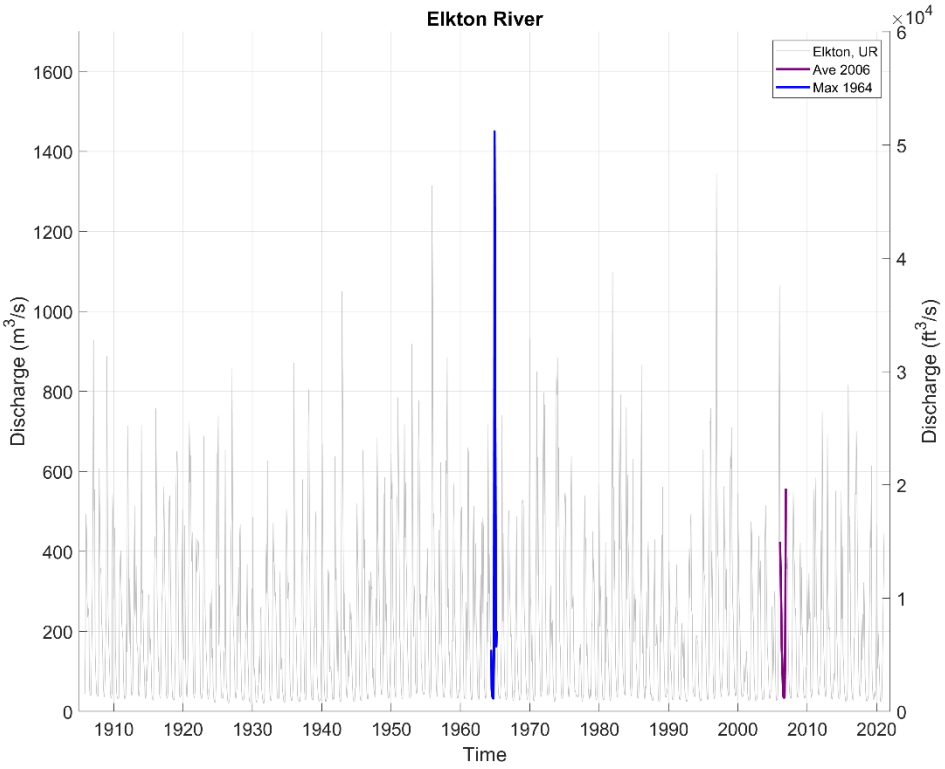

Table 2. Manning-*n* values for various land-cover types (from Bunya and others, 2010, Tables 4 and 5).

Description	Manning-*n* Value
Open water	0.020
Sand beach, bare ground, recreational grass	0.030
Fallow, transportation	0.032
Pasture	0.033
Grassland, farmed wetlands, urban grassy pasture, herbaceous wetland	0.035
Agriculture, bare rock	0.040
Low-density urban/commercial	0.050
Shrub land	0.070
Transitional, orchard, vineyard	0.100
Medium-density urban	0.120
Woody wetland	0.140
High-density urban	0.150
Deciduous forest	0.160
Mixed forest	0.170
Evergreen forest	0.180

Multiple model runs were undertaken to simulate the effects of tides, river flow, and tsunamis before these were compared across all "dynamic-tide" runs. **Table 1** shows summary information for each of the model runs completed for this study. In this report we will focus initially on comparisons between static- and dynamic-tide run results to illustrate the importance of incorporating tides in tsunami simulations for this high energy system. For dynamic-tide simulations, the effects of spring[4] tide, tidal phase, and river flow conditions are examined. Most of the simulations are done for one day under an average spring freshet[5] condition as observed in 2006 (**Figure 3**). Longer simulations (12 to 24 days) are done for tidal runs that were used to provide the initial condition at the start of the coupled tide-tsunami simulations.

Finally, **Figure 4** presents a map identifying the locations (virtual gauge stations) where time series information has been extracted from the simulations in order to generate plots of tsunami currents and water levels. These data are useful for better understanding the complex nonlinear responses of the tsunamis as they interact with tides and riverine flows.

[4] Spring tides occur twice each lunar month when the Earth, sun, and moon are nearly in alignment, producing high tides that are a little higher than normal.

[5] A term used to describe a spring thaw resulting from snowmelt.

Figure 4. Map showing the locations of virtual water level stations in the Umpqua Estuary used to observe tsunami currents and water level time series information. Inset example shows the simulated XXL1 water levels for Run05a (flood tide) and Run06a (ebb tide) at station 5 (blue circle) located near the mouth of the Umpqua River (RM0). The shading in the inset indicates the total variability at this station from all simulations. Blue to yellow shading in the main panel defines the offshore bathymetry and subaerial topography.

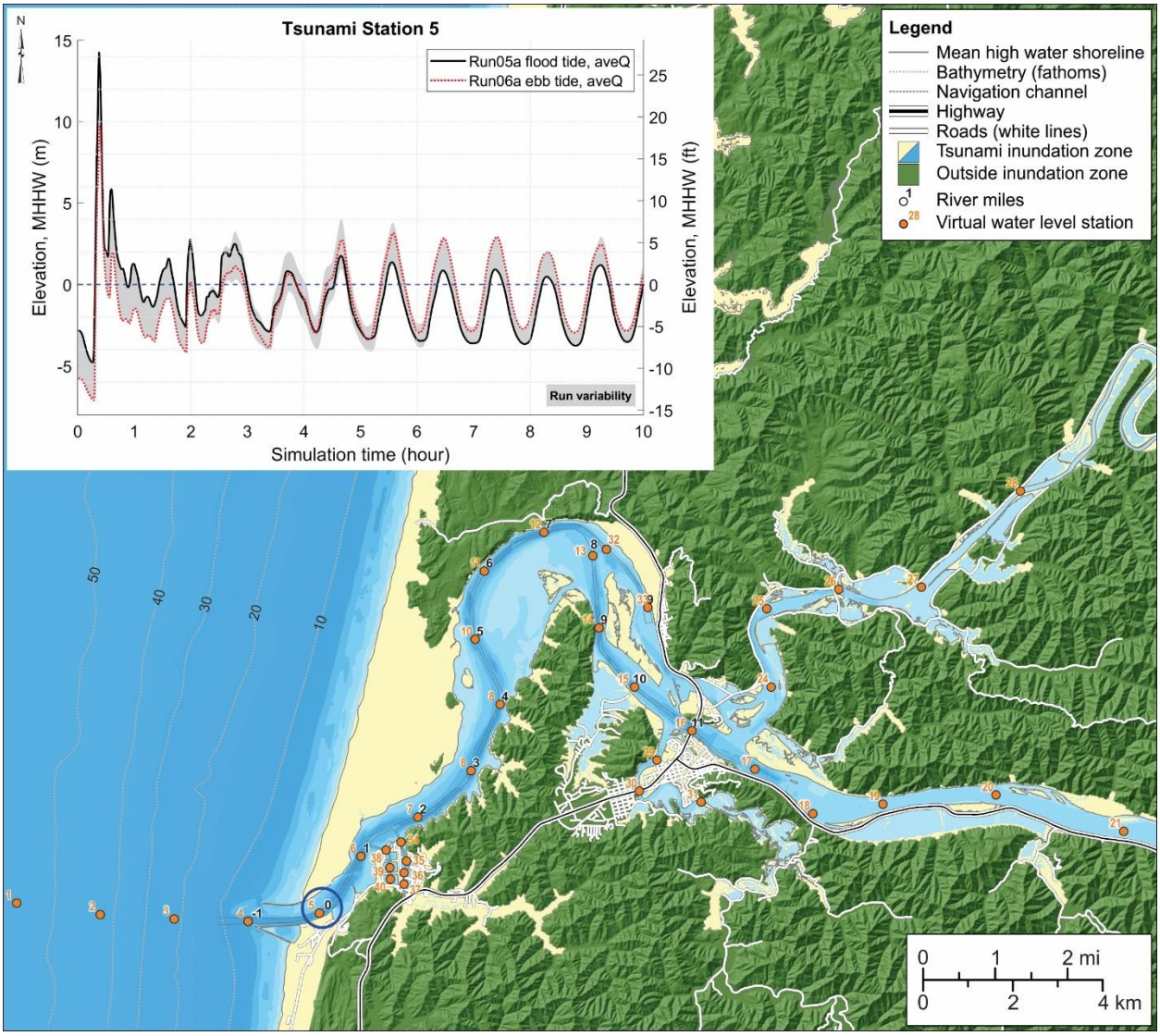

3.0 MODEL VALIDATIONS

3.1 Tides

We first validate the model for tidal elevations. We used an average river flow event in May 2006 to evaluate the tidal modeling. **Figure 5** provides a comparison between the predicted tides at the NOAA Halfmoon Bay tide prediction station[6] with the model results determined by SCHISM. As can be seen in **Figure 5**, our 2D model replicates the predicted tide data well. Some of the mismatch may be explained by our omission of wind effects in the simulation. Also note that the NOAA-predicted elevation may also have errors. Besides including wind, better accuracy may be achieved with the 3D version of SCHISM, especially when using 3D baroclinic SCHISM (Burla and others, 2010).

All dynamic-tide runs discussed in this report consist of three separate runs, with the first two being preparation for the last run:

- A tidal run (with river flow) that starts ~10 days before the tsunami event and ends at least one day after the event in order to cover all simulations
- A static-tide run with tsunami only (with no river flow or tides)
- A final dynamic-tide run that is initiated from the tidal run at a given tidal phase and at the start of the earthquake event and uses the information at the ocean boundary from the other two runs as well as bed deformation inside the domain. Comparison of results from this run and the sum of the other two runs reveals nonlinearity due to tide-river-tsunami interaction.

Figure 5. Comparison of modeled and predicted tidal elevations defined for the Halfmoon Bay tidal prediction station near the mouth of the Umpqua River.

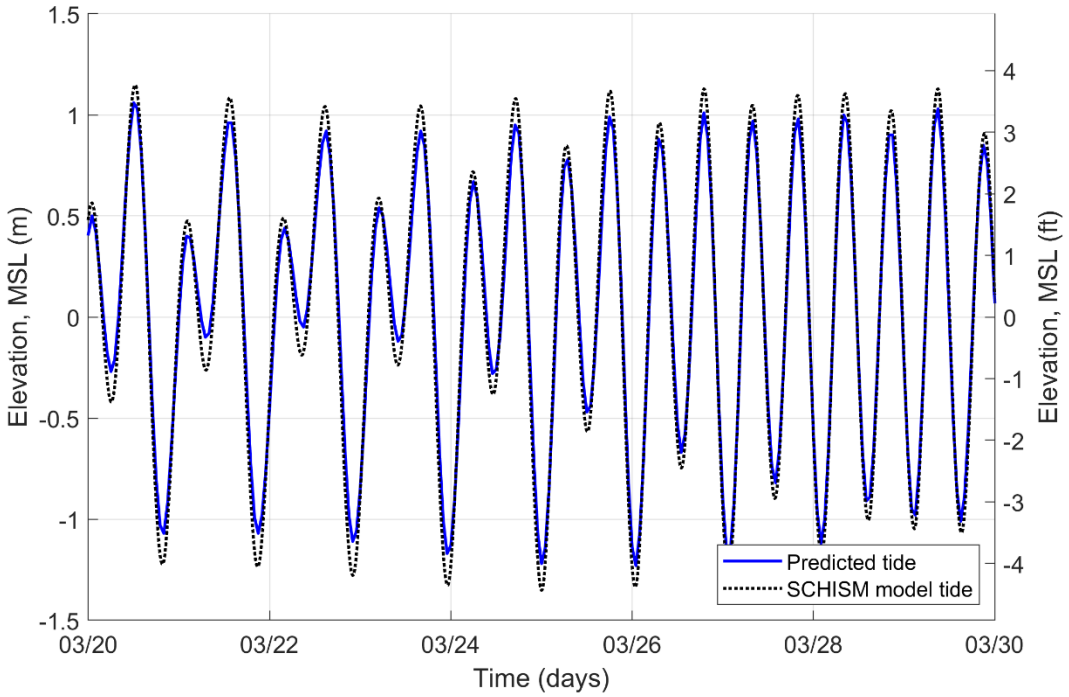

[6] https://tidesandcurrents.noaa.gov/noaatidepredictions.html?id=9433445

3.2 The Great Alaska 1964 Tsunami

Wilson and Torum (1968) report that the Alaska 1964 tsunami reached a height of ~4.3 m (14 ft) just offshore the Umpqua River mouth. Lander and others (1993) noted that the tsunami reached ~3.3 m (11 ft) within the Winchester Bay marina. It is not clear what datums were used to define the tsunami height estimates, while the specific observation locations are also unclear. For example, Wilson and Torum (1968) reported that the peak tsunami wave height of 4.3 m (14 ft) offshore the mouth, was above mean high water (MHW). However, that datum would have produced greater inundation when converted to the MLLW datum and likely more damage. In contrast, descriptions provided in Lander and others (1993), suggest that the water elevations were expressed relative to MLLW, since that is a datum commonly used by mariners. The latter is more consistent with our model results.

Damage from the Alaska tsunami was small, estimated at no more than $5,000 in 1964, with negligible damage 17.7 km (11 mi) upriver at the city of Reedsport (Lander and others, 1993). The latter is probably not surprising given the relatively broad, sinuous river channel and shallow tidal flats. Here we revalidate the model using higher-resolution DEM data developed for the Umpqua Estuary.

The static-tide run uses MHHW as the vertical datum — 2.54 m (8.34 ft) based on the South Beach tide gauge station datum — whereas the other two runs (tidal and dynamic-tide runs) use MSL (1.36 m; 4.46 ft). For the 1964 event, we initiated the tide model from March 10, 1964. The model was then restarted at 00:00 GMT on March 28, a few hours before the earthquake that occurred at 03:36 GMT on March 28, 1964 (19:36 pm PDT on March 27, 1964), with the 1964 tsunami wave signal added at the ocean boundary. These latter data were calculated from a previous large-domain run undertaken by Priest and others (2013), extended to one simulation day here. The first tsunami wave reaches the mouth of the Umpqua River at approximately 4 hours, 5 minutes after the Alaskan earthquake (23:41 pm PDT on March 27, 1964). Unfortunately, we are unable to directly compare model results with observed water levels within the Umpqua Estuary as there is no operational tide gauge station. Nevertheless, we can provide some nominal comparison of the simulation with the few qualitative observations available to us, such as those noted previously.

The Alaska 1964 tsunami waves coincided with a spring flood tide, which likely exacerbated local impacts (Zhang and others, 2011). The tsunami waves are visible during the subsequent ebb and flood and persisted more than one day after the earthquake (**Figure 6**). As noted above, Lander and others (1993) describe several observations of surges associated with the 1964 event. However, aside from one location out in the surf, north of the Umpqua River mouth, the rest of the observations are qualitative, making it difficult to compare model versus real world results. Our analyses confirm that the maximum tsunami height occurs at the mouth, where the simulated tsunami reaches ~3.9 m (12.8 ft; **Figure 6**) above MLLW, which is close to the observation of Schatz and others (1964) and Lander and others (1993). At the entrance to the Winchester Bay marina, our modeled peak water level reaches ~3 m (9.8 ft) and is ~3.2 m (10.5 ft) at the head of the marina; Lander and others (1993) report a peak water level observation of “plus 4.2 m” (14 ft) at the marina entrance. This suggests our modeling may be underestimating the maximum tsunami water levels in this part of the harbor; however, as noted previously there is no record of where the observation was made. During that first surge into Winchester Bay, there is a note that the harbor manager tried to evacuate his car and trailer (no location provided), but it was swamped by the tsunami (Lander and others, 1993). Our evaluation of the model DEM suggests that the most likely place for tsunami wave overtopping may have occurred near the southwestern corner of the marina (just west of station 40 in **Figure 7**), where ground elevations are lower. Nevertheless, we do not see overtopping in our modeling, but the simulated water levels are sufficiently close and the limited inundation that may

have occurred could be explained in terms of localized "greenwater" overtopping or, simply, wave splash. For subsequent tsunami peak surges, our model results are entirely consistent with reported descriptions in Lander and others (1993). Of further importance, the timing of our modeled tsunami surges (first, second, and third peaks) are completely consistent with the reported timing of the waves in Lander and others (1993).

Figure 6. Simulated water level elevations at the mouth of the Umpqua River during the 1964 event from the dynamic-tide simulation; vertical datum is MLLW.

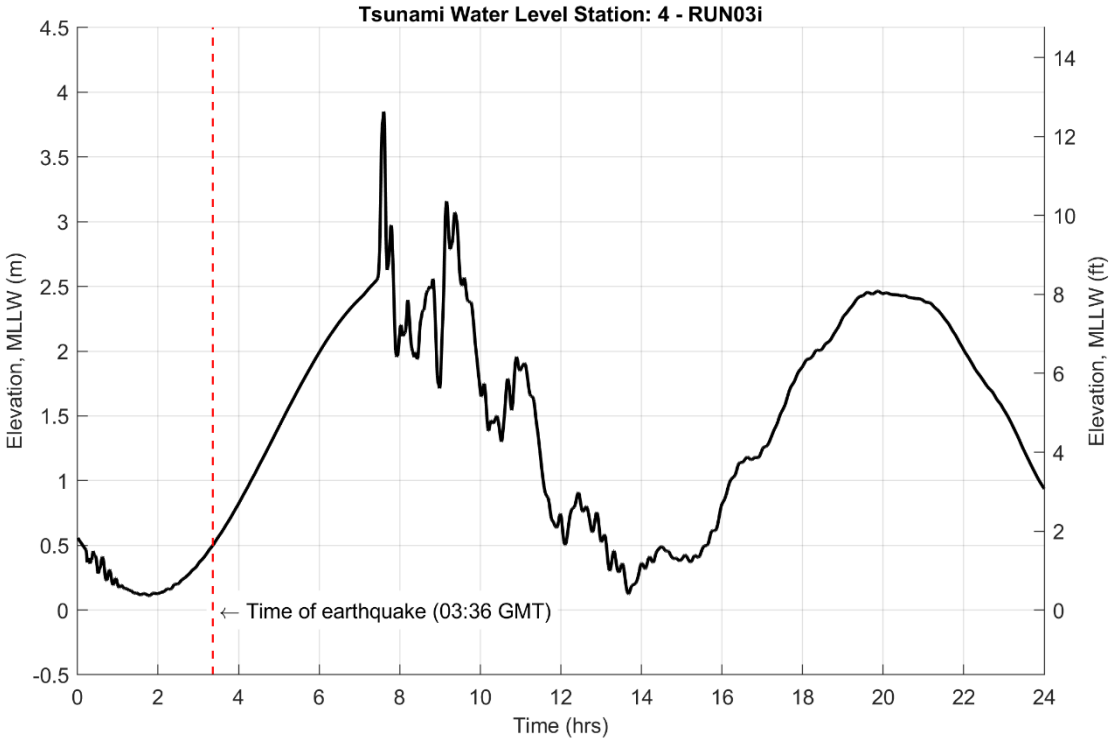

North of the Umpqua River mouth (**Figure 7**), there is a single estimate of a maximum tsunami amplitude of 1.68 m (5.5 ft), located about 2.4 km (1.5 mi) north of the mouth and 0.85 km (0.5 mi) west of the beach (Lander and others, 1993); the observation point places it out in the ocean, west of the surf zone. Assuming the site is correct, this would imply that the observation must have been made by a person on a boat, such that the reference height is the height of the tsunami wave above the normal tide. Converting the simulated maximum water level for the same location to MLLW, we get a modeled water level of 4.07 m (13.4 ft); subtracting the tide yields a water level residual of ~1.53 m (5 ft), which is broadly similar to the reported observation. These comparisons suggest that the SCHISM model is capturing the complex interaction between tsunami waves and tides and can produce reasonable results when compared to a few discrete observations.

Because the Alaska 1964 event remains the largest far-field tsunami to strike the Oregon coast in the last century, these data are useful for assisting with the development of maritime tsunami guidance for the Umpqua Estuary. **Figure 8** and **Figure 9** present the simulated maximum water levels and current velocities generated for the Alaska 1964 tsunami. For tsunami currents (**Figure 9**) we use the binning approach as proposed by Lynett and others (2014; **Table 3**), after finding a strong relationship between

current velocity and damage caused by the 2011 Tōhoku tsunami on ports and harbors on the California coast. In general, Lynett and others found that for velocities ranging from 1.5 to 3 m/s (3 to 6 knots), moderate tsunami damage tended to occur to port facilities and moored vessels. When the current velocities increased to ~3–4.5 m/s (6–9 knots), ports and docks were subject to major damage. Extreme damage occurred when current velocities exceeded 4.5 m/s (9 knots).

Figure 7. Simulated maximum water levels relative to the MLLW tide datum at the mouth of the Umpqua River and in the Winchester Bay marina. Figure includes a single observation point of the Alaska 1964 tsunami amplitude located offshore. The combined amplitude and tide at this location closely matches the simulated water levels. Numbered gray circles are virtual water level stations.

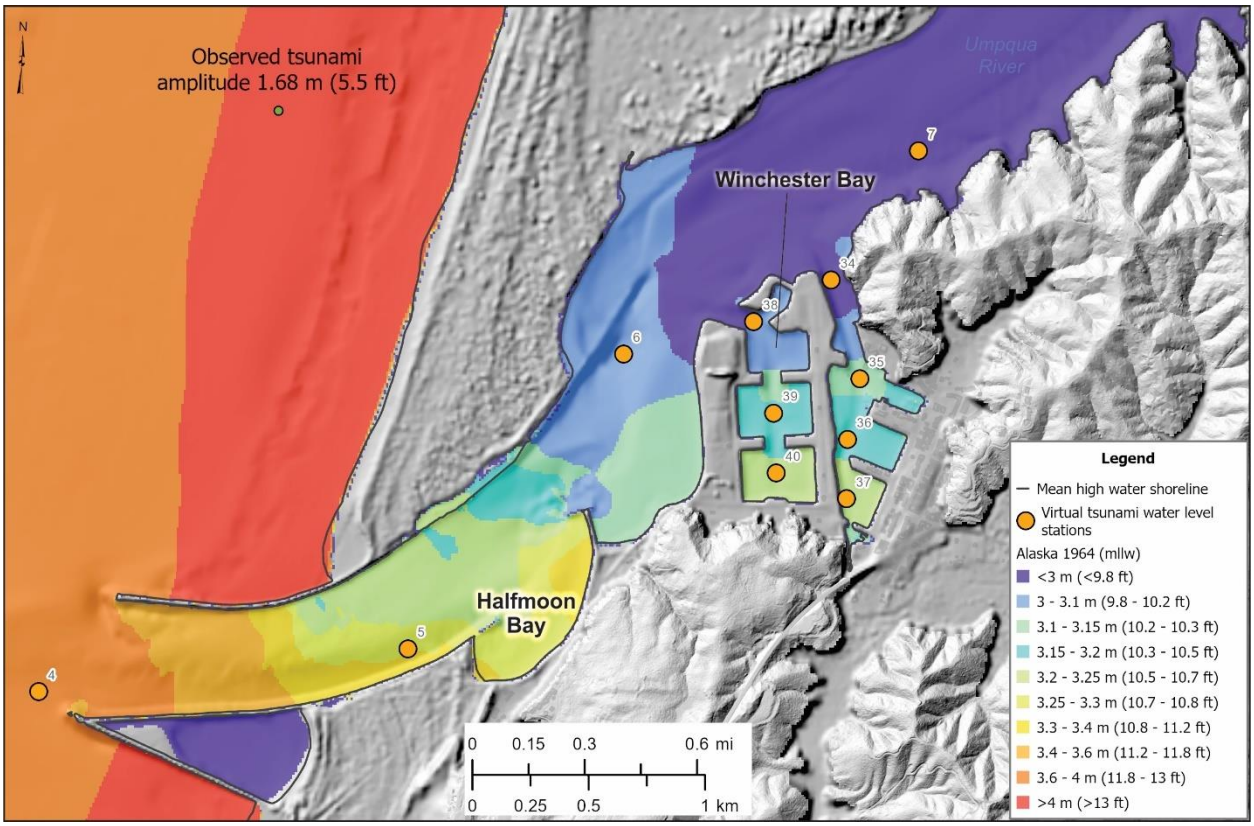

As can be seen in **Figure 8**, maximum water levels (relative to mean sea level) range from 1.2 to 1.5 m (4 to 5 ft) adjacent to the mouth of the Umpqua River. Water levels decrease rapidly after entering the mouth and reach ~0.6 m (2 ft) near Winchester Bay. Maximum tsunami water levels continue to decrease upriver and by the time the tsunami reaches Reedsport, the maximum water levels are close to normal. At Reedsport, the tsunami waves are reduced to an amplitude (half the wave height) of ~0.15 m (0.5 ft). On the open coast, water levels are highest both north and south of the estuary mouth, where they reach ~2.1 m (6.9 ft).

Evident from **Figure 9**, the modeled currents are generally low throughout the Umpqua Estuary. The strongest currents (3–6 knots) are observed between the estuary mouth and the entrance to Winchester Bay marina (between RM-1 and RM1). Elsewhere in the estuary, the tsunami current velocities are generally below the 1.5 m/s (3-knot) current threshold (**Figure 9**). According to Lander and others (1993, p. 99), damage from the 1964 tsunami was done by the initial tsunami surge as "two drag boats were broken loose from their moorings … [and] the bait stand also broke loose." Lander and others (1993, p.

99) further noted that "The tidal current entered the small boat basin with great speed." As discussed previously, damage was minor.

Table 3. Damage index and corresponding damage type (after Lynett and others, 2014).

Damage Index	Associated Current Velocity	Damage Type
0		no damage/impacts
1	< 1.5 m/s (< 3 knots)	small buoys moved
2	1.5–3 m/s (3–6 knots)	1-2 docks/small boast damaged and/or large buoys moved
3		moderate dock/boat damage (< 25% of docks/vessels damaged and/or midsized vessels off moorings)
4	3–4.5 m/s (6–9 knots)	major dock/boat damage (< 50% of docks/vessels damaged and/or midsized vessels off moorings)
5	> 4.5 m/s (> 9 knots)	extreme/complete damage (> 50% of docks/vessels damaged)

Figure 8. Simulated maximum water levels for the Alaska 1964 tsunami relative to the dynamic tidal heights.

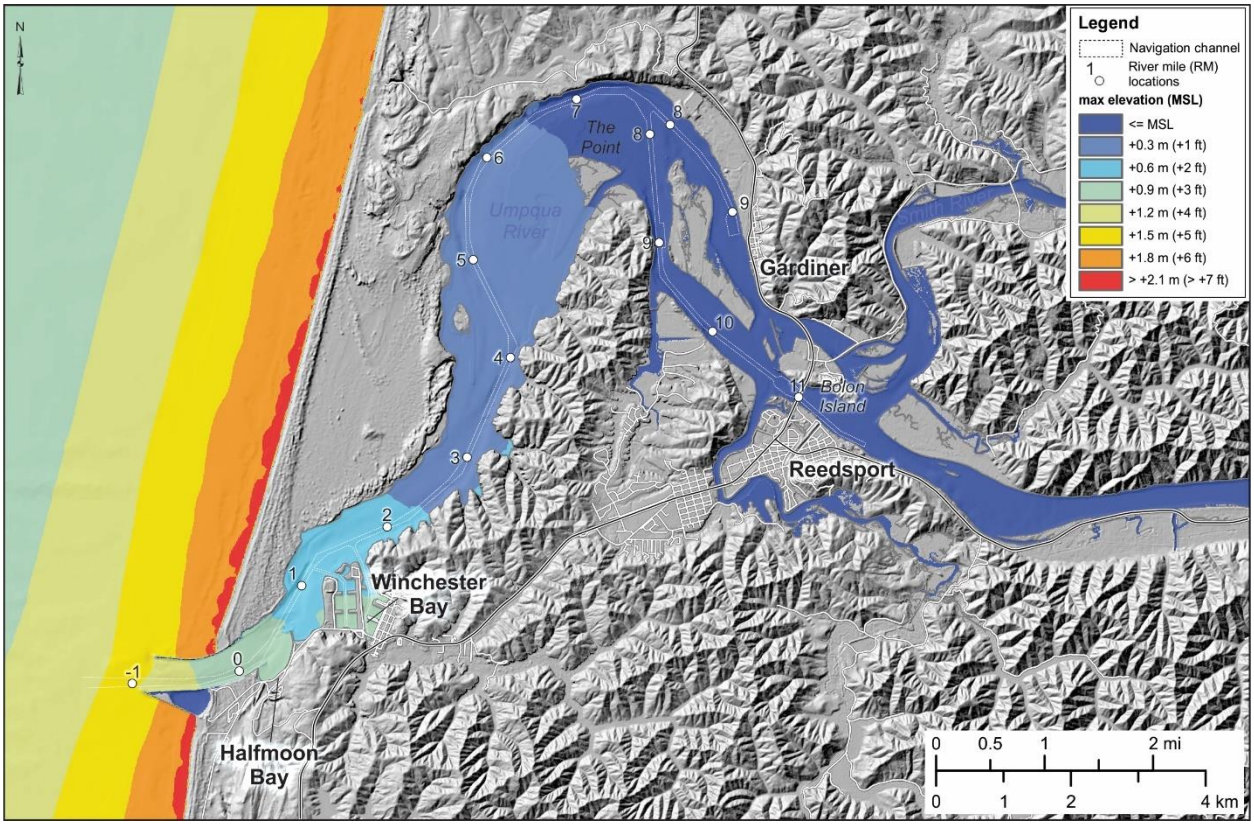

Figure 9. Simulated maximum currents for the Alaska 1964 tsunami using dynamic tides.

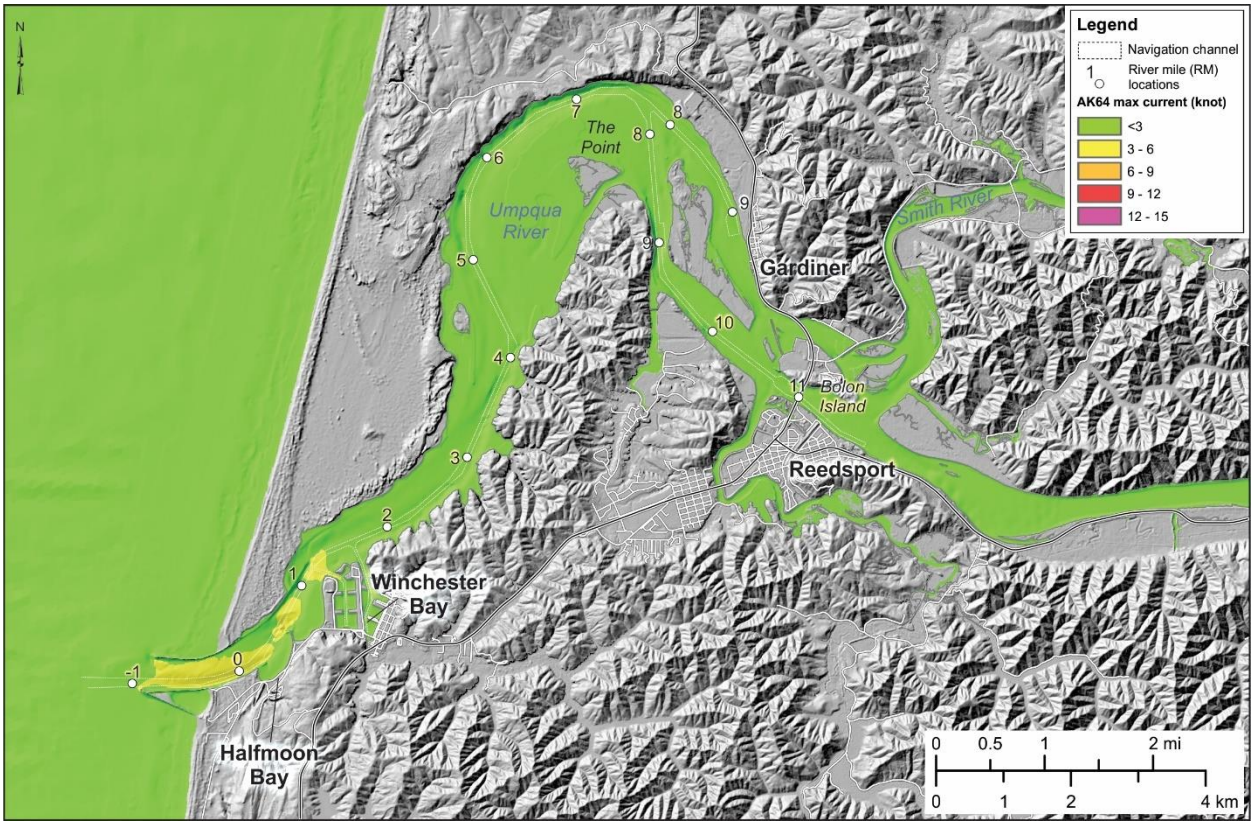

4.0 STATIC AND DYNAMIC TSUNAMI SIMULATIONS

4.1 Static-Tide Results

Simulations involving static-tide modeling were implemented for only the XXL1 local CSZ scenario, to allow for direct comparisons between model results using the original and updated digital elevation models. As a reminder, these runs do not include river flow and use a frictionless bathymetry (**Table 1**, group 2), making them consistent with previous modeling efforts undertaken for the Oregon coast from 2009 to 2013 (Priest and others, 2009; Witter and others, 2011; Priest and others, 2013). The vertical datum used in our static run modeling is MHHW defined at the South Beach tide gauge.

The major difference between the latest simulation (Run01c), described in this report, and the previous modeling effort (Run01b), besides simulation period (twenty-four hours versus eight hours), is the adoption of an updated digital elevation model (**Figure 10 A**, *top*) that include the following bathymetric improvements:

- A relatively moderate (1–3 m; 3.3–10 ft) decrease (shallowing) of water depths in the nearshore region (orange color, **Figure 10 A**) across large areas seaward of the North Umpqua Spit.
- A more substantive (3–5 m; 10–16 ft) decrease (shallowing) in water depths in the surf zone (brown color, **Figure 10 A**) immediately west of the North Umpqua Spit.
- A region of low to moderate (0.5–3 m; 1.6–10 ft) increase (deepening) in water depths offshore the Umpqua River mouth (pale blue, **Figure 10 A**).
- Within the estuary and along the river channel, large areas where the local bathymetry has become deeper (pale blue to dark blue, **Figure 10A**).

Comparisons of the inundation extents produced from our latest simulation versus modeling undertaken in 2013 (Priest and others, 2013) indicate that for most areas within the estuary, differences between the two modeling efforts are relatively minor (yellow, **Figure 10B**). Overall, we find little difference in the inundation extents along the open coast, with an equal mixture of both areas now removed from the XXL1 tsunami inundation zone (rose color, **Figure 10B**) versus newly flooded areas (cyan color). More substantive change occurs up the Umpqua and Smith rivers, especially in distal ends of small tributary valleys where the latest modeling indicates increased flooding (cyan color, **Figure 10B)**. These changes are very similar to results seen in our Coos Bay modeling (Allan and others, 2020).

As can be seen in **Figure 11** (*top*, maximum water levels; *bottom*, currents), the entire Umpqua North Spit is overtopped under the maximum-considered XXL1 scenario. Because the estuary geometry serves as an effective dissipater of short-wavelength tsunami waves, the greatest impact caused by an XXL1 tsunami (**Figure 11**, *top*; hot colors) is in the lower estuary between the mouth and approximately Reedsport. Both modeled tsunami water levels and current velocities can be expected to yield catastrophic results throughout this area, with the communities of Winchester Bay, Gardiner, and Reedsport severely impacted. The XXL1 tsunami loses much of its energy upstream of Reedsport but still manages to travel an additional 22 km (14 mi) beyond Reedsport. Finally, strong tsunami currents exceeding 6.2 m/s (12 knots) will impact the entire estuary (**Figure 11**, *bottom*; red-brown-purple colors), contributing to the destruction of buildings and infrastructure located in the inundation zone.

Figure 10. ***(A)*** **Bathymetric (DEM) changes defined for 2021 compared with original 2013 DEM. Warm colors indicate bathymetry is shallower relative to 2013 DEM, whereas darker blue colors indicate deeper conditions. Gray color indicates negligible DEM change. Green areas are those outside the tsunami zone.** ***(B)*** **latest static (MHHW) run modeling (Run01c) compared with results from 2013 (Run01b).**

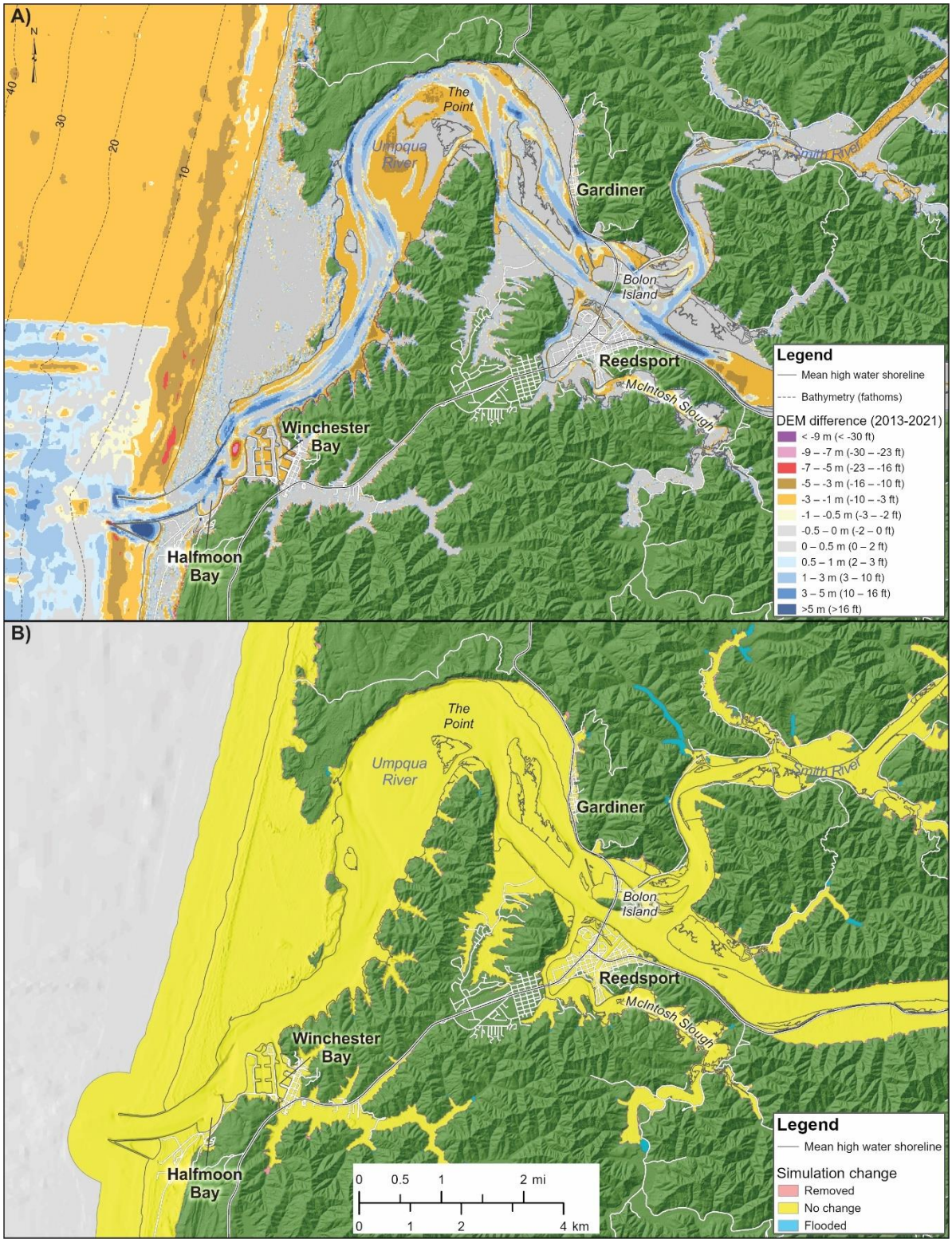

Figure 11. ***(top)*** **Maximum tsunami elevation and** ***(bottom)*** **current velocities, in knots, generated for the XXL1 (Run01c) simulation, modeled using MHHW, no river flow, a frictionless landscape, and updated DEM.**

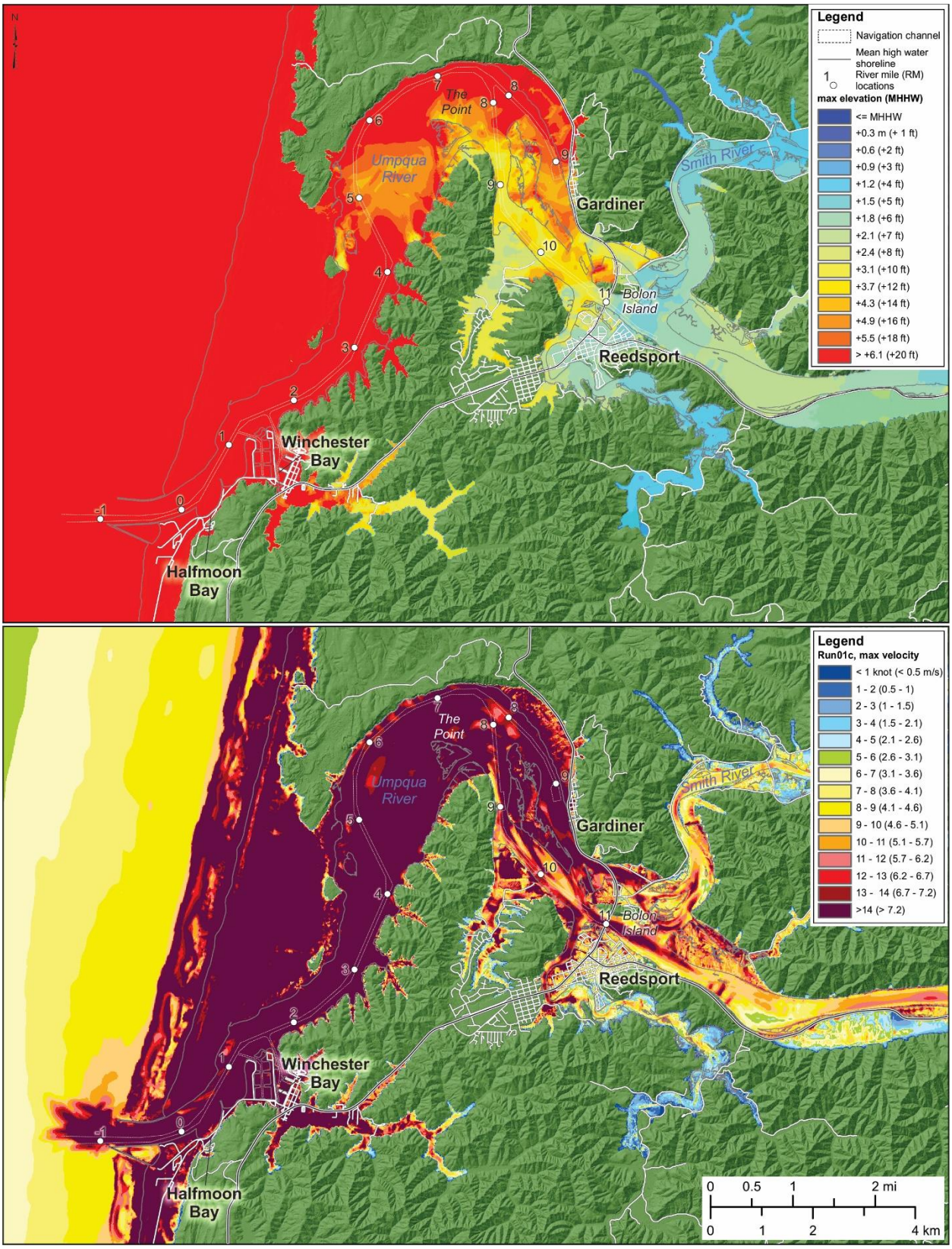

To further highlight the transformation in the tsunami as it propagates up along the Umpqua navigation channel, we define the maximum tsunami water level along the length of the channel, which extends upriver from offshore of the mouth of the Umpqua River to past downtown Reedsport (**Figure 12**). **Figure 12** also includes simulation results based on the original DEM. The maximum water level is defined as:

$$\max \text{wl} = FD - d \tag{1}$$

where *FD* is the maximum flow depth and *d* is the elevation of the ground or bathymetric surface after subsidence.

As can be seen in **Figure 12**, the largest tsunami waves are concentrated just inside the estuary, downstream of river mile (RM) 2 and adjacent to the river mouth. At Winchester Bay, the XXL1 tsunami reaches ~14 m (46 ft). Channel morphology and shallowing within the estuary cause the tsunami waves to decrease in height after entering the estuary. For example, between RM3 and RM5 the maximum tsunami water levels decrease from a peak of ~12 m (40 ft) to ~5 m (16 ft). From RM5 to RM8, the tsunami wave increases in height again to ~8 m (26 ft). This is due to the reinforcement of a second wave front that overtopped the coastal dune to the north of the Umpqua River mouth. From RM8 to RM 11, the tsunami rapidly decreases in height again and by the time the wave reaches Reedsport at the Highway 101 bridge (RM11), the height of the tsunami has fallen to ~2 m (6 ft). Thus, the most significant transformation occurs upriver of RM7, where the tsunami loses significant energy due to the wave reflection near the sharp turn of the channel (The Point, **Figure 12**). The tsunami waves continue past Reedsport, traveling up the Umpqua and Smith rivers.

Figure 12. Maximum tsunami water levels interpolated along the Umpqua Estuary navigation channel for XXL1 using the original (2013) DEM and static tidal elevation and with the updated DEM (Run01c).

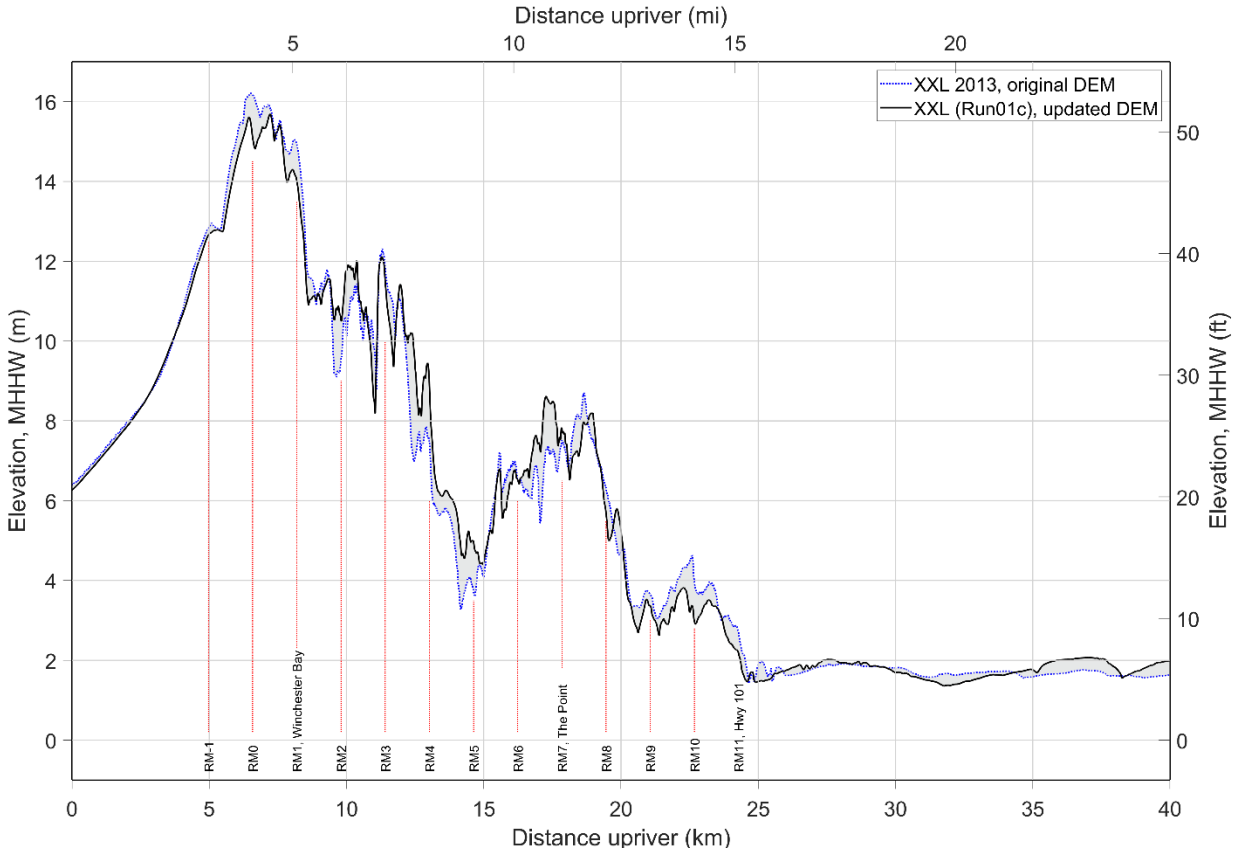

4.2 Dynamic-Tide Results

4.2.1 Tidal effects: flood versus ebb conditions

The addition of dynamic tides introduces a great deal of complexity into the results, due to the nonlinear interaction between tides, river flow and tsunamis in the Umpqua Estuary. The predicted maximum velocity exhibits more local extremes along the coast and within the lower estuary, especially near the mouth, where the interaction is found to be strongest due to powerful currents and shoaling of tsunami waves (compare **Figure 13** with **Figure 11**). Differences between the old and new modeling are noticeable in the lower estuary, downstream of RM5, where recent bathymetric-topographic changes have been captured (**Figure 14**). Figure 14 shows differences in current velocities between the static tide modeling approach using the updated DEM (Run01c) and the latest results (Run05a), which incorporate dynamic (flood) tide conditions and friction. Velocity differences less than −0.5 knots (cool colors, i.e., blues) indicate that the flood (Run05a) currents dominate, whereas currents greater than 0.5 knots (warm colors, i.e., reds) indicate that original (Run01c) conditions dominate. The region between –0.5 and 0.5 knots denotes little difference between the simulations.

Figure 13. Maximum tsunami velocities (in knots) generated for the XXL1 (Run05a) simulation, modeled using dynamic tides, average river flow, and friction. Note: timing of the wave arrival coincides with a flood tide at South Beach, Newport.

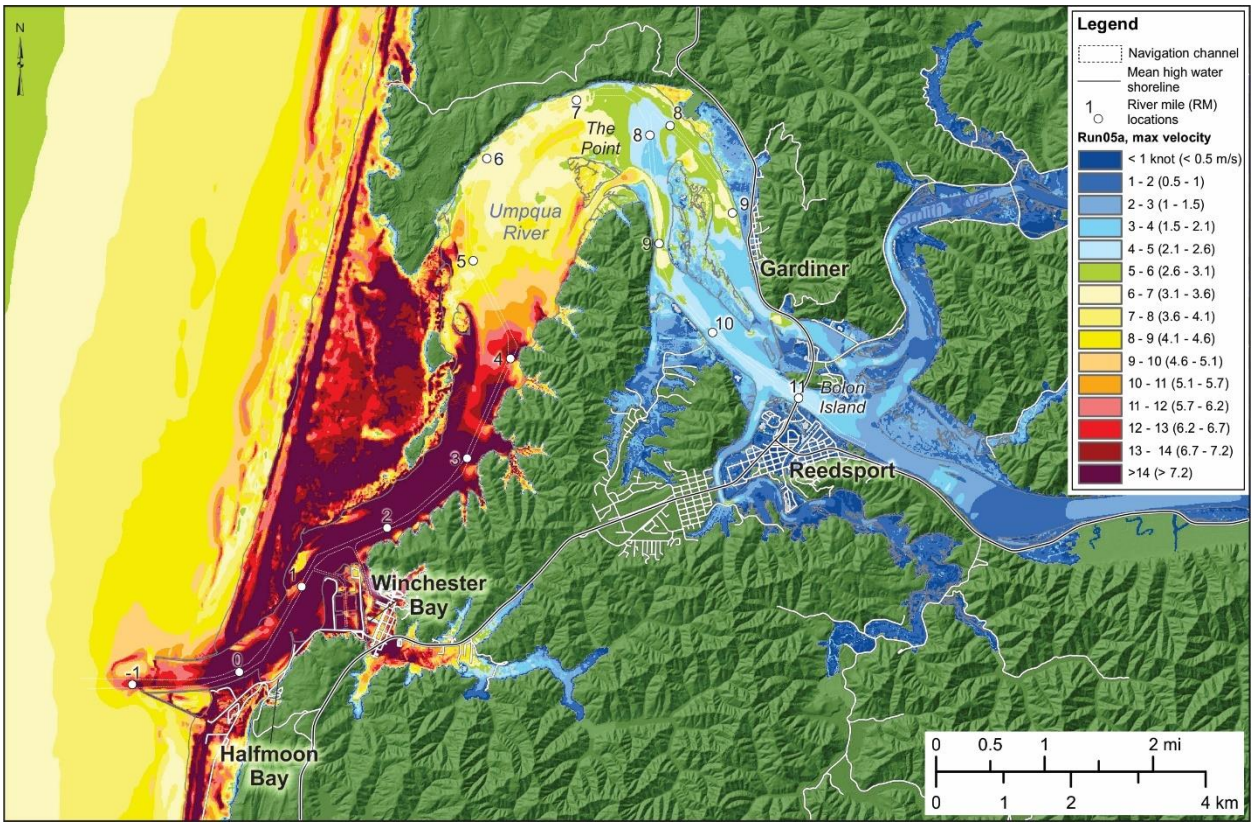

As can be seen in **Figure 14**, virtually the entire estuary is characterized with warm colors, which indicates a very significant reduction in the overall current velocity. This change is almost entirely a function of the incorporation of friction in our latest modeling, especially on land. **Figure 14** also highlights areas where bathymetric changes have occurred. For example, cooler colors in the navigation channel adjacent to Winchester Bay indicate slightly stronger current velocities associated with the latest simulation effort, which may be the product of recent DEM improvements. Similarly, warm to hot colors up the Smith and Upper Umpqua rivers indicate that the original 2013 modeling produced stronger currents in those areas.

Figure 14. Maximum tsunami velocities (knots) expressed as the difference between original modeling (Run01c) and new modeling (Run05a) that incorporate dynamic tide, river flow, and friction. Blue colors (< 0.5 knots) indicate Run05a currents dominate, whereas red colors (> 0.5 knots) indicate that Run01c currents dominate.

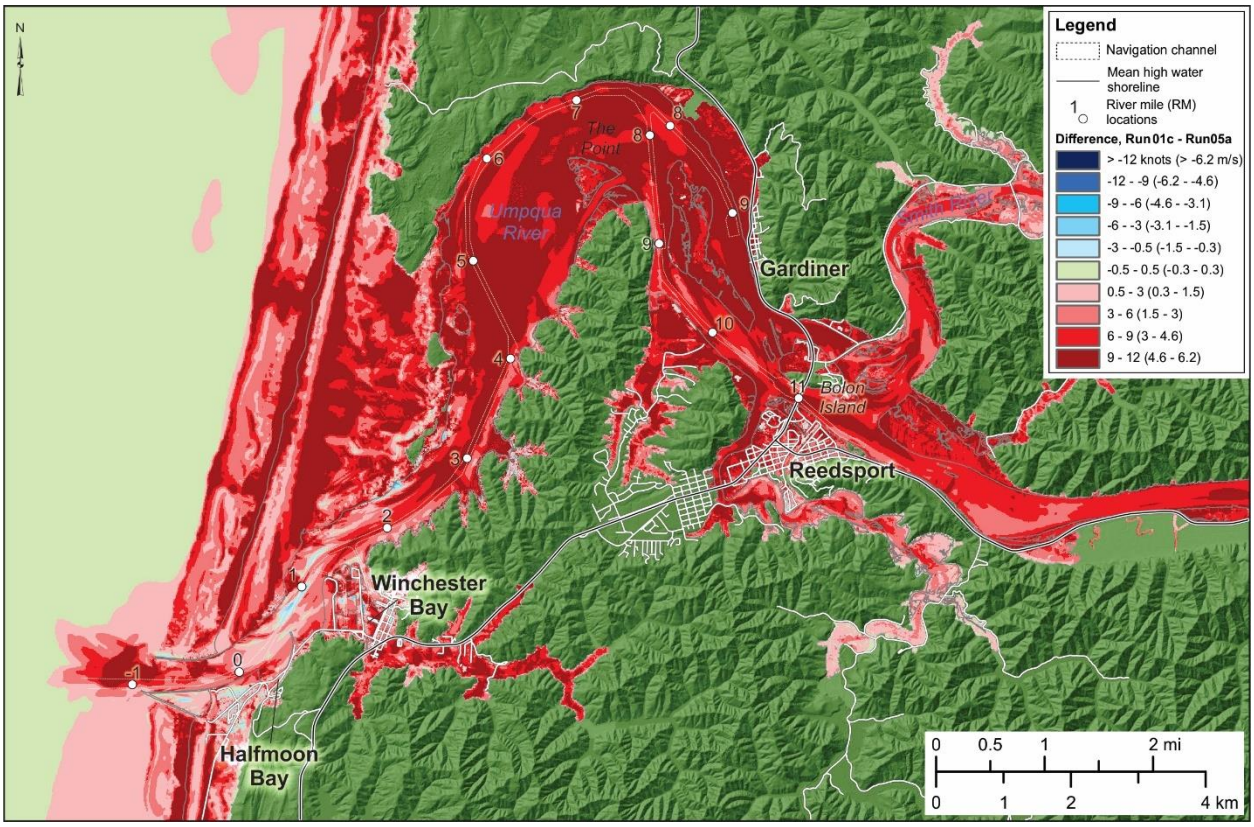

Tsunami wave patterns are highly dependent on the tidal phase at which the tsunamis arrive. The conventional understanding is that tsunamis arriving with a flood spring tide are generally more damaging compared with other tidal stages. To understand these differences, we generated a difference map (**Figure 15**), which allows us to compare tsunami currents at ebb stage (Run06a) with those at flood stage (Run05a). Our results for the Umpqua River confirm that tsunamis arriving with a flood spring tide (bright blue colors) are generally more damaging compared with the same event on an ebb tidal stage. This is true along much of the estuary, but especially upriver of Winchester Bay. Overall, our simulations confirm that flood conditions produce inundation that extend the farthest inland. The latter is evident in **Figure 15** by the abundant light blue in areas such as the north Umpqua Spit and in low-lying areas between RM6 and RM11. These differences are almost entirely due to the tidal elevation difference.

The situation becomes a little more complex in the shallow waters of the lower estuary, where tsunamis arriving at ebb and flood slack are usually more energetic — compare **Figure 15** (ebb) to **Figure 17** (ebb slack). As can be seen in **Figure 15**, strong currents (warm colors) dominate the ebb phase (Run06a) within the Umpqua Estuary mouth (between RM-1 and RM1), in the area offshore the north Umpqua Spit, within Winchester Bay harbor, and in the shallow areas on the north bank of the river channel between RM2 and RM5. The presence of rings of strong currents at Halfmoon Bay probably reflects the formation of gyres as the tsunami interacts with the jetties and the bay mouth.

Figure 15. Maximum tsunami velocities (in knots) expressed as the difference between ebb (Run06a) and flood (Run05a) simulations assuming average river flow and friction. Blue colors (< 0.5 knots) indicate Run05a currents dominate, whereas red colors (> 0.5 knots) indicate that Run06a currents dominate.

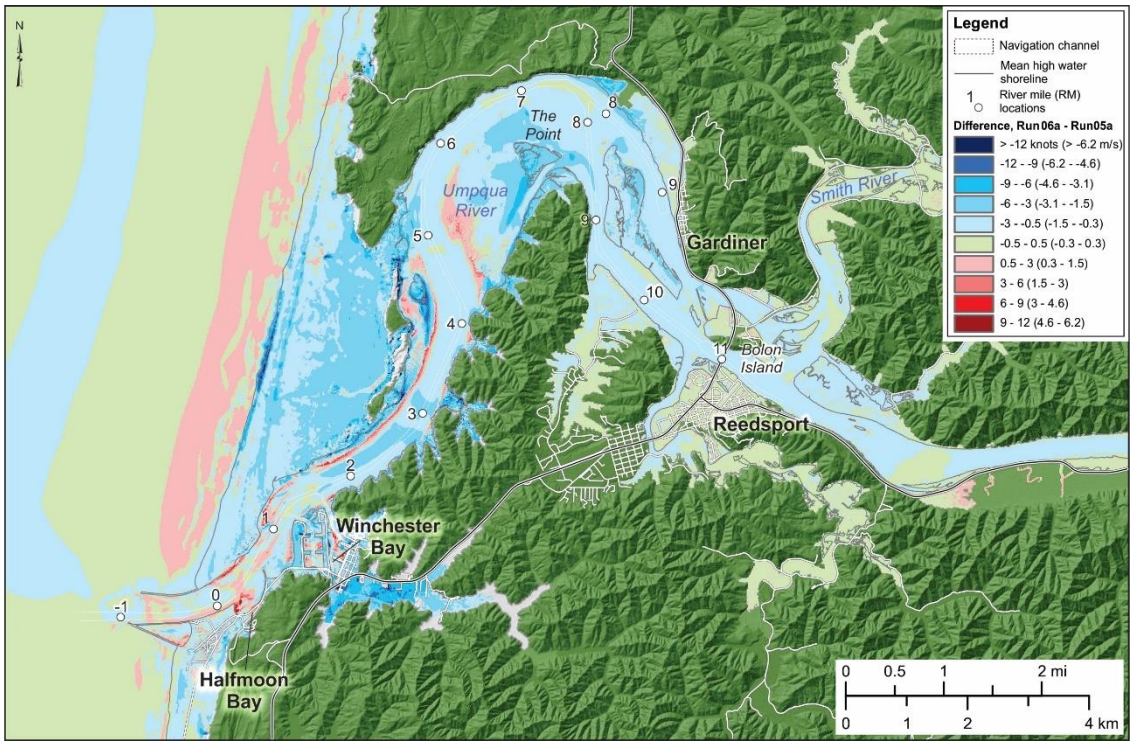

Figure 16. Maximum tsunami velocities (in knots) expressed as the difference between flood slack (Run07a) and flood (Run05a) simulations, average river flow and friction. Blue colors (< 0.5 knots) indicate Run05a currents dominate, whereas red colors (> 0.5 knots) indicate that Run07a currents dominate.

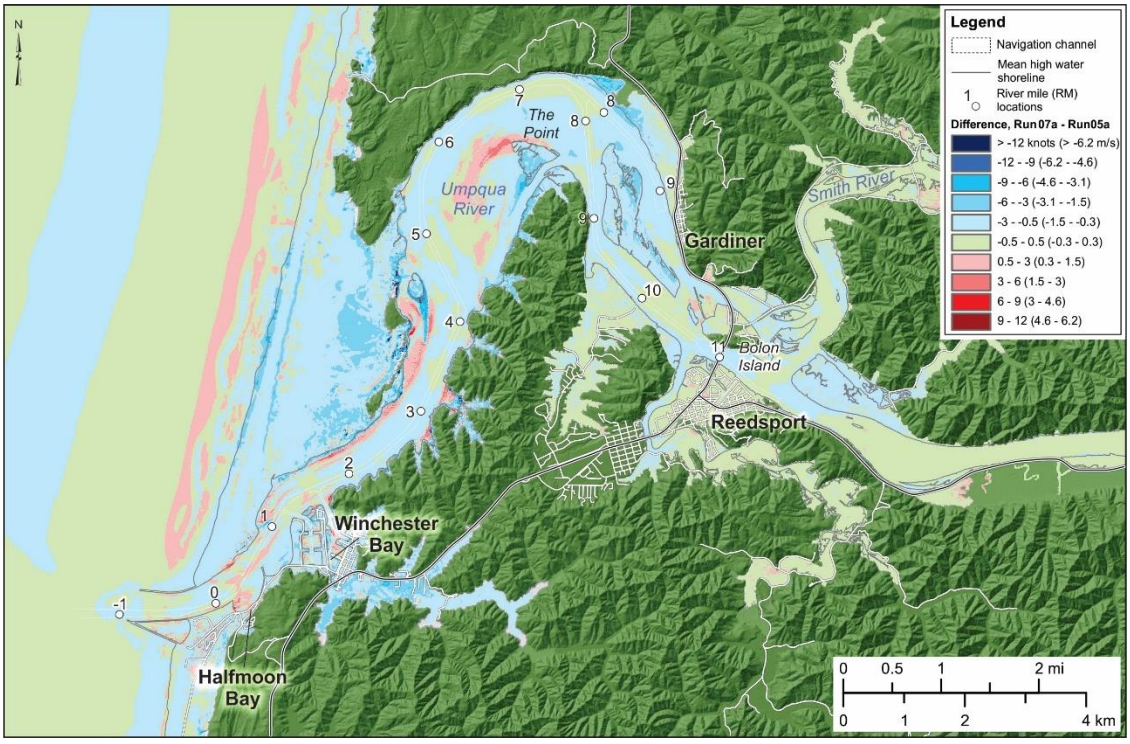

Tsunamis arriving at flood slack reveal generally stronger current velocities near the river mouth and along the north Umpqua riverbank (warm colors between RM0 to RM5, **Figure 16**) when compared to the flood stage (**Figure 15**). However, the response appears to be more muted during ebb slack (**Figure 17**), with our simulation indicating stronger current velocities mainly in the nearshore and seaward of the north Umpqua Spit.

Figure 17. Maximum tsunami velocities (in knots) expressed as the difference between ebb slack (Run08a) and flood (Run05a) simulations, average river flow and friction. Blue colors (< 0.5 knots) indicate Run05a currents dominate, whereas red colors (> 0.5 knots) indicate that Run08a currents dominate.

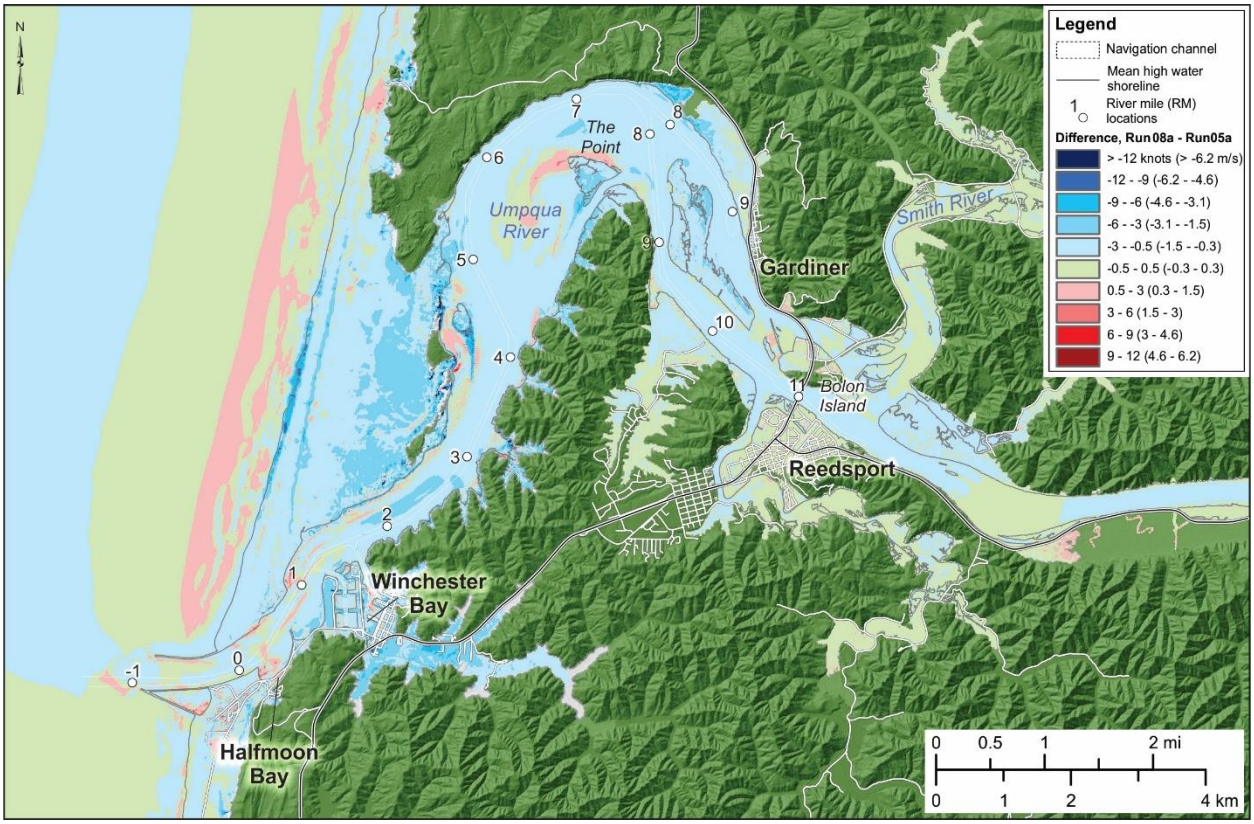

The collision between the tidal and tsunami currents at the Umpqua River mouth (e.g., **Figure 15**) suggests that the ebb scenario is particularly dangerous for boats of all sizes. **Figure 18** and **Figure 19** present time series information of tsunami currents and water levels for two sites in the Umpqua Estuary: landward of the river mouth (station 5 at RM0) and near The Point (~station 13 at RM8), station locations are identified in **Figure 4**). Unlike our findings at the mouth of the Columbia River (Allan and others, 2018b), time series data from the Umpqua indicate there is very little difference in the tsunami current velocities associated with ebb and flood conditions. This is consistent with our observations at Coos Bay (Allan and others, 2020). However, once the first wave has passed, current processes become more complex at the mouth as subsequent incoming tsunami waves interact with preceding tsunamis (i.e., reflection), offshore directed flows during the drawdown and with strong outgoing tides. Our simulations indicate that ebb currents become especially dominant after several hours (e.g., t = 2.5 and t = ~3.5 hours; **Figure 18**, top). These results contrast strongly with the simulated water levels, which clearly indicate that a tsunami arriving at flood tide consistently produces the highest generated water levels during the initial 4 hours of tsunami activity (**Figure 18**, bottom). However, our simulations indicate that after 4

hours, the ebb tide plus tsunami produces the highest water levels (not shown in the figure). However, by this stage the tsunami water levels are significantly reduced (~60%) when compared with the first 4 hours.

Figure 18. Time series for Run05a (flood) and Run06a (ebb) showing the modeled *(top) u* and *v* tsunami currents and *(bottom)* water levels at water level station 5 located at the mouth of the Umpqua Estuary simulated on an average river flow. Note: positive *u* indicates eastward directed currents, whereas negative *u* denotes westward directed currents; positive *v* indicates northward directed currents, whereas negative *v* denotes southward directed currents. Note also how rapidly currents reverse direction and water levels change in the first few hours.

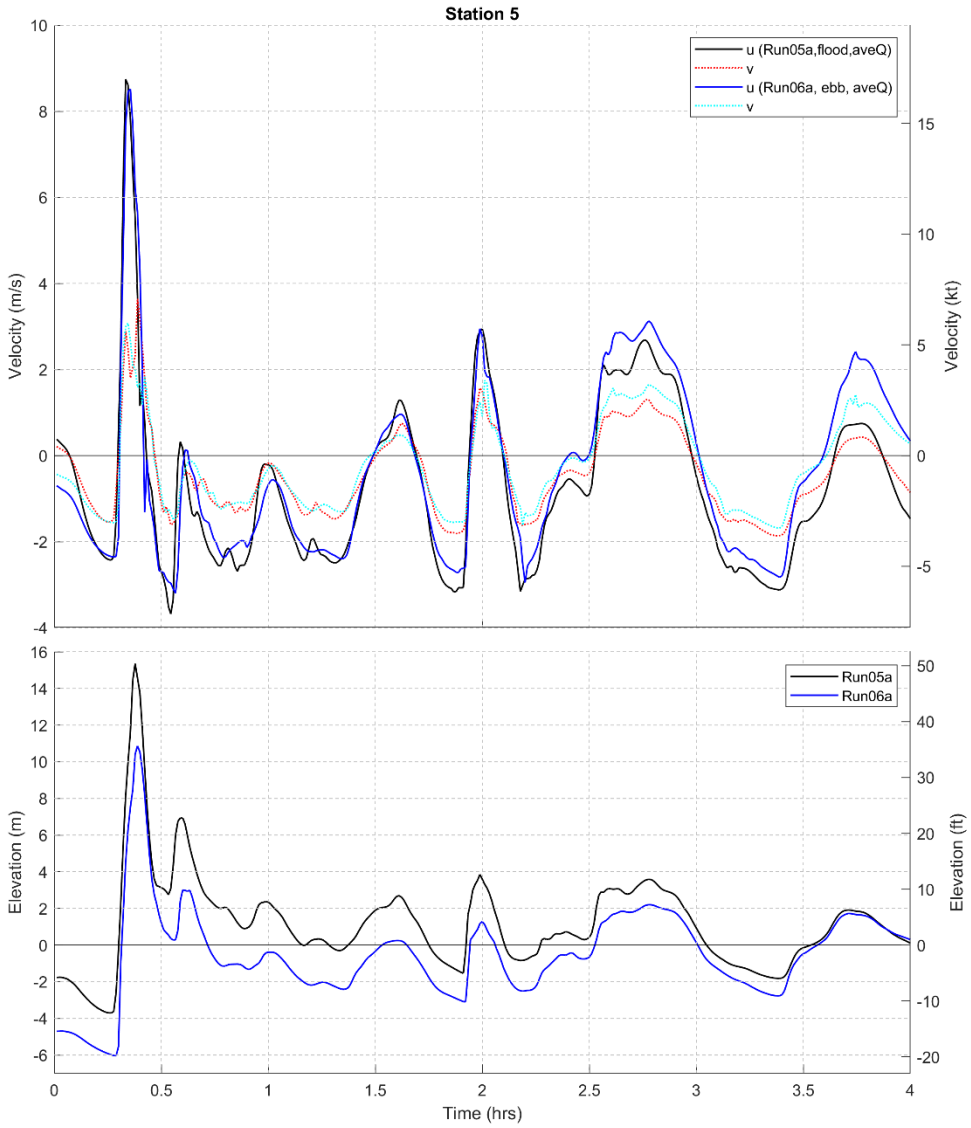

Further upriver at RM8, it is evident from **Figure 19** that the XXL1 tsunami has lost a considerable amount of energy, with the maximum tsunami wave height now having decreased to ~2 m (6 ft; **Figure 19**, bottom); the difference between flood and ebb conditions are even more apparent here. Overall, our findings indicate that the flood scenario continues to produce the strongest current velocities. Differences

between the Umpqua and Coos Bay sites and the Columbia River are likely due to a smaller tidal prism (tidal volume), highly irregular (meandering) channel geometry and morphology which imposes greater attenuation effects, shallower bathymetry, and possibly lower river discharge. We find similar patterns characterizing the other two earthquake scenarios modeled in this study (L1 and AKMax).

Figure 19. Time series for Run05a (flood) and Run06a (ebb) showing the modeled *(top) u* and *v* tsunami currents and *(bottom)* water levels at water level station 13 located near Reedsport simulated on an average river flow. Note: positive *u* indicates eastward directed currents, while negative *u* denotes westward directed currents; positive *v* indicates northward directed currents, while negative *v* denotes southward directed currents. Note also how rapidly currents reverse direction and water levels change in the first few hours.

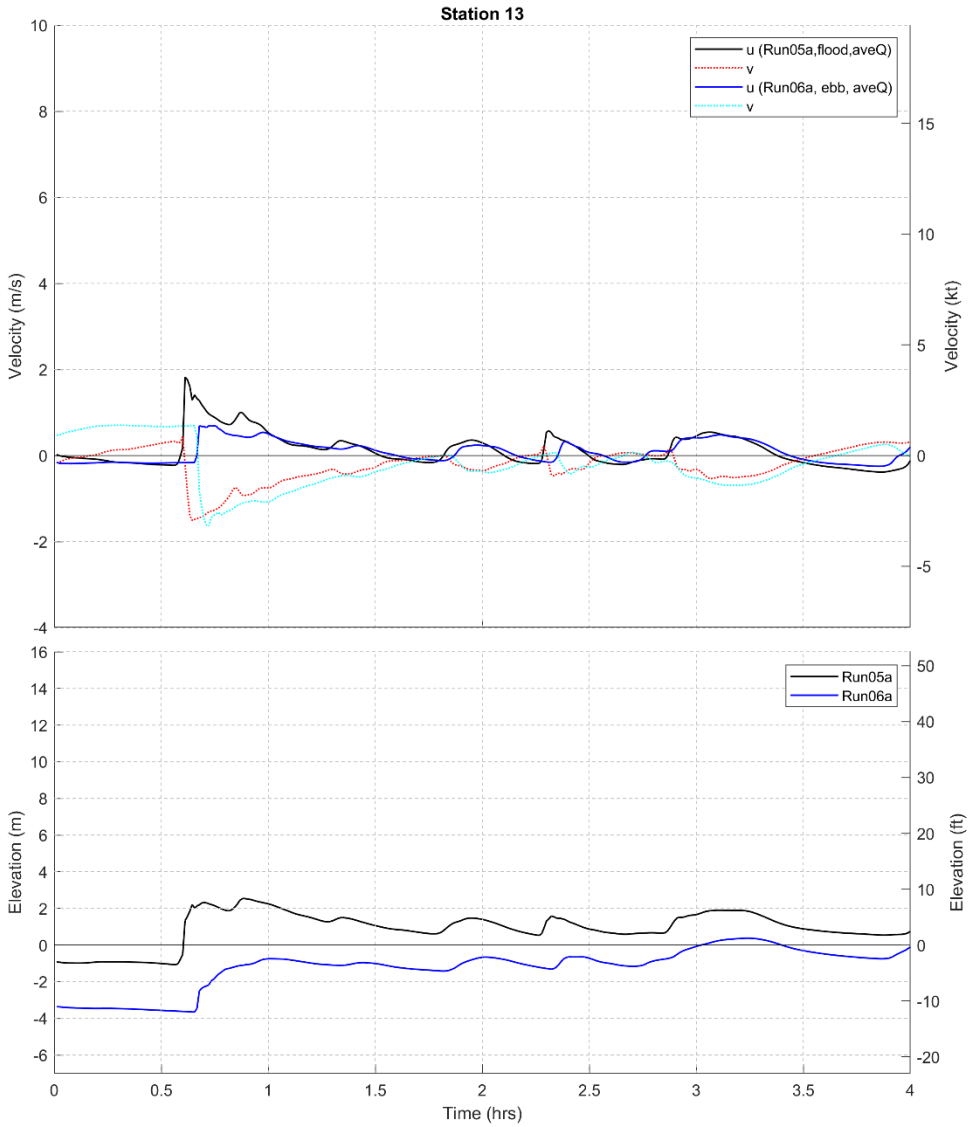

4.3 Wave Arrival Times

Knowledge of tsunami wave arrival times is vital to both terrestrial and maritime evacuation planning, since arrival times determine how much time the public will have to respond. In defining the tsunami arrival times along the Umpqua Estuary, we examined water levels through time series for select stations within the system, the locations of which are presented in **Figure 4**. Tsunami wave arrivals were defined for the dynamic tide simulations and were based on three criteria:

1. An initial wave arrival time, which reflects the moment at which the water level begins to depart from the normal background tidal signal
2. The time associated with the peak water level for the first wave
3. The time associated with the highest water level, regardless of which wave

The reason for the latter is because, although the first wave generally produces the highest water level, at a number of upriver sites, the maximum water level occurs much later.

4.3.1 Local Cascadia tsunami wave arrival times

Figure 20 presents the XXL1 wave arrival times (after earthquake shaking starts) for select sites along the Umpqua Estuary, and **Figure 21** shows an ensemble of the maximum tsunami water levels determined from the various simulations along the length of the navigation channel. A detailed description of the final ensemble maps is provided in Section 5. Included in **Figure 21** are the expected wave arrival times at some locations along the river.

As can be seen in **Figure 20** and **Figure 21**, the largest tsunami waves are concentrated at the mouth of the estuary, where, depending on the tide, the tsunami waves reach ~10–14.5 m (33–48 ft) in height. Included in **Figure 21** is the Run01c simulation (black line) that reflects a static (fixed) tide and assumes no frictional effects (i.e., Manning's n=0). This scenario produces a larger tsunami (~16 m; 53 ft). Run01c is akin to the original modeling of the coast, but now using an updated DEM. While Run01c is reasonable for use in evacuation planning on land, it is not ideal for maritime planning where nonlinear interactions between tides, river flow and tsunami occur. Hence, Run01c is included for comparative purposes to demonstrate how different the results look when conditions closer to reality are considered.

Between the mouth (~RM-1) and RM2, the tsunami water levels decrease significantly (**Figure 21**). Much of this effect can be attributed to the overall geomorphology of the river channel, along with the broad region of generally lower ground elevations that comprises the north Umpqua Spit. This is further aided by an abrupt change in channel orientation, from east-west at the mouth, to more north-south within the lower estuary. Combined, these effects allow much of the tsunami energy to be dispersed over a large area. Additional effects such as bathymetric shallowing dissipate more of the tsunami energy. These effects contribute to a considerable amount of energy loss within the first 8 km (five miles) of the navigation channel, such that by the time it reaches "The Point", the tsunami is largely a 2 m (6 ft) high bore (**Figure 20**). A second tsunami wave enters the estuary ~34 minutes after the start of earthquake shaking.

Between RM5 and RM11 (i.e., just west of The Point to Reedsport) the maximum tsunami water levels continue to decrease in height, dropping from ~1.6 m high (5.2 ft) to ~1 m (3 ft) at the Highway 101 bridge between Reedsport and Bolon Island. Our results also confirm that a tsunami arriving on a flood tidal regime (Run05a) produces the farthest upriver penetration of the tsunami, extending well up the Umpqua and Smith rivers (not shown). Finally, flatlining of the tsunami water levels upstream of ~RM4 (**Figure 21**, Run06a, Run07a, and Run08a) is due to nonlinear interactions between the tide and tsunami that results in attenuation (loss of energy) of the tsunami.

Figure 20. Tsunami wave arrival times defined for XXL1 (local) for specific locations along the Umpqua Estuary. Times reported are in minutes. Red numbers correspond to the initial wave arrival (the point at which the water level begins to depart from normal), whereas bold black numbers reflect the time at which the maximum water level occurs. Light black numbers are river miles. Background image reflects the integration of the maximum water levels determined from all XXL1 model simulations to form an "ensemble" result of maximum water levels. Example water level time history plot (inset) is for station 5 (RM0), near Halfmoon Bay.

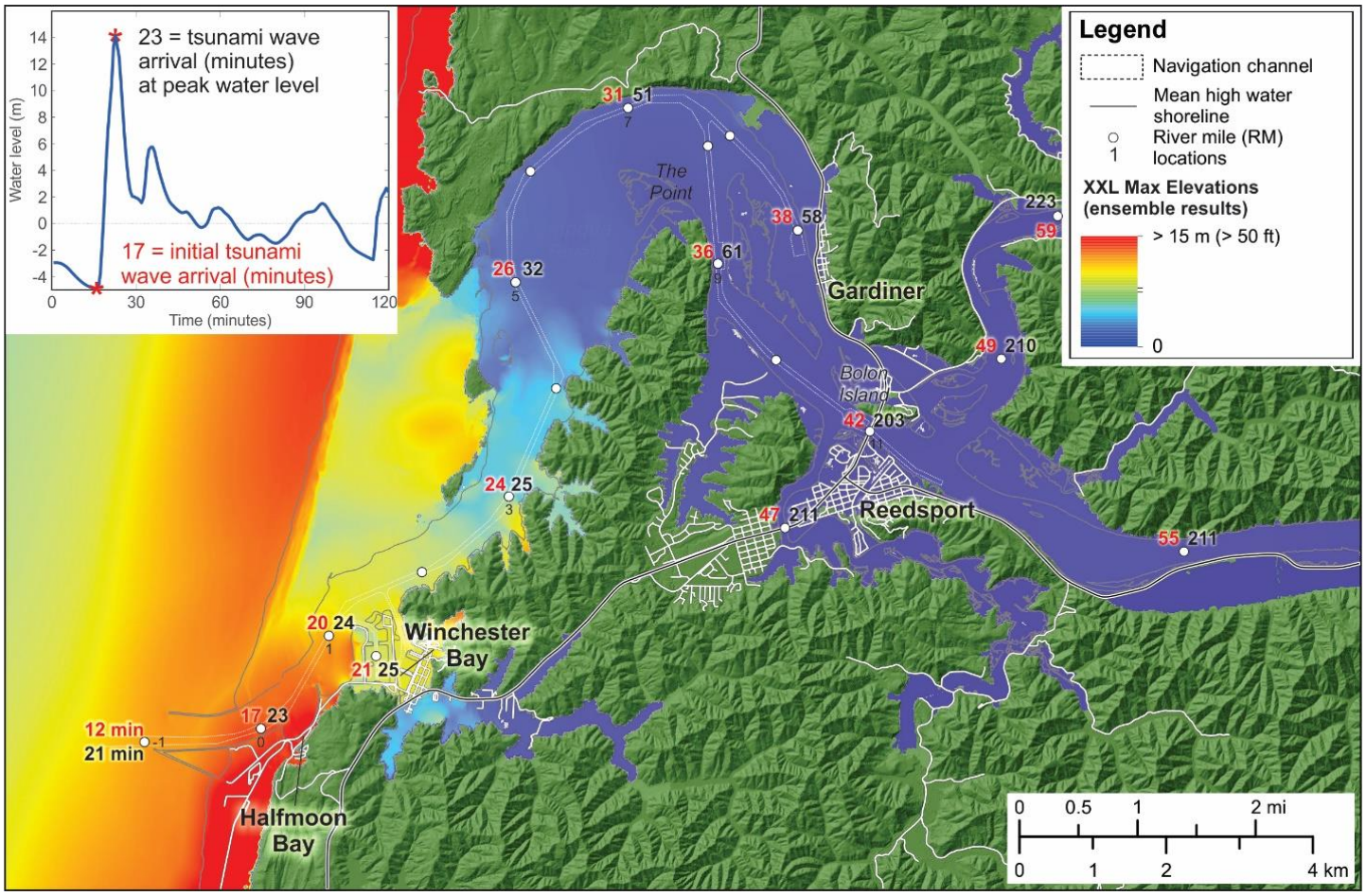

Figure 21. Maximum tsunami water levels interpolated along the Umpqua Estuary navigation channel for various XXL1 (local) simulations. Gray shading covers the spectrum of responses associated with various tidal stages modeled using an average river flow. RM is river mile.

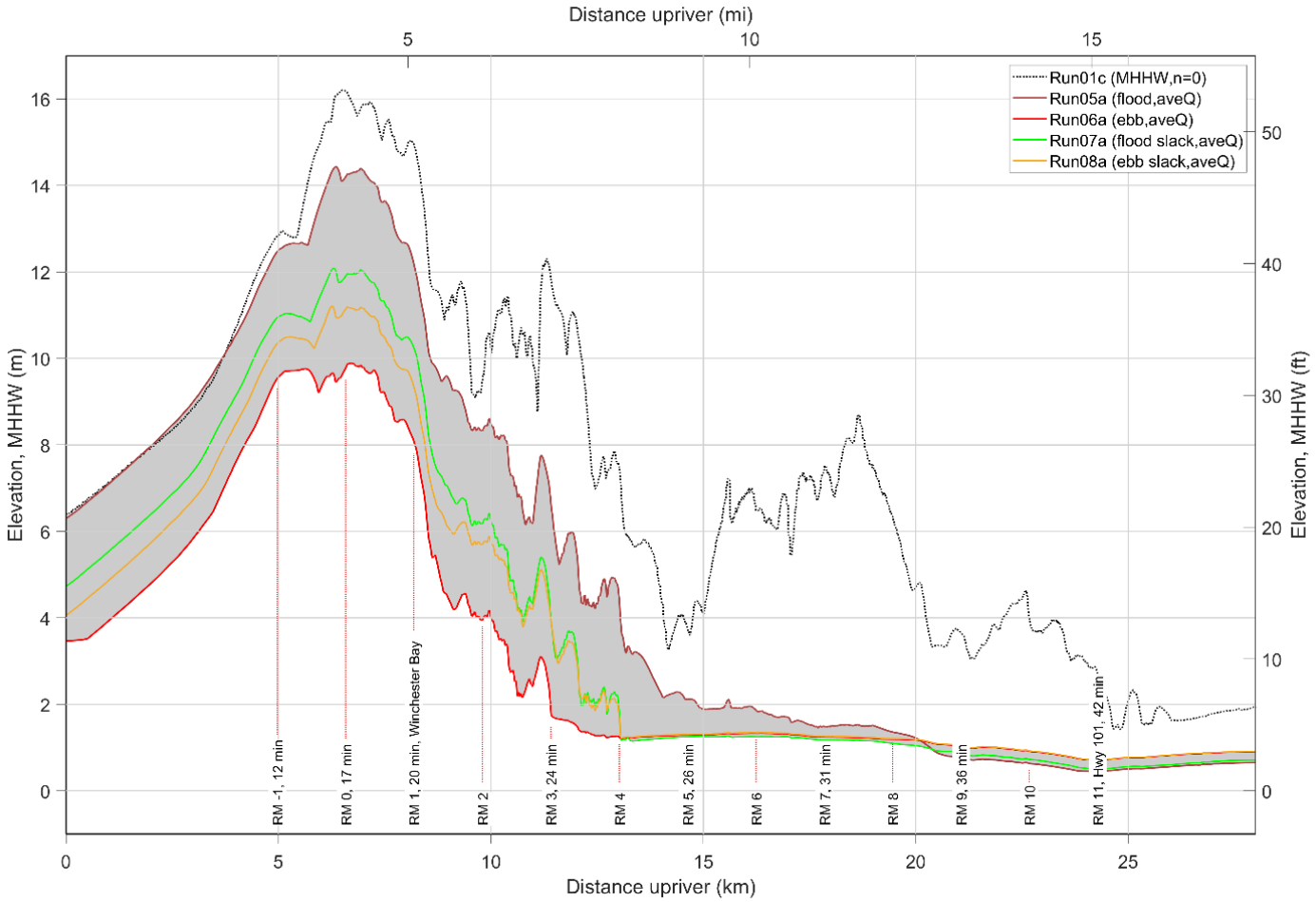

The initial tsunami wave arrives at the mouth of the Umpqua River ~12 minutes after the start of earthquake shaking, and the peak wave arrives some 9 minutes later — 21 minutes following the onset of shaking (**Figure 20**). All times shown in Figure 21 are relative to the start of earthquake shaking. Initial wave arrivals at Halfmoon Bay and Winchester Bay are 17 and 21 minutes, and the wave peak arrives at 23 and 25 minutes respectively. Between RM4 and RM9, the tsunami wave slows, reaching the sites ~32 and 61 minutes respectively. Changes in water levels at Reedsport begin to occur (initial tsunami arrival) at ~42 minutes, and, although the first wave peak reaches Reedsport ~66 minutes after the earthquake occurred, the maximum tsunami water level occurs over 3.6 hours later. This last response reflects a later tsunami wave arrival (**Figure 20** and **Figure 22**).

To better understand the timing of the tsunami wave sequence travel and arrival at sites upriver from the estuary mouth, we performed a wavelet analysis[7] (e.g., Torrence and Compo, 1998) of the tsunami frequency bands for selected sites along the Umpqua Estuary. This approach allows for further assessment of differences in the energy within the tsunami time series (the time-varying frequency content of the tsunami signal), allowing us to more definitively track the tsunami as it travels. As noted by Torrence and Compo (1998), converting a time series of water levels into time-frequency space allows one to determine the dominant modes of energy variability and, further, how those modes change over time. Essentially, the approach allows one to track the dominant energy signal of the tsunami as it propagates upriver.

Figure 22 presents the results of the wavelet analysis for two sites in the Umpqua Estuary: Winchester Bay (RM1, station 6) and Reedsport (RM11, station 16). The plots indicate that most of the energy in the tsunami signal is concentrated in the tsunami band for periods <=1 hours (the y-axis), with some energy also present at both higher and lower frequencies. The change in the tsunami power over time is captured on the x-axis (time in hours), which shows the signal over 24 hours (the length of the model simulation). The shaded regions on either end (shaped like the keel of a boat) indicate the "cone of influence (COI)," where edge effects become important and errors are introduced from the analyses. The latter occurs because the approach assumes the time series is cyclic. As a result, below the COI line, the results are not reliable.

At Winchester Bay, the initial peak signal in the time domain occurs at ~21 minutes and is within the range of the peak wave arrival time at RM1 presented in **Figure 20**. Additional peaks occur at 2, 2.6, and 3.5 hours (**Figure 22**) as later arriving tsunami waves reach the site; the time between tsunami peaks averages ~29 minutes. Of importance, the dominant energy signal at Winchester Bay is strongest during the first five hours after the earthquake, with the energy decreasing over time. Much of this energy is expended by hour 10 and becomes negligible by hour 15; see later discussion on tsunami currents. Near Reedsport, the peak signal occurs ~ 49 minutes after the earthquake, and there is significantly less energy in the signal compared with the Winchester Bay station.

Finally, the dominant energy band identified with a period of ~1 hour in **Figure 22** reflects resonance activity that is observed within the estuary and on the shelf offshore of the river mouth. This mode of activity is likely due to the development of edge waves (gravity waves) excited by the subsidence (as seiches) and the ensuing tsunami. This resonance is present at the majority of the water level stations and spans the entire simulation period. Animations of the tsunami striking the area demonstrated periodic peaks and troughs as these edge waves arrive from both the south and north as free waves. Analyses of the dominant signals at the Columbia River by Allan and others (2018b) did not reveal this level of resonance there, which suggests that there are unique characteristics about the shelf morphology adjacent to the Umpqua River that may be contributing to the resonance.

[7] https://noc.ac.uk/business/marine-data-products/cross-wavelet-wavelet-coherence-toolbox-matlab

Figure 22. Wavelet analysis of the XXL1 (local, flood tide, Run05a) tsunami water level time series at Winchester Bay (RM1) and near Reedsport. Hot colors indicate significant energy; shaded regions on either end indicate the "cone of influence" (COI), where edge effects become important (so should be discarded); solid contour is the 95% confidence level. Time (x-axis) in hours is after the earthquake.

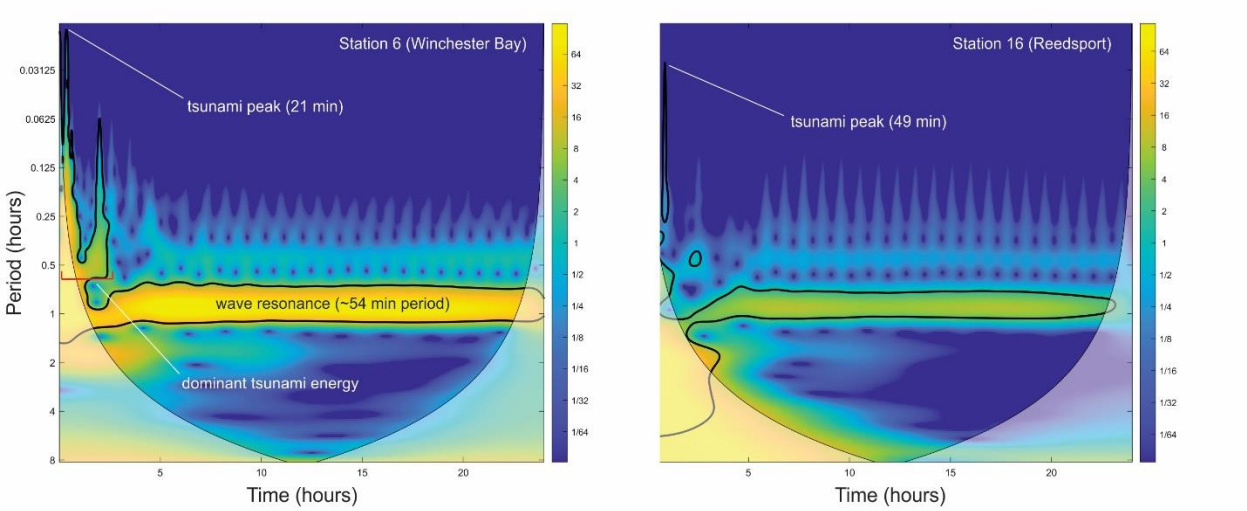

4.3.2 Distant (AKMax) tsunami wave arrival times

The AKMax distant tsunami reaches the Umpqua mouth ~3 hours, 50 minutes after the earthquake, with the maximum wave height occurring eight minutes later after the water levels began to rise (**Figure 23**). Within the lower estuary, the peak tsunami wave typically arrives ~6–9 minutes after the wave begins to arrive. Longer wave arrival times for the maximum wave are evident farther up the estuary (e.g., ~7 hours after the earthquake at Reedsport) that are caused by later arriving tsunami waves accompanied by the different tidal stages. **Figure 24** shows the maximum tsunami water levels for the various simulations along the length of the navigation channel. Included in the figure are the expected wave arrival times at various locations along the river channel. We also include results from the 1964 Alaska tsunami (solid blue line) because this event represents the largest distant event to have impacted the Oregon coast in modern history.

As can be seen in **Figure 24**, the largest tsunami waves are concentrated at the estuary mouth, where the eastern Aleutian tsunami reaches ~0.9 m (3 ft) to 3.8 m (12.5 ft) in height (relative to MHHW), depending on the tidal stage. Between the mouth and RM4, there is an appreciable decrease in the tsunami water levels, which is similar to what we saw for the local XXL1 scenario (**Figure 21**). This is caused by changes in the channel configuration and morphology, shallowing up the estuary, and tsunami dispersion effects. The nonlinear interaction between the tsunami, tidal stage, and tidal hydraulics is especially noticeable for distant tsunamis and is characterized by the significant differences in simulated water levels observed between flood and ebb. As can be seen in **Figure 24**, a distant tsunami arriving at ebb tide is suppressed resulting in a peak tsunami of no more than 0.9 m (6 ft), compared to the same scenario occurring at flood tide. This is entirely due to the effects of the outgoing tide, which effectively negates the tsunami confining its effects only to the area near the river mouth. Upriver of RM4, maximum water levels decrease significantly. Accordingly, these data strongly suggest that any distant tsunami arriving during an ebb tide is unlikely to cause significant flooding or accompanying damage.

Figure 23. Tsunami arrival times defined for AKMax (distant) for discrete locations along the Umpqua Estuary. Times reported are in minutes and are relative to the initial (3 hr, 50 min) wave arrival at the mouth of the Umpqua River. Red numbers correspond to the initial wave arrival (the point at which the water level begins to depart from normal), whereas bold black numbers reflect the time at which the maximum wave arrives. Background image reflects the integration of the maximum water levels determined from all AKMax model simulations to form an "ensemble" result of maximum water levels. Example water level time history plot is for virtual water station 5 (RM0) near Halfmoon Bay.

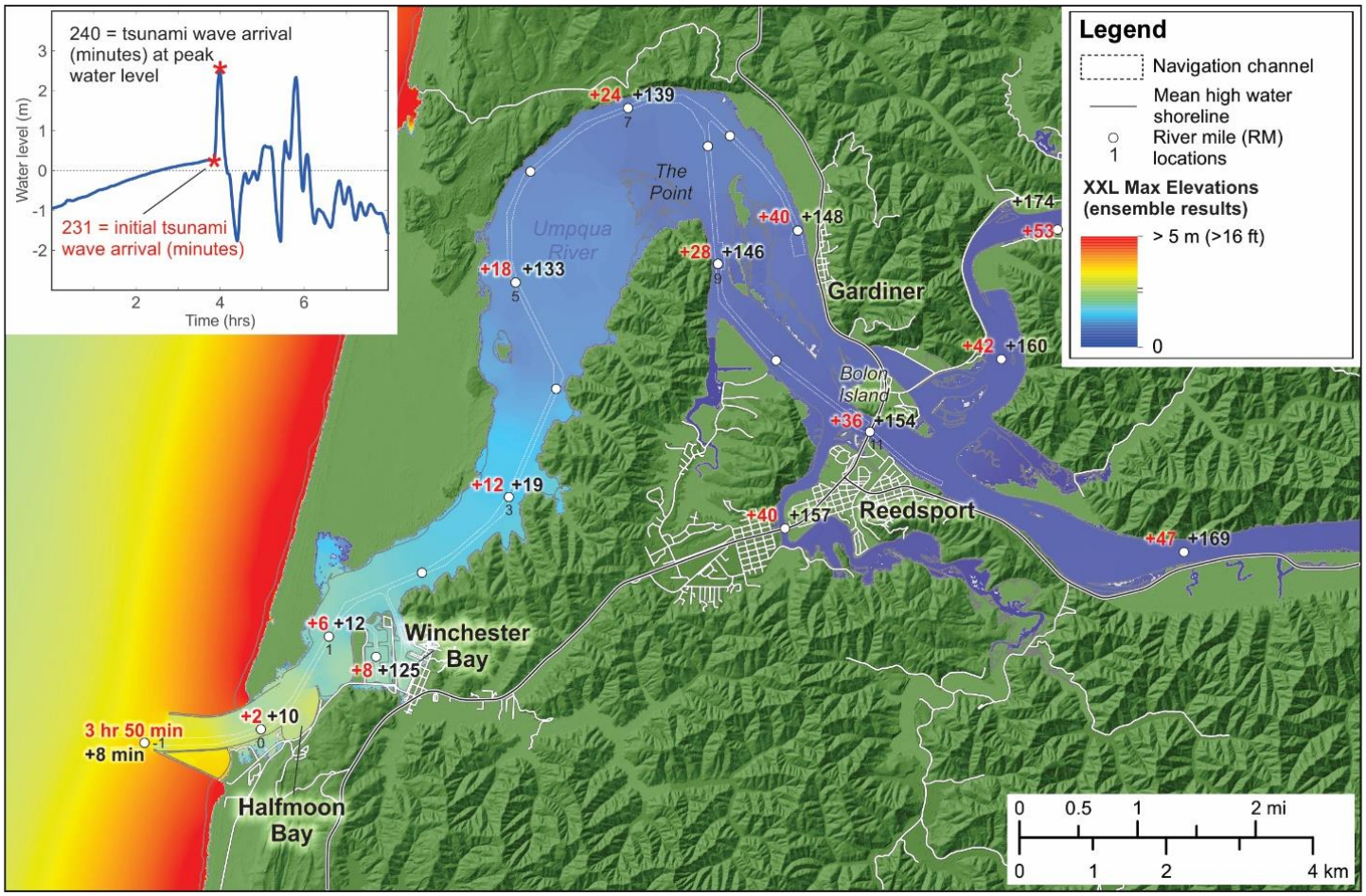

Figure 24. Maximum tsunami water levels interpolated along the Umpqua Estuary navigation channel for various AKMax simulations. Included in the plot are the expected wave arrival times (after RM-1, wave arrivals reference time after 3 hours, 50 minutes). Gray shading covers the spectrum of responses associated with various tidal stages modeled using an average river flow. RM is river mile. Run01c is the simulation using a static MHHW tide and zero friction.

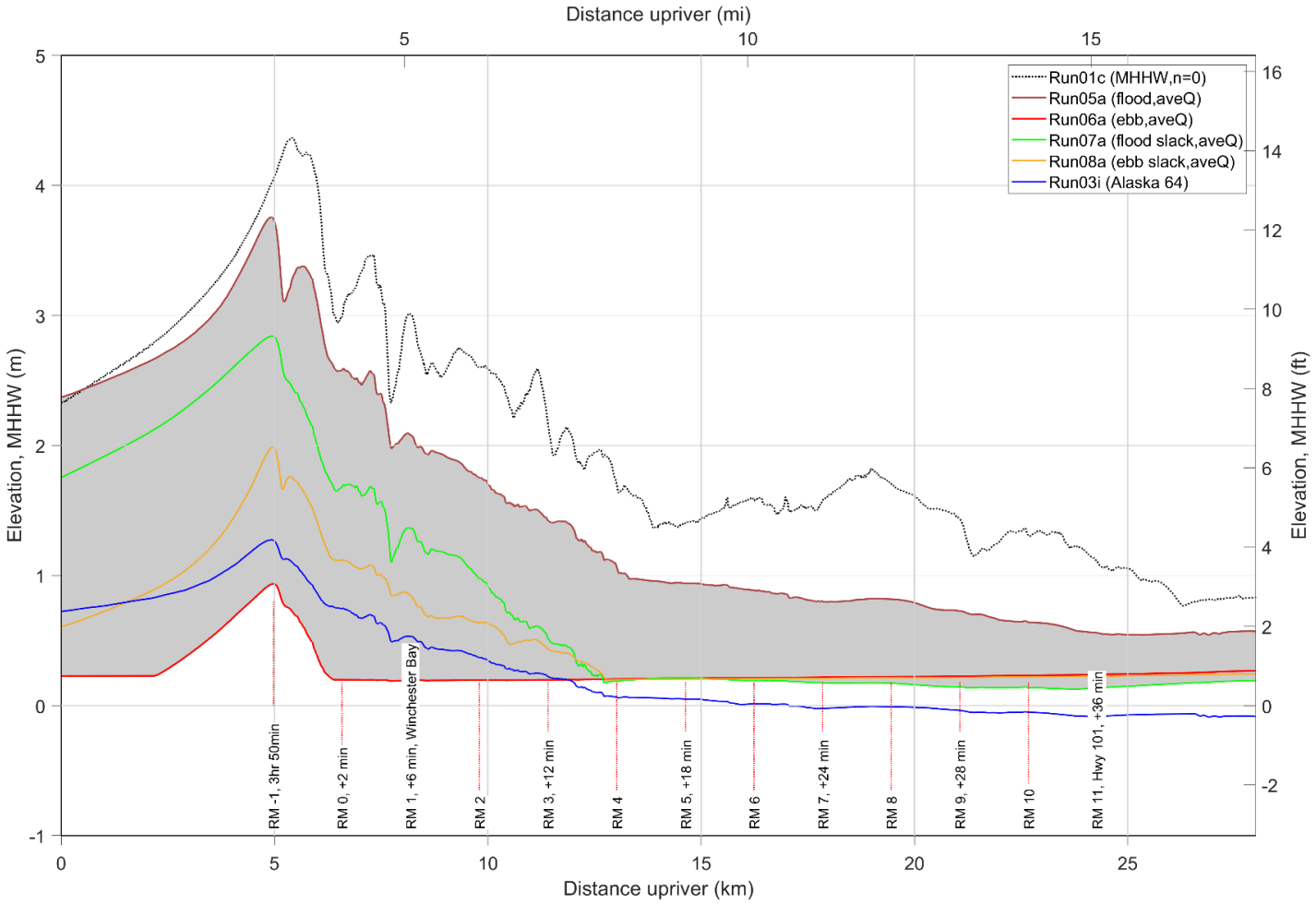

As noted previously, the initial tsunami reaches the Umpqua River mouth in ~3 hours, 50 minutes (**Figure 23** and **Figure 24**). The tsunami can be tracked up the Umpqua Estuary using wavelet analysis, as shown in **Figure 25.** At Winchester Bay, the tsunami may be identified by an initial peak, indicating the tsunami arrives at ~238 minutes after earthquake shaking begins. Several other peaks reflect later arriving waves. Overall, the tsunami persists for at least 10 hours (highlighted by the bright yellow shading at a period of two hours in **Figure 25**). The time between hour 10 and 15 coincides with low (ebb) tide such that the incoming tsunami waves are effectively dampened. However, with the transition to high tide at 15 hours, the tsunami is once again able to penetrate up the estuary. This effect is even apparent at station #16 located near Reedsport. Nevertheless, by hour 15, there is effectively little energy left and the distant tsunami can be effectively ignored upriver of this station.

Figure 25. Wavelet analysis of the AKMax (distant, flood tide, Run05a) tsunami water levels time series at Winchester Bay (RM1) and near Reedsport. Hot colors indicate significant energy. Shaded regions on either end indicate the COI, where edge effects become important. Solid contour is the 95% confidence level. Time (x-axis) in hours is after the earthquake.

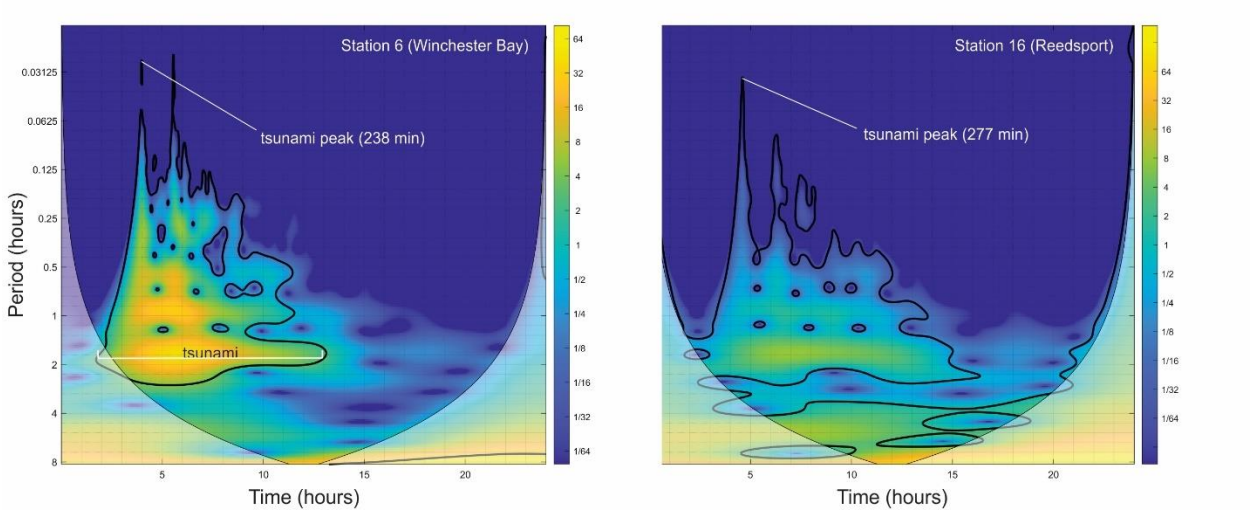

5.0 ENSEMBLE MODEL RESULTS

Due to uncertainties in the timing of a local or distant tsunami, coincident with different tidal stages, we derive "ensemble" modeling results for each earthquake source. The approach effectively combines maximum water levels, currents, vortices, and minimum water levels for each scenario into a single merged raster for each of these parameters. This allows us to incorporate the uncertainty characterized by the range of tsunami/tide/flow combinations, providing a more conservative model estimate of the tsunami effect for incorporation into appropriate response guidance. To generate the ensemble product, we produced individual rasters for each model simulation in Esri ArcGIS® and for each of the previously mentioned parameters. We then created the ensemble raster by using the ArcGIS "mosaic to new raster" tool with the maximum value defined for each grid cell. For the minimum flow depth, we used the minimum value assigned to the grid cell.

5.1.1 Local (XXL1 and L1) tsunami ensemble results

5.1.1.1 XXL1 and L1 water levels

Figure 26 presents the merged maximum water levels for both an XXL1 and an L1 local event. The plots demonstrate two contrasting responses: the extreme water levels that will be experienced along the open coast (hot colors), and the generally much lower water levels (cool colors) upriver of The Point. Between these two areas is a large region in which the water levels are expected to be highly variable (varying shades of yellow to red), with localized peaks at Winchester Bay (~8.8 m in the harbor; 29 ft) decreasing to 1.5 m (5 ft) at The Point, relative to MHHW for an XXL1 size event. Although high tsunami water levels will also be experienced during the L1 event, it is evident from **Figure 26** (*bottom*) that the effects are not as extreme as those of the XXL1 event. Overall, L1 water levels tend to be ~3.1 m (10 ft) in the channel at Winchester Bay, before decreasing to ~1.6 m (5.2 ft) near The Point. Both figures highlight several sites at the shore where tsunami flooding (and hence damage) is likely to be extreme (red colors), including Winchester Bay and Halfmoon Bay. Catastrophic conditions will characterize the XXL1 scenario, especially at Winchester Bay. Damaging waves and strong currents will affect much of the area within the lower Umpqua Estuary, especially between the mouth and RM5 (**Figure 26**). For the L1 scenario, the impacts are generally less severe, with the strongest velocities and greatest potential for damage concentrated nearest to the estuary mouth.

Time series information for select stations along the river is presented in **Figure 27** (XXL1) and **Figure 28** (L1). These data have been truncated to span the first 12 hours of the simulations, providing improved insight into the variability and range of modeled water levels; the datum used is MHHW. Included in the figure are the simulated tsunami waves occurring on a flood (black line) and ebb (red line) tide. The gray shading in each plot defines the envelope (range) of variability from the combined suite of simulations. Apparent in the figures are differences in the maximum tsunami water levels, with the flood condition generally producing the highest tsunami waves, while the ebb condition highlights the role of lower tides and later arriving tsunami waves. In some later arriving waves, however, the variability of levels is not always bounded by these two phases, suggesting complex nonlinear interaction among river flow, tsunamis and tides. Differences in the heights of the simulated water levels are also more obvious between the maximum-considered XXL1 (**Figure 27**) and L1 (**Figure 28**) scenarios. This is a function of the amount of slip that occurs during the subduction zone earthquake. Both time series highlight the extreme peaks of the tsunami waves at the mouth (station 4), which decreases rapidly by the time the tsunami reaches RM7 (station 12), near The Point. At Reedsport (station 16), the XXL1 tsunami wave reflects an ~2-m (6-ft) high bore with a steep wave front. Water levels remain high for at least six hours before subsiding. At that point, the L1 bore is reduced to ~1 m (3 ft) high. However, as indicated previously, tsunami waves continue to impact the area for at least 10 to 15 hours after the event.

Figure 26. Ensemble model results of the maximum tsunami water levels generated by a XXL1 *(top)* and L1 *(bottom)* CSZ (local) earthquake. Cartoon showing water level time history and attributes is for virtual water station 5 (RM0) near Halfmoon Bay.

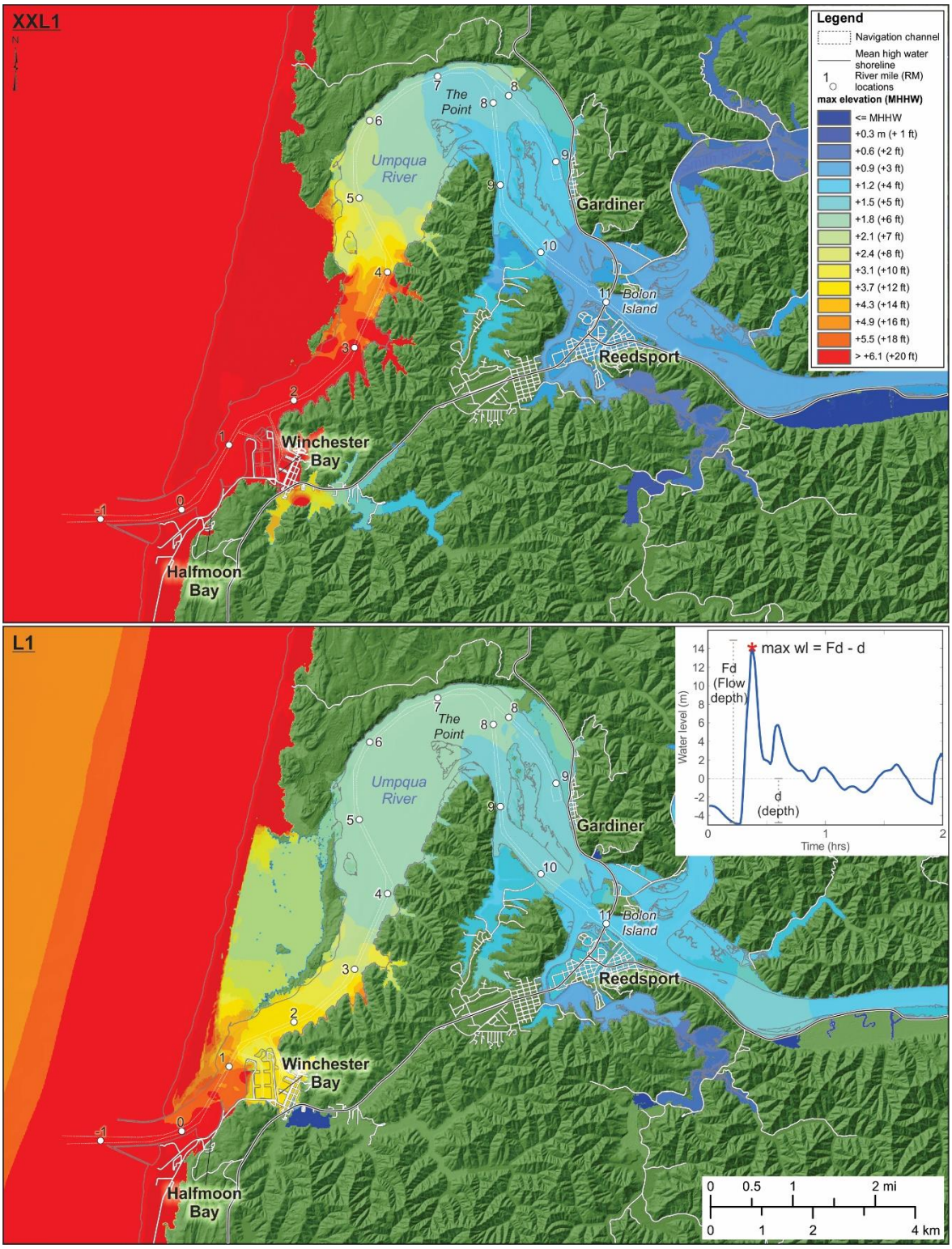

Figure 27. Time series showing the modeled water levels for two simulations of a CSZ tsunami (XXL1) traveling along the navigation channel from the Umpqua River mouth to Reedsport. Gray shading denotes the envelope of variability in the water levels from all simulations.

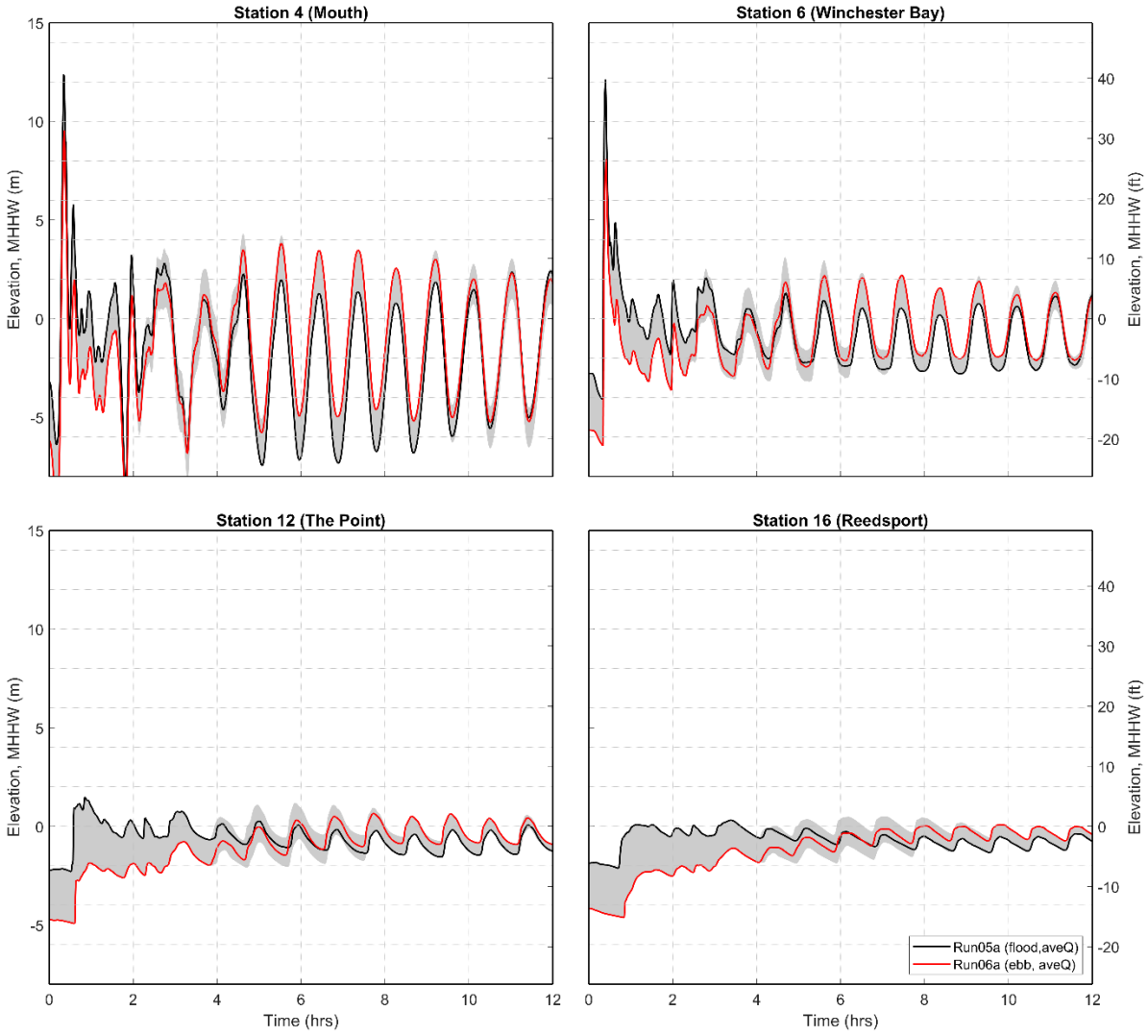

Figure 28. Time series showing the modeled water levels for two simulations of a CSZ tsunami (L1) traveling along the navigation channel from the Umpqua River mouth to Reedsport. Gray shading denotes the envelope of variability in the water levels from all simulations.

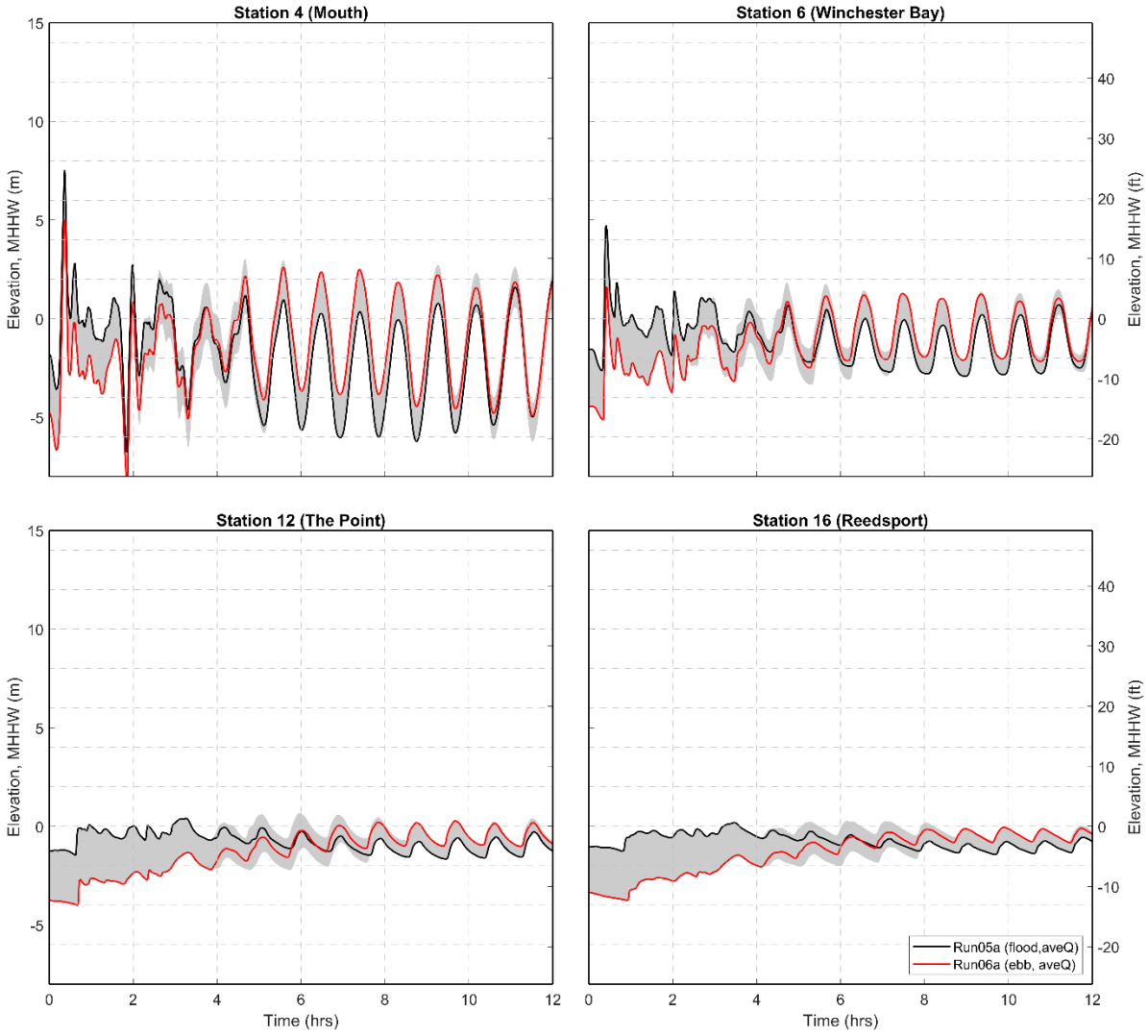

5.1.1.2 XXL1 and L1 tsunami currents

Figure 29 presents the modeled currents for the Umpqua Estuary. For the purposes of assisting with maritime guidance, we have binned the current velocities into five categories consistent with the work of Lynett and others (2014). As a reminder, they observed that current velocities exceeding 4.5 m/s (> 9 knots) were found to result in extreme damage to ports and harbors, while little to no damage was found to occur at velocities < 1.5 m/s (< 3 knots).

Modeling of the tsunami currents for an XXL1 event indicates catastrophic conditions will predominate across much of the lower estuary, with large tsunami waves and very strong currents prevalent between the mouth and just east of The Point (i.e., RM-1 to ~RM8, **Figure 29**, *top*). In this scenario, extreme currents (> 4.5 m/s; > 9 knots) will significantly affect Winchester Bay harbor, where damage is expected to be devastating. Farther upriver, near The Point (station 12, RM7), our simulations indicate that there is a notable change in the modeled current velocities (**Figure 29**). There, the XXL1 currents decrease from 3–4.5 m/s (6–9 knots) to 1.5–3 m/s (3–6 knots), with a further decrease in current velocity near Reedsport. As can be seen in **Figure 29** (*bottom*), simulated currents generated by the L1 scenario are not as severe as those produced by an XXL1 event. For the L1 scenario we find that extreme currents (> 4.5 m/s; >9 knots) will largely be concentrated near the estuary mouth and Halfmoon Bay, and along the navigation channel seaward of Winchester Bay (**Figure 29**, *bottom*) and within the entrance channel to the marina.

Differences in the simulated current velocities are most apparent when we compare the time series of modeled currents for both XXL1 (**Figure 30**) and L1 (**Figure 31**). As can be seen for both scenarios, strong currents dominate the mouth and Winchester Bay before decreasing in strength as the tsunami waves travel upriver. These changes are largely a function of frictional effects, but also of changes in channel configuration and the general shallowing along the estuary, which helps to dissipate the tsunami energy. At station 12, the XXL1 simulation indicates strong currents (~3 m/s; 6 knots) occur in the first hour of the event, before they fall below the 1.5 m/s (3 knots) velocity/damage threshold (**Figure 30**). At Reedsport, the strongest simulated currents during an XXL1 event occur briefly on a flood tide. Should the XXL1 event occur during an ebb tide, it is unlikely to produce damaging currents in the vicinity of the Reedsport docks. Similar patterns are observed for the L1 scenario. However for L1, the tsunami currents fall below the 1.5 m/s (3 knot) velocity/damage threshold upriver of The Point (**Figure 31**). This suggests that damaging effects from an L1 tsunami is likely to be minor to none at Reedsport. In summary, our simulations indicate that flood conditions allow greater upriver penetration of the tsunami and areas subject to strong currents.

Figure 29. Ensemble model results of the maximum tsunami currents generated by a *(top)* XXL1 and (*bottom)* L1 CSZ earthquake.

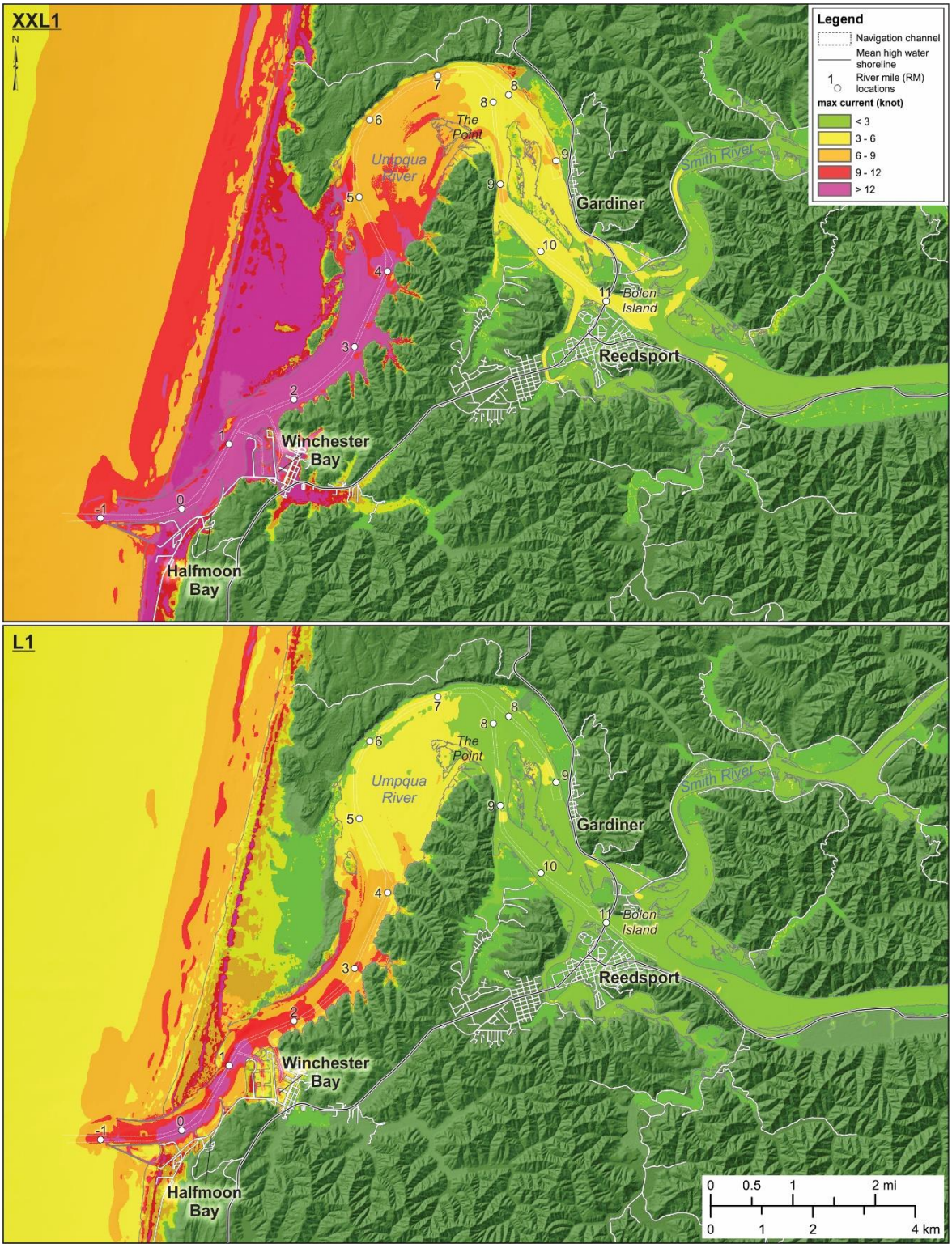

Figure 30. Time series showing the modeled currents generated for two simulations of a CSZ tsunami (XXL1) traveling along the navigation channel from the Umpqua River mouth to Reedsport. Gray shading denotes the envelope of variability in the tsunami currents from all simulations.

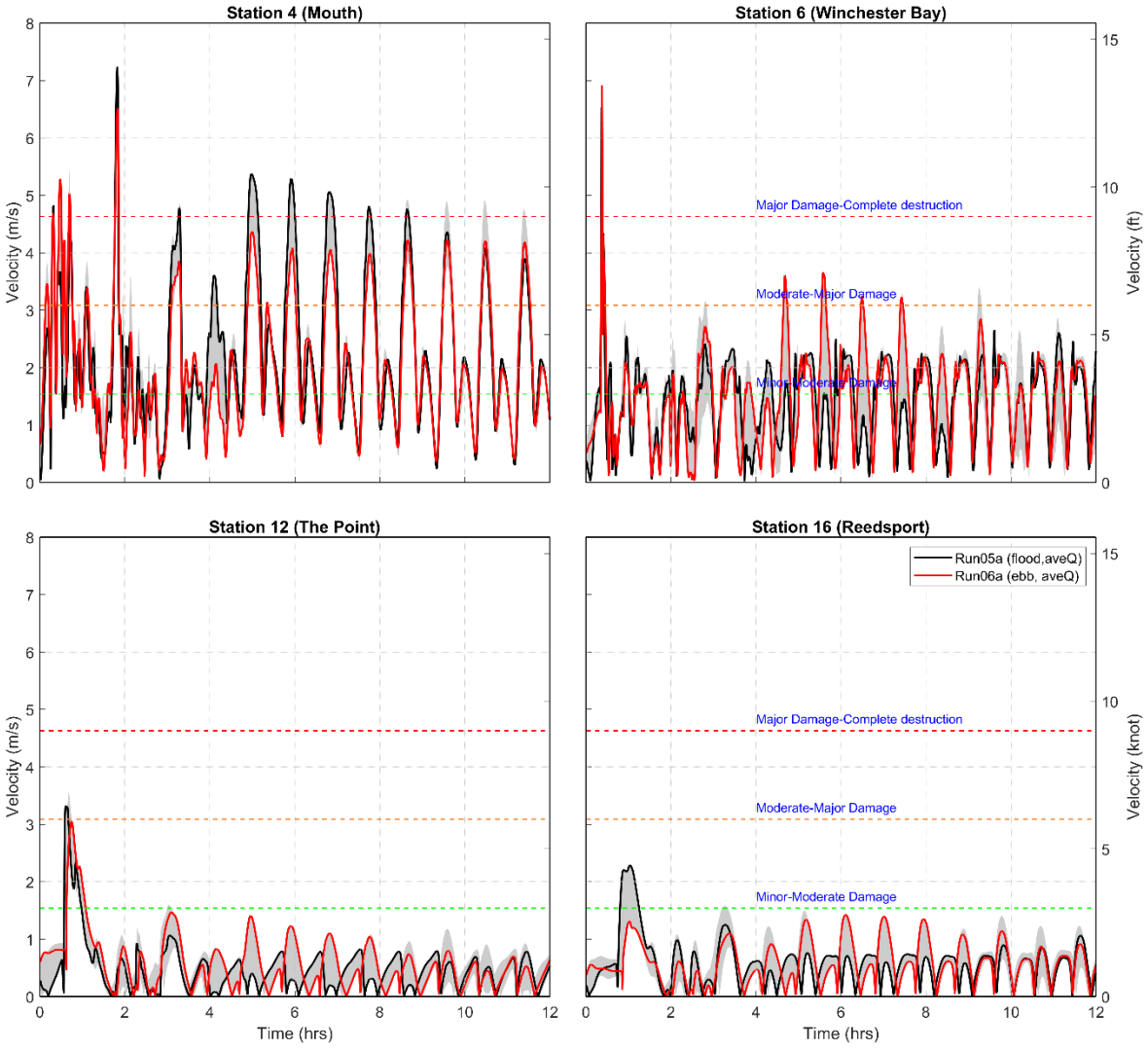

Figure 31. Time series showing the modeled currents generated for two simulations of a CSZ tsunami (L1) traveling along the navigation channel from the Umpqua River mouth to Reedsport. Gray shading denotes the envelope of variability in the tsunami currents from all simulations.

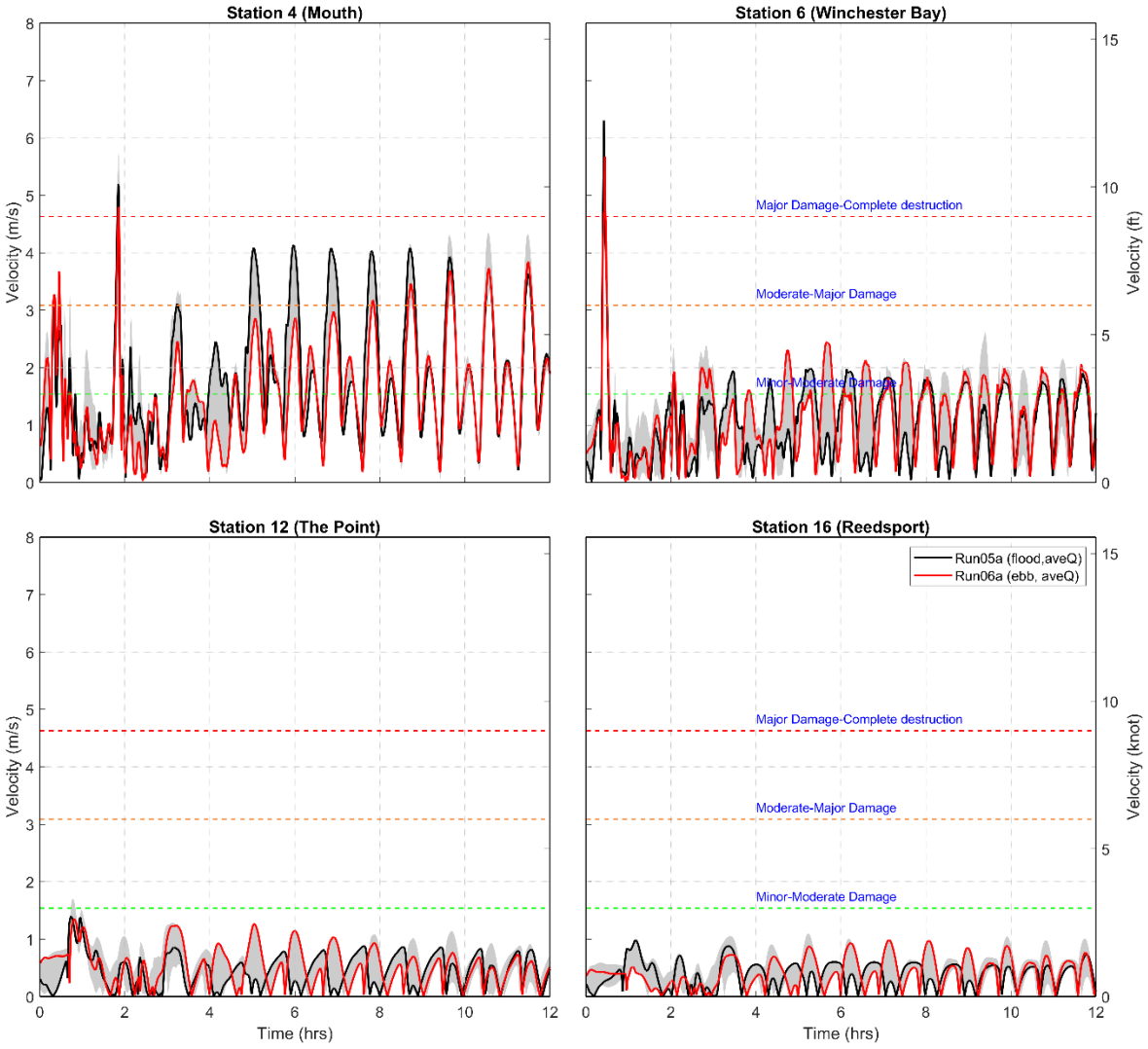

Knowing how long strong currents can be expected to persist following a CSZ earthquake is also important to mariners and emergency officials. Because performing such analyses is computationally demanding, developing ensembles of these types of results is not practical. Instead, we focus on evaluating the current durations for just the estuary and offshore region and the two most important model simulations: flood (Run05a) and ebb (Run06a) conditions. Our approach involves querying the full simulation data using a Fortran script to extract the first 12 hours of model data for every grid node; we ignored data after hour 12 because the tsunami is largely over by then. These data are subsequently processed in MathWorks MATLAB® and converted to Esri form using a python script. For our purposes, we use the following velocity thresholds to distinguish the duration of the currents: 1.5 m/s (3 knots), 3 m/s (6 knots), and 4.5 m/s (9 knots).

The duration of each of the current velocity bins — 1.5–3 m/s (3–6 knots) and 3–4.5 m/s (6 to 9 knots) — is presented in **Figure 32**. We have chosen not to include the results for currents > 4.5 m/s (9 knots) because their effect is confined entirely to the estuary mouth, west of Halfmoon Bay. Flood conditions are shown on the left side of the figure, and ebb conditions are on the right. Not surprisingly, currents of 1.5–3 m/s (3–6 knot) affect the entire estuary for at least one hour (**Figure 32**A). This pattern is repeated for the ebb scenario (**Figure 32**C). Tsunami-generated currents of 1.5–3 m/s (3–6 knots) are expected to persist for more than four hours in the lower estuary, between the mouth and Winchester Bay (dark purple colors). These flood currents dominate the area from Winchester Bay to ~RM2 for 2–3 hours. The patterns shown for the ebb scenario (**Figure 32**C) are broadly similar to the flood scenario, except that these currents persist over a larger portion of the estuary (mouth to ~RM4). Finally, currents in the 3–4.5 m/s (6–9 knots) range are comparable between flood (**Figure 32**B) and ebb (**Figure 32**D) conditions and are dominant in the mouth, where the currents persist for up to three hours.

Figure 32. Duration of CSZ XXL1 tsunami current velocities for *(left)* Run05a (flood tide scenario) and *(right)* Run06a (ebb tide scenario).

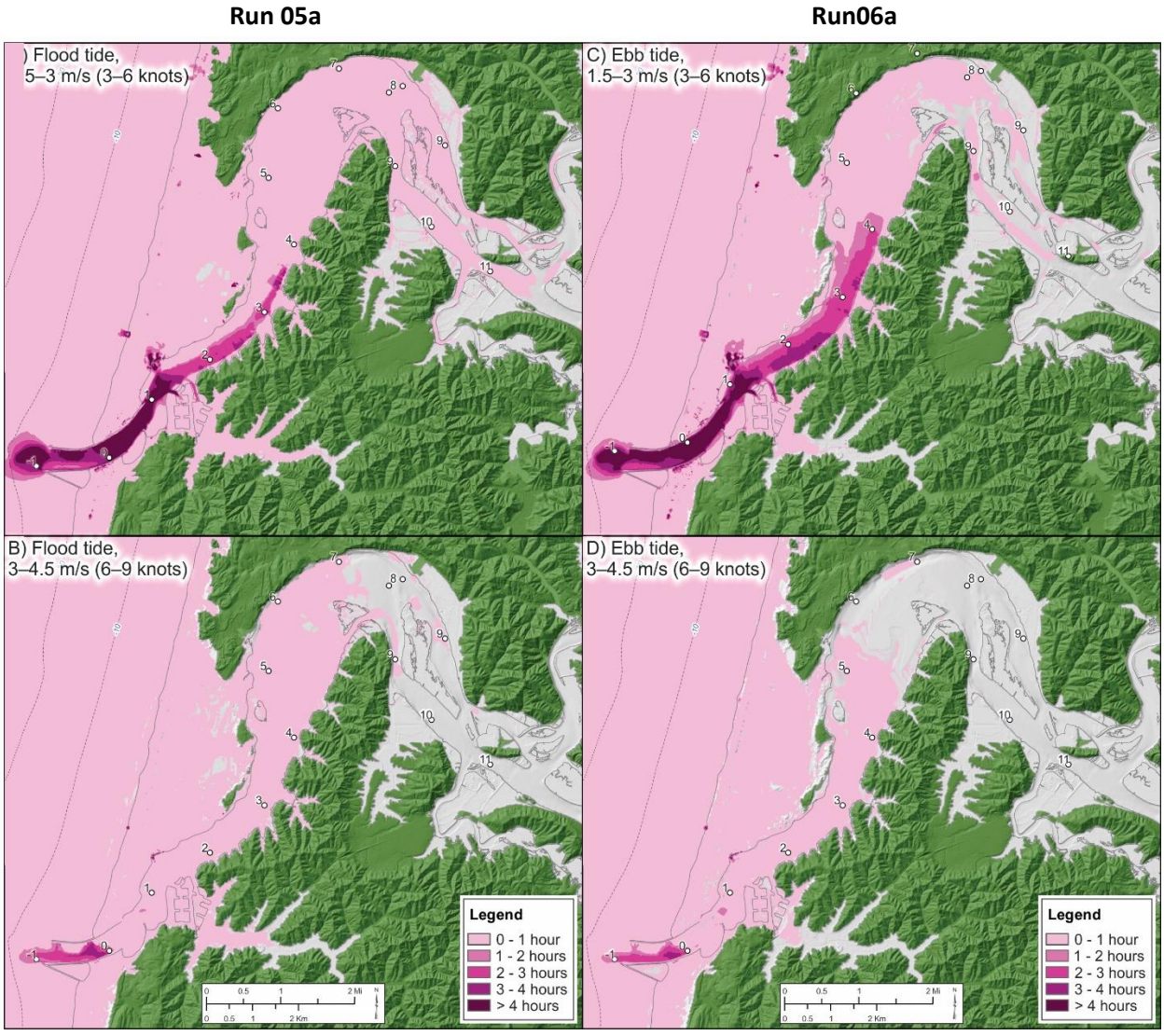

5.1.1.3 XXL1 and L1 vorticity

Vorticity, or rotation, of water forms gyres and whirlpools, which can affect maritime operations, particularly the ability of a vessel to maintain headway. Vorticity is defined as:

$$\text{Vorticity} = \left|\frac{\partial v}{\partial x} - \frac{\partial u}{\partial y}\right| \quad (2)$$

where ∂v is the change in north velocity, ∂u is the change in east velocity, ∂x is the change in distance east, and ∂y is the change in distance north. In general, values greater than 0.1 (0.01 units of 1/s = velocity changing 1 m/s over 100-m distance) are akin to very strong shear force on the water. **Figure 33** presents the calculated vorticity generated by both the XXL1 and L1 tsunamis. Our modeling reveals that the entire marina at Winchester Bay could experience strong rotation potential. Similar conditions can be observed under the L1 scenario. These results are probably due to the increased volume and flow of water into the marina and their corresponding interaction with various piers and wharfs, and the entrance breakwater. Our results indicate there is no rotation at the estuary mouth. This is likely due to the width of the estuary mouth, the relatively straight east-west jetties, the length of the jetty throat, and the absence of any additional structure on the jetties (e.g., groins) that could potentially disrupt flow and cause gyres to form.

Figure 33. Ensemble model results of the maximum vorticity generated by a *(top)* XXL1 and *(bottom)* L1 CSZ tsunami.

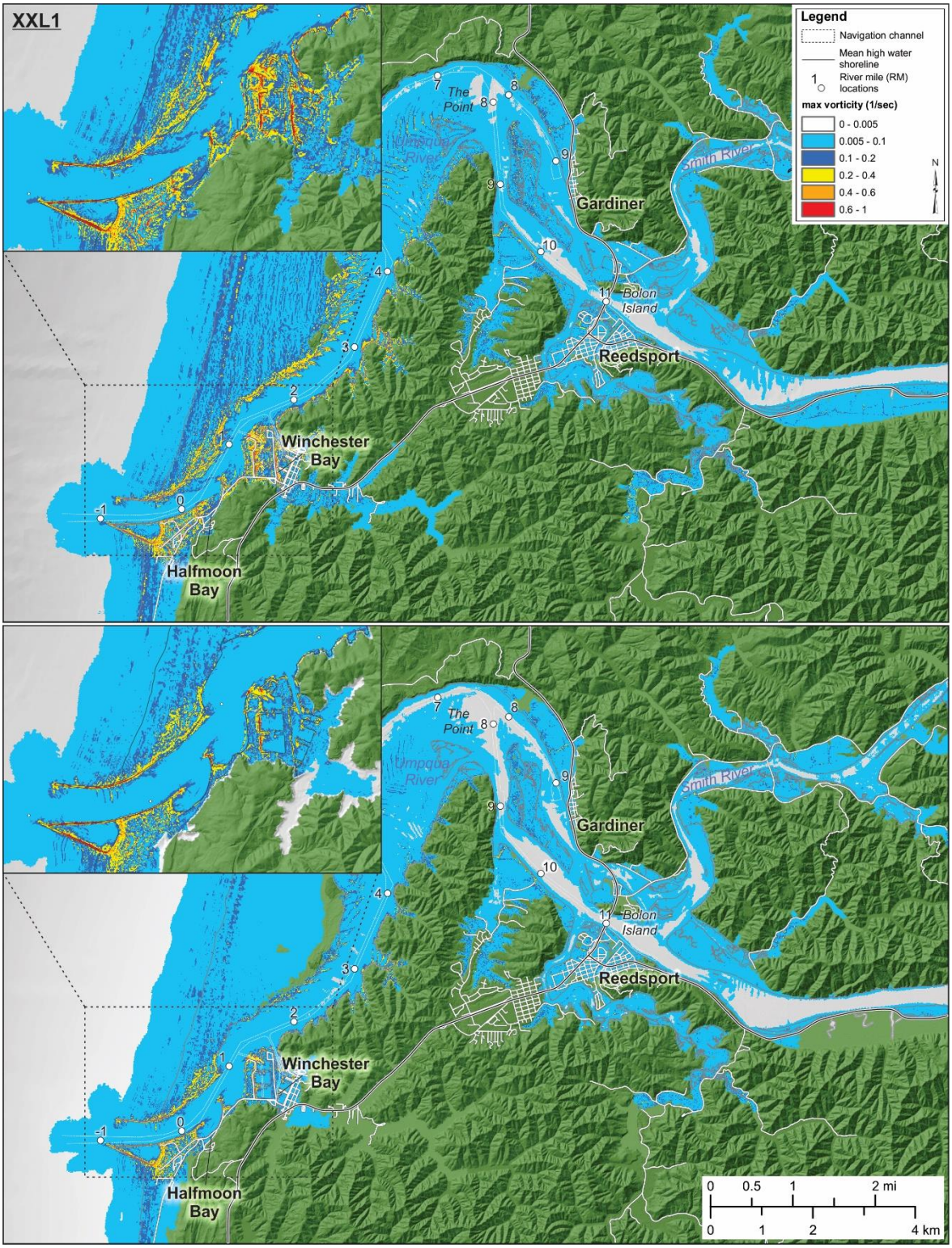

5.1.2 Distant (AKMax) tsunami ensemble results

5.1.2.1 AKMax Water Levels

Figure 34 presents the merged maximum water levels and currents for the maximum-considered eastern Aleutian Island (AKMax) distant tsunami event. As with the local scenarios, the highest tsunami water levels are observed along the open coast, especially west of the north Umpqua Spit. Dangerous conditions are also observed at the mouth of the estuary, in Halfmoon Bay, and within Winchester Bay. Simulated water levels for the AKMax tsunami indicate that water levels could exceed 3.7 m (12 ft) above MHHW at the estuary mouth, and ~2.4 m (8 ft) within Winchester Bay (**Figure 34** *top*). Maximum-simulated tsunami water levels indicate a rapid decrease in water levels from RM2, located just north of Winchester Bay, upriver to Reedsport. Our simulations indicate that at Reedsport, the tsunami water levels are <0.6 m (<2 ft).

Time series information for select stations along the river is presented in **Figure 35**. As with the local scenarios, these data have been truncated to span the first 12 hours of the simulations, providing improved insight into the variability and range of modeled water levels. The datum used is MHHW. The gray shading in each plot defines the envelope (range) of variability from the combined suite of simulations. The solid black line indicates the tsunami arriving on a flood tide, and the red line defines the tsunami arriving at ebb. The time series data highlight the more extreme nature of the tsunami waves at the mouth of the Umpqua Estuary (station 4) and to a lesser degree at Winchester Bay (station 6). As noted previously, the simulated tsunami waves rapidly decrease in height upriver of RM2, with maximum water levels of about 0.5 m (1.8 ft) observed at Reedsport (station 16). During ebb conditions, the tsunami waves are further reduced and increasingly attenuated.

5.1.2.2 AKMax currents

More telling are the modeled tsunami currents, which indicate potentially dangerous currents occurring at the mouth of the Umpqua Estuary (**Figure 34**, *bottom* and **Figure 36**). Strong currents that range from 3 to 4.5 m/s (~6–9 knots) are prevalent at the mouth, in the navigation channel by Halfmoon Bay, and at the entrance to the Winchester Bay marina (**Figure 34** *bottom*). Of greatest concern will be the interaction of the incoming tsunami waves with opposing currents generated particularly during an ebb tide, coupled with seaward-directed tsunami drainage, which will likely contribute to the amplification of wind waves occurring in the vicinity of the mouth (Allan and others, 2018a). Upriver of RM4, effects from the tsunami fall below the critical velocity/damage threshold of 1.5 m/s (3 knots; **Figure 34**, *bottom*). This suggests that a distant tsunami originating from Alaska is unlikely to have a significant effect on maritime operations occurring upriver of RM4, specifically in the vicinity of Reedsport. Nevertheless, as a precaution, maritime vessel operators based at Reedsport may want to consider adding additional drag anchors and/or mooring ropes to larger vessels. In contrast, strong currents are expected within the Winchester Bay marina, and appropriate care should also be taken to safeguard vessels that may be within the marina at the time a distant tsunami arrives. For these operators, evacuation upriver toward Reedsport may be feasible, depending on how long it takes to get a vessel underway, the size of the vessel, and the speed at which a vessel can travel upriver. Providing conditions seaward of the estuary mouth allow, offshore evacuation is another possibility for vessels located in Winchester Bay.

Figure 36 presents the modeled AKMax tsunami currents for the same stations defined previously. As noted earlier, the modeled currents are strongest at the mouth (station 4) and rapidly weaken as the tsunami progresses upriver (**Figure 36**). By the time the tsunami reaches The Point (station 12), the tsunami-generated currents fall below the 1.5-m/s (3-knot) velocity/damage threshold. As a result,

because of the combination of relatively small tsunami waves and low currents observed at Reedsport, maritime operations upriver of RM4 are unlikely to be significantly impacted by a distant tsunami.

The duration in which tsunami currents are expected to exceed 1.5 m/s (3 knots) for the AKMax scenario is presented in **Figure 37** for both flood (Run05a, *left plots*) and ebb (Run06a, *right plots*) conditions. Longer current durations characterize the flood scenario, especially along the navigation channel near the estuary mouth, where currents in the 1.5–3 m/s (3–6 knot) range are expected to last for more than four hours (**Figure 37**A). During ebb conditions, the AKMax tsunami currents are suppressed (**Figure 37**B), with durations on the order of 1–3 hours concentrated at the mouth and within Winchester Bay marina (**Figure 37**C). At the higher velocity of 3–4.5 m/s (6–9 knots), our results indicate that strong tsunami currents arriving on a flood tide will persist for less than one hour in the navigation channel at the mouth and within the entrance to the Winchester Bay marina (**Figure 37**B), but is even more muted during ebb conditions (**Figure 37**D). These results suggest that different maritime planning responses may be warranted for flood and ebb conditions when dealing with a distant tsunami event. Overall, these results confirm that a tsunami arriving at flood tide will generally produce stronger currents for longer durations compared with the same event arriving at ebb tide.

5.1.2.3 AKMax vorticity and minimum flow depth

Figure 38 (*top*) presents the calculated vorticity potential, and **Figure 38** (*bottom*) shows the water depth below the minimum trough of the tsunami. The former provides insights about areas subject to strong rotation, and the latter is important with respect to the potential for vessel grounding. As with the local scenarios, areas of cool to hot colors indicate potential for rotation and the development of gyres and whirlpools in **Figure 38 (***top*). Overall, we find little evidence for significant vorticity within the Umpqua Estuary caused by an AKMax distant tsunami. Areas with the strongest potential occur in the navigation channel near Halfmoon Bay, and within the entrances to the Winchester Bay marina. Both areas could be impacted by strong incoming and outgoing currents, leading to shear and the formation of whirlpools. Our analyses suggest that within the navigation channel the effects of passing tsunami troughs are likely to cause grounding issues in most areas of the upper estuary. This is evident in **Figure 38** (*bottom*) along the navigation channel, which shows simulated minimum water depths ranging from 6 to 10 m (20 to 33 ft).The potential for grounding (**Figure 38,** *bottom*) is largely confined to areas such as Reedsport, and within the marina at Winchester Bay, where minimum water depths during the tsunami drawdown may be reduced to 1.3 to 4 m (4.3 to 10 ft); gray areas in **Figure 38** *(bottom*) indicate exposure of the estuary floor during periods of drawdown.

Figure 34. Ensemble model results of the maximum tsunami *(top)* water levels and *(bottom)* currents generated by a maximum-considered distant earthquake and tsunami (AKMax) occurring on the eastern Aleutian Islands. Cartoon showing water level time history and attributes is of station 5 (RM0) near the Umpqua River mouth.

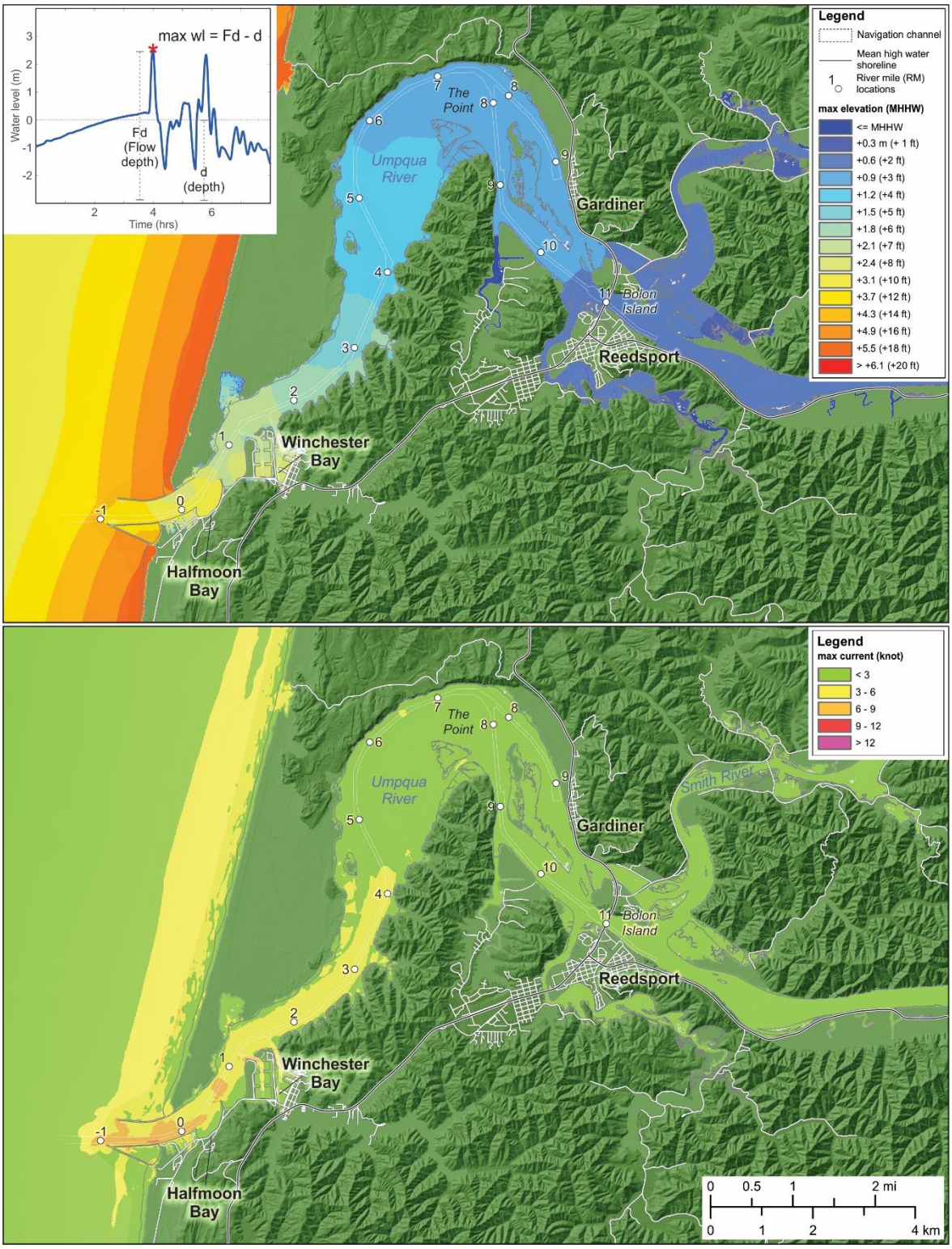

Figure 35. Time series showing the modeled water levels for the AKMax tsunami traveling along the navigation channel from the Umpqua River mouth to Reedsport. Gray shading denotes the envelope of variability in the water levels from all simulations.

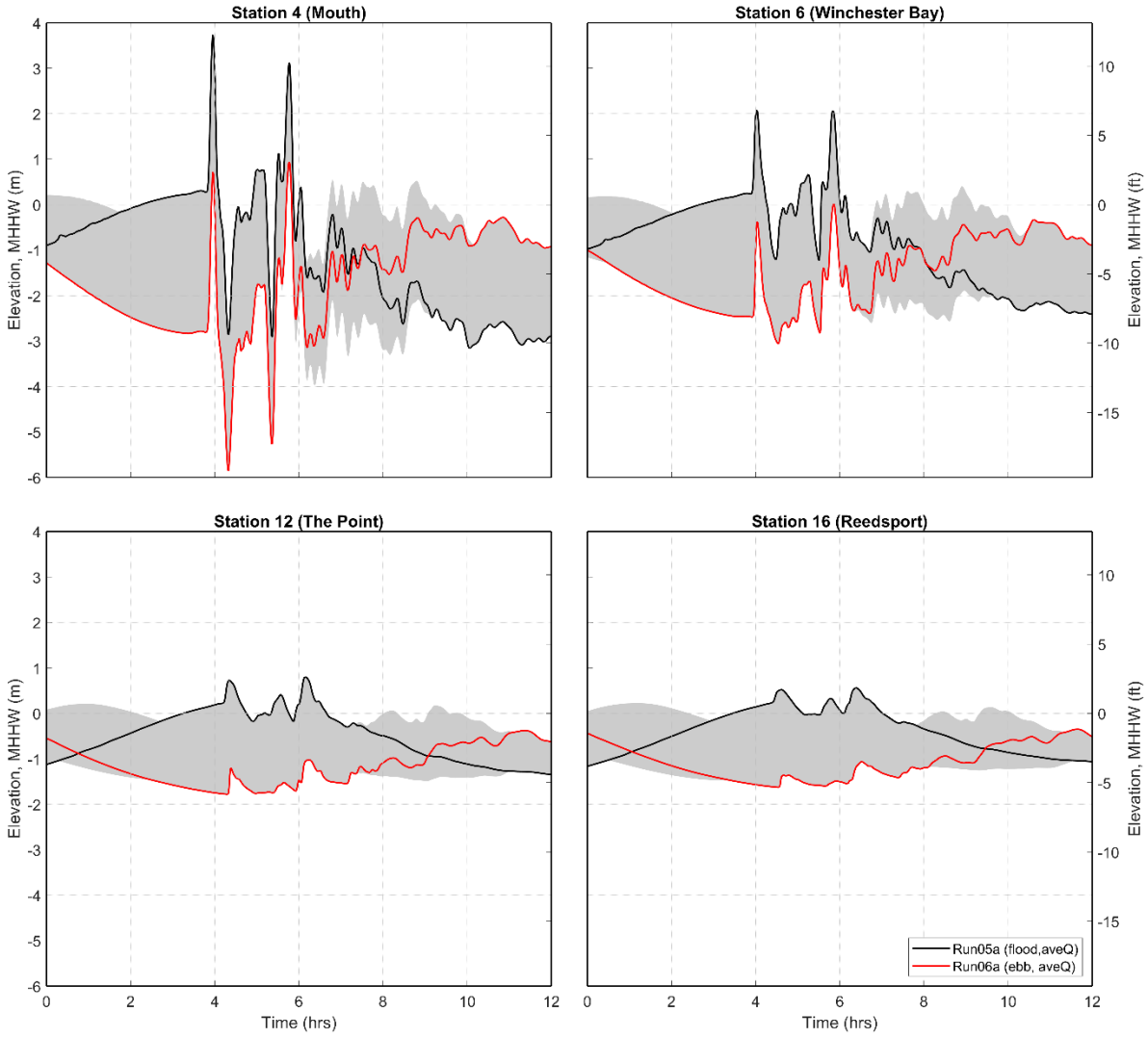

Figure 36. Time series showing the modeled currents for the AKMax tsunami traveling along the navigation channel from the Umpqua River mouth to Reedsport. Gray shading denotes the envelope of variability in the tsunami currents from all simulations.

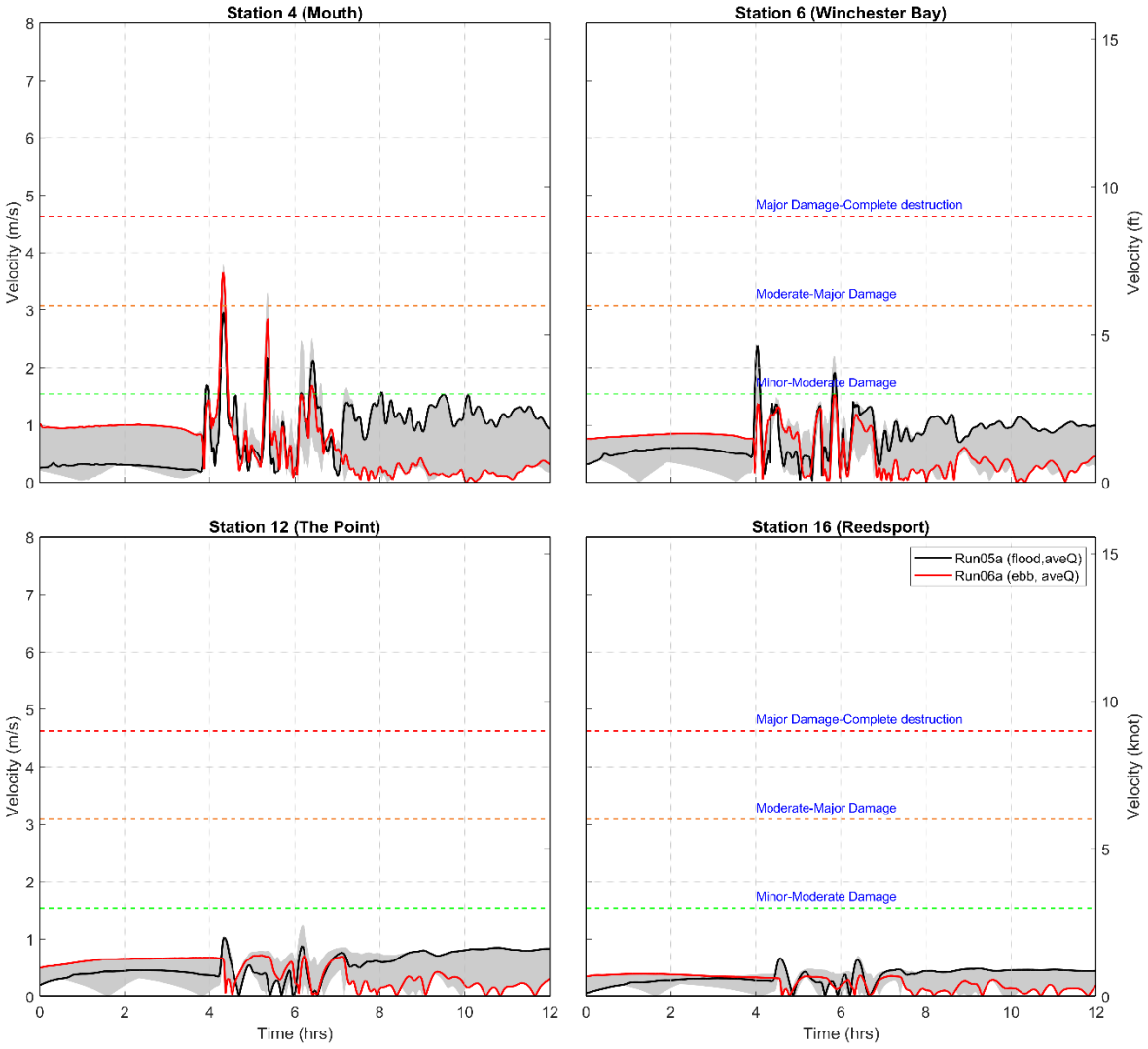

Figure 37. Duration of AKMax tsunami current velocities for *(left)* Run05a_pmel01 (flood tide scenario) and *(right)* Run06a_pmel01 (ebb tide scenario).

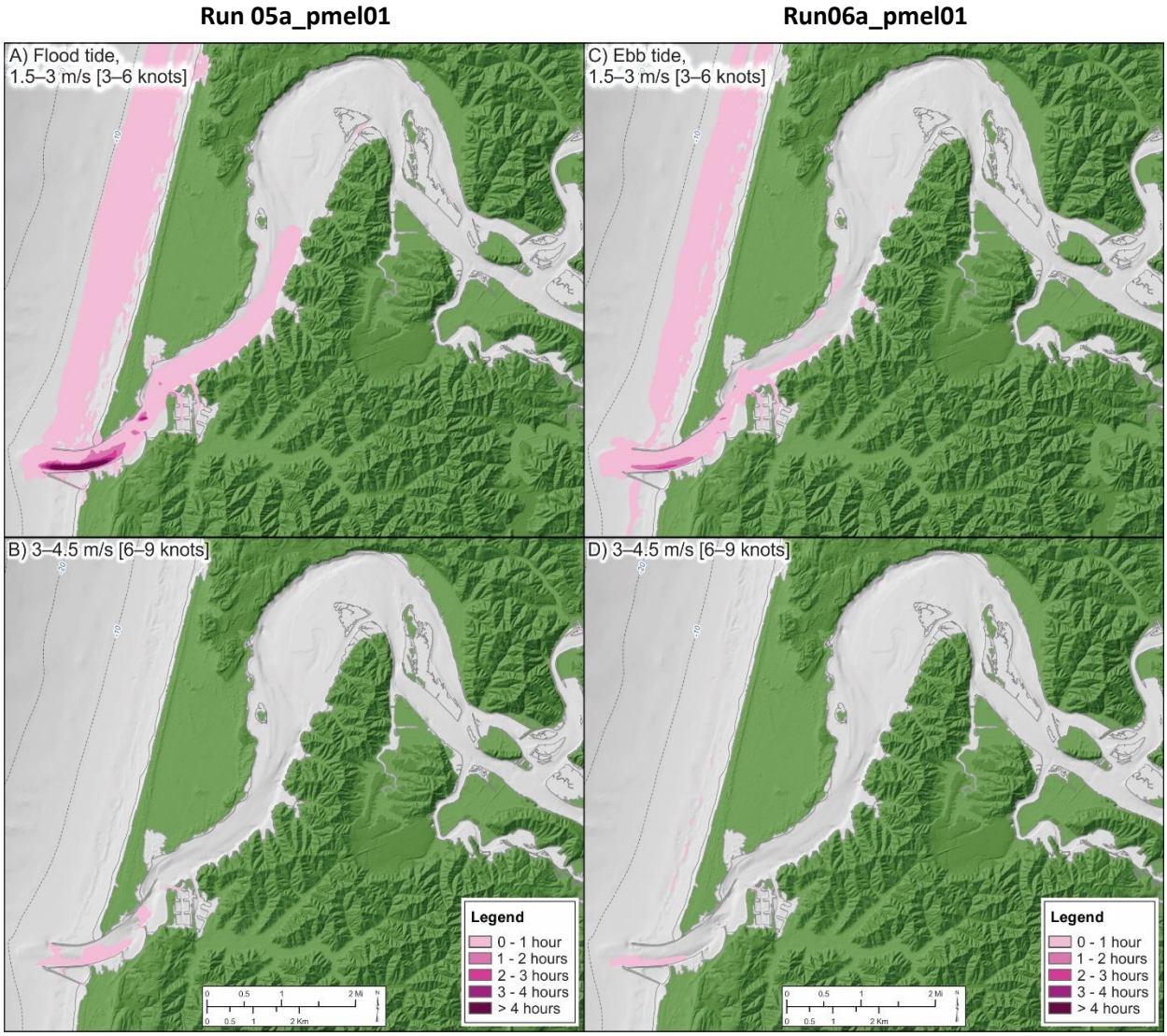

Figure 38. Ensemble model results of the *(top)* maximum vorticity and *(bottom)* minimum water depths generated by a maximum-considered distant earthquake and tsunami (AKMax) occurring on the eastern Aleutian Islands. Cartoon showing water level time history and attributes is of station 5 (RM0) at the Umpqua River mouth.

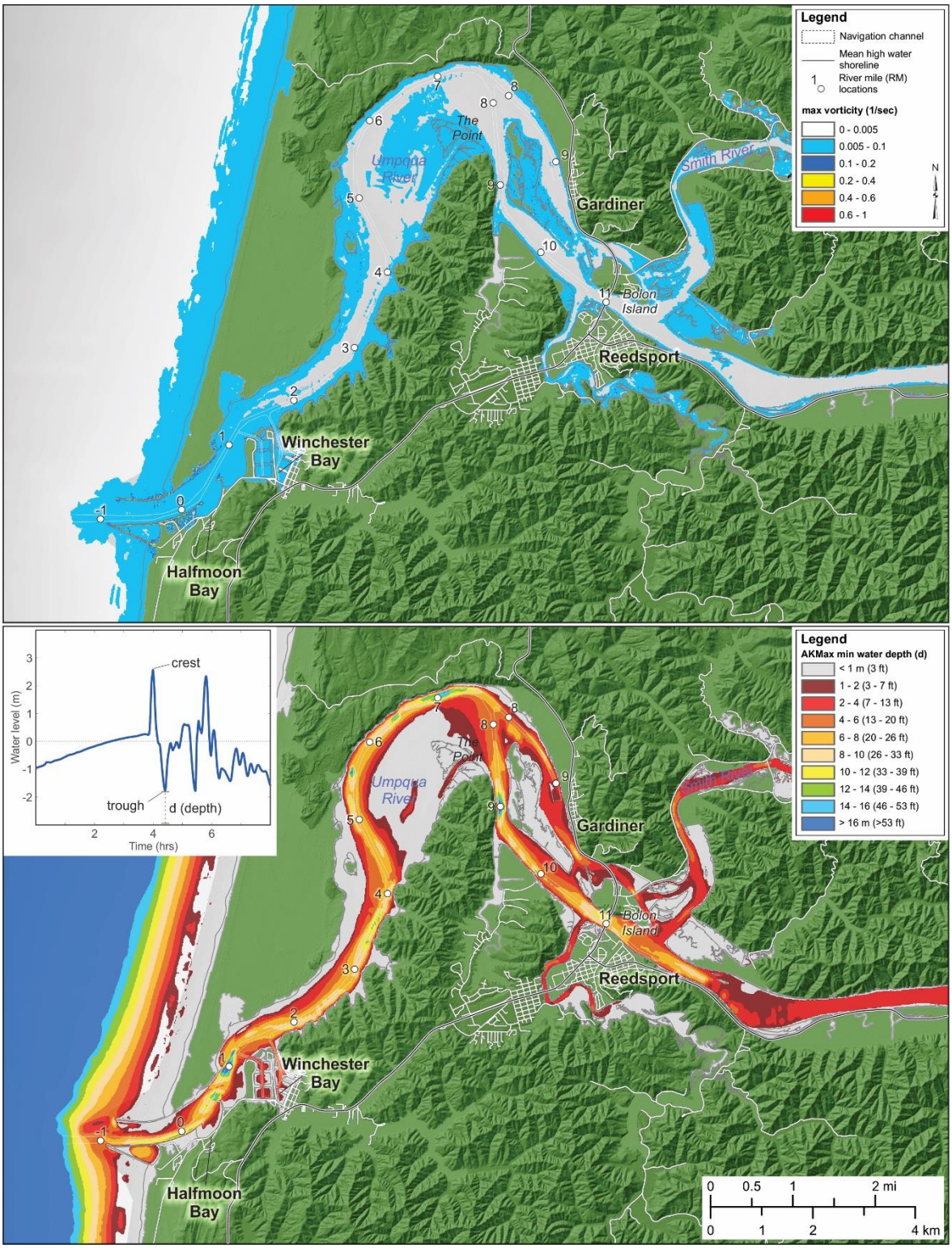

6.0 UMPQUA ESTUARY MARITIME GUIDANCE

Our review of the scientific literature indicates that tsunami-generated currents pose a potential threat to the maritime community, especially within ports and harbors (Borrero and others, 2015; Lynett and others, 2014; Uslu and others, 2010). There is general agreement in the literature that damage from tsunamis within ports and harbors begins at current velocities of ~1.5–2 m/s (3–4 knots). However, the same cannot be said for conditions on the ocean. Vessel vulnerability to open ocean currents is difficult to assess because it depends not only on the strength of the currents but, importantly, on the size of the vessel, its cargo load, and on prevailing antecedent conditions (wave heights and winds). An additional factor is the ability of smaller boats to remain isolated far offshore for potentially extended periods. All these factors have implications for where to best send mariners in the event of a tsunami.

Lynett and others (2014) attempted to address the issue of offshore tsunami evacuation by comparing the maximum-simulated currents with depth for a distant tsunami affecting Crescent City, California. They noted that maximum currents of ~0.5 m/s (1 knot) are expected well offshore, where ocean depths reach 180 m (100 fathoms) deep. In contrast, they found large variations in current velocities occurred closer to shore, in water depths shallower than 45 m (25 fathoms). To avoid dangerous currents, Lynett and others (2014) concluded that vessels should evacuate to depths of ~55 m (30 fathoms) for distant tsunami events (**Table 4**). In Japan, Suppasri and others (2015) noted that Japanese fishermen have practiced offshore evacuation (known as "oki-dashi") for generations, although prior to 2011, such a response was not recommended by the national government. This is because steering a boat toward a tsunami is dangerous and difficult, requiring expert knowledge of the offshore conditions as well as luck. Nevertheless, Japan's Fisheries Agency (2006 in Suppasri and others, 2015) indicated in its guidelines that for a tsunami warning, boats should evacuate offshore to water depths >50 m (27 fathoms) (**Table 4**).

Since 2011, a number of Japanese Prefectures have developed recommendations for offshore tsunami evacuation. For example, Aomori Prefecture advised that in the case of a 5-m (16-ft) tsunami warning, the required sea depth for evacuation was 50 m (27 fathoms), which increased to 150 m (82 fathoms) for a 10-m (33 ft) tsunami warning (Suppasri and others, 2015). In the Tokushima Prefecture, a 4-m (13-ft) tsunami warning requires evacuation to 70-m (38-fathom) water depth, and evacuation to 110-m (60-fathom) water depth is recommended for a 6-m (20-ft) tsunami (**Table 4**). Although the focus in Japan is on a locally generated tsunami, the same rules appear to apply for a distant tsunami. Most recently, however, Iwate Prefecture officials indicated that they would no longer recommend offshore maritime evacuation for a local tsunami (Dr. Anawat Suppasri, written commun., March 2018).

In the United States, considerable modeling and mapping efforts undertaken by National Tsunami Hazard Mitigation Program (NTHMP) state programs have led to the development of maritime guidance for each state. These recommendations include a range of potential depths for maritime evacuation purposes covering both local and distant scenarios (National Tsunami Hazard Mitigation Program, 2017). In Oregon, the currently recommended minimum depth is 55 m (30 fathoms) for the maximum-considered distant tsunami (DOGAMI, 2014); for the local XXL1 tsunami, the recommended depth for evacuation is 182 m (100 fathoms). For the distant event ("AKMax"), distances to safety range from a low of 2 km (1.2 mi) in Douglas County to as much as 16 km (10 mi) offshore from Lane County. Assuming a mean boat speed of 2–3 m/s (4–6 knots), reaching safety could take as little as 11 min to as much as 133 minutes. In contrast, distances to safety for an XXL1 event increase significantly and range from 30 to 66 km (19–41 mi) depending on the vessel's position along the Oregon coast. These distances place boaters a long way from the shore in potentially hazardous seas (Allan and others, 2018a).

Table 4. Maritime tsunami evacuation depths previously identified.

Location	Scenario	Tsunami Height (m)	Tsunami Height (ft)	Recommended Evacuation Depth (m)	Recommended Evacuation Depth (ft)	Recommended Evacuation Depth (fathoms)	Reference
Crescent City	distant			55	180	30	Lynett and others (2014)
Japan's Fisheries Agency	local			50	164	27	Suppasri and others (2015)
Japan, Aomori Prefecture	local	5	16	50	164	27	Suppasri and others (2015)
	local	10	33	150	492	82	
Japan, Tokushima Prefecture	local	4	13	70	230	38	Suppasri and others (2015)
	local	6	20	110	360	60	
Japan, Iwate Prefecture	local**						
Oregon, USA	distant			55	180	30	DOGAMI (2014), NTHMP (2017)
Oregon, USA	local			183	600	100	DOGAMI (2014), NTHMP (2017)
Oregon, USA	distant local			45 250[#] 350[##]	150 820 1150	25 137 200	Allan and others (2018a)
Columbia River, Oregon	distant local			45 146	150 480	25 80	Allan and others (2018b)
Coos Bay, Oregon	distant local (L1) local (XXL1)			45 146 274	150 420 900	25 80 150	Allan and others (2020)

Note: **Offshore evacuation for a local tsunami is prohibited (A. Sappasri, written commun., 2018).

[#] All coastal counties except Curry County; [##] Curry County

After evaluating the tsunami currents, their durations, and water depths, Allan and others (2018a) proposed a trizone hazard region for both distant and local tsunamis affecting the Oregon coast. For an XXL1 event, they identified a high hazard zone (depths < 150 m; 82 fathoms) where strong, dangerous currents would predominate. Between 150 and 250 m (82–109 fathoms) water depth, Allan and others (2018a) defined a moderate hazard region where the simulated tsunami currents ranged from 2 to 2.6 m/s (4 to 5 knots). However, within this region the duration in which the current velocities exceed 2 m/s (4 knots) was found to be < 1 minute north of Stonewall Bank, increasing to 1.5–5.5 minutes south of the bank. Thus, it may be possible for a vessel to be moving through the moderate hazard area at the time of the event and, provided the vessel is able to maintain a westward direction and speed, the chance of survival improves. At depths > 250 m (137 fathoms), the tsunami currents fall below 2 m/s (4 knots). For the AKMax scenario, Allan and others (2018a) recommended that vessels north of Stonewall Bank evacuate to depths > 45 m (25 fathoms). Strong, dangerous currents can be expected at depths < 28 m (15 fathoms).

In an examination of new tsunami model data generated for the Columbia River Estuary, Allan and others (2018b), revised the estimates for offshore evacuation staging areas based on an assessment of the combined effects of tsunami, tides, and river discharge (**Table 4**). They recommended that vessels seaward of the Columbia River mouth evacuate to depths greater than 46 m (25 fathoms/150 ft) for a distant tsunami event. They noted further that dangerous currents (> 2.6 m/s; 5 knots) caused by such a tsunami are expected to occur at depths shallower than 27 m (15 fathoms; 90 ft). For a local CSZ event, Allan and others (2018b) recommended that vessels seaward of the Columbia River mouth evacuate to depths greater than 146 m (80 fathoms), specifically identifying Astoria Canyon as a potential staging area. More recently, Allan and others (2020) reconfirmed the choice of a 46 m (25 fathoms; 150 ft) staging area for distant tsunamis at Coos Bay. For a CSZ local tsunami, Allan and others (2020) recommended mariners head to ~146 m depth (80 fathoms), which occurs ~18.5 km (10 nm) west of Coos Bay. However, since this depth is associated with an L1 tsunami event, they recommended proceeding farther westward toward deeper water (**Table 4**).

6.1 Maritime Guidance for a Local Tsunami

Given that initial wave arrival for a locally generated tsunami is expected to occur at the Umpqua River mouth in as little as ~12 min, with a peak wave at 21 minutes, there is insufficient time for mariners moored in Winchester Bay or along the navigation channel to respond to this event other than to evacuate by foot to high ground. Hence, maritime evacuation planning for a locally generated tsunami is generally limited to those vessels already operating out on the open ocean. For vessels seaward of the Umpqua River mouth, the most effective strategy is to evacuate immediately toward deeper water and, accordingly, toward decreasing tsunami-generated currents. However, steering a vessel toward an approaching tsunami is dangerous and difficult and should only be attempted if land-based evacuation is impossible (Allan and others, 2018a). In this scenario, there will be little to no warning for operators out on the ocean. Telltale signs of a locally generated earthquake and approaching tsunami may include:

- a background ocean roar
- changes in boat motions
- stronger ocean currents
- muddier water
- vessels located closer to shore may witness clouds of dust appearing along the coastline and in the hills, where landslides may be occurring.

As previously mentioned, Allan and others (2018a) completed a comprehensive analysis of tsunami currents generated by both local and distant events for the entire Oregon coast, and proposed a trizone hazard region for maritime evacuation based on certain thresholds of tsunami currents. Using a similar approach at the Umpqua River (**Figure 39**), we note the following:

- the most dangerous currents (>2 m/s; >4 knots) generated by a Cascadia XXL1 tsunami occur in water depths <182 m (<100 fathoms).
- for a maximum-considered XXL1 Cascadia event, the safest area to stage vessels occurs in water depths >285 m (>156 fathoms), where currents fall below 1.5 m/s (3 knots; western most blue dashed line in **Figure 39**). This places vessels ~33 km (18 nm) west of the Umpqua River mouth.

Because of the extreme (and rare) nature of an XXL1 CSZ event, we identify a more probable (but still conservative) area of dangerous currents based on the L1 CSZ scenario (**Figure 39**). Using this scenario, we note the following:

- the most dangerous currents (>1.5 m/s; >3 knots) generated by an L1 tsunami occur in water depths <118 m (<65 fathoms). This region of dangerous currents is defined as the yellow + orange zone in **Figure 39** and should therefore be avoided. Although not shown in **Figure 39**, dangerous currents caused by a Cascadia event will be experience as far upriver as Reedsport. Within the yellow and orange hazard zones, wind generated waves and swell may be greatly amplified by strong opposing tsunami currents making this region especially dangerous.
- low current velocities (<1.5 m/s; <3 knots) associated with the L1 scenario occurs seaward of ~118 m depth (65 fathoms; **Figure 39**). Safety improves significantly with additional westward travel as tsunami-generated currents will continue to decrease with increasing water depth. The preferred staging area is in depths greater than 182 m (100 fathoms; 600 ft) located ~27 km (14.6 nm) west of the river mouth.
- the L1 shallower staging area is located ~17.6 km (9.5 nm) west of the river mouth.

In these circumstances, mariners should prepare to potentially remain offshore for days due to the likelihood that navigation within the lower estuary could be dangerous if not impossible for some time. This is because of a combination of expected changes to bay hydraulics due to the likely failure and destruction of the Umpqua River jetties, changes in the locations of sandbanks, side channel collapse and infilling of the navigation channel, and the presence of debris throughout the estuary. More importantly, in this scenario, all ports in the lower estuary are likely to be heavily damaged. As a result, vessel operators should develop plans to evacuate to potentially safe ports located to the south of Cape Mendocino on the California coast.

For vessels operating within the Umpqua Estuary, the options are limited. Wave arrival times and water levels are presented in **Figure 20** and **Figure 21** for multiple sites along the river. Maritime operators should be aware of these arrival times and, if caught out on the estuary, attempt to evacuate to the nearest point of high ground and evacuate uphill. Depending on proximity to the estuary mouth, this may be feasible for operators in smaller, faster boats. Modeling indicates that large tsunami waves and powerful currents caused by a local CSZ event could reach 9–18 m (30–59 ft) above the tide (depending on whether it is an XXL or L1 earthquake), with the largest wave being the first wave. Although the most extreme tsunami wave heights will be experienced in the first 1–2 hours following the earthquake, tsunami waves are expected to continue to affect the area for at least 10 hours after the event. Accompanying the initial peak wave will be dangerous currents that exceed ~4.6 m/s (~9 knots) near the mouth, and decreases upriver. Strong currents in the 1.5 to 3 m/s (3–6 knot) range will persist for at least six hours after the event. Any vessels located within the Umpqua lower estuary or navigation channel at the time a CSZ event occurs will likely be transported farther up the estuary, where they could become

grounded, and/or destroyed. From RM7 (The Point) to Reedsport, our simulations indicate a rapid loss in tsunami energy, characterized by both significant decreases in the modeled wave heights and currents. In general, we find that the Reedsport area will be mainly impacted by the initial wave. Later arriving tsunami waves exhibit significantly less energy, and are characterized by both smaller wave heights and lower current velocities. Accordingly, vessels located near Reedsport may survive the event. Vessels distributed throughout the estuary will be subject to grounding potential.

Figure 39. Offshore maritime evacuation zones for the Umpqua River study area. Orange zone defines areas affected by dangerous tsunami currents from a distant event. Yellow area defines areas affected by dangerous currents from a local Cascadia tsunami. Maritime safety improves with farther westward travel.

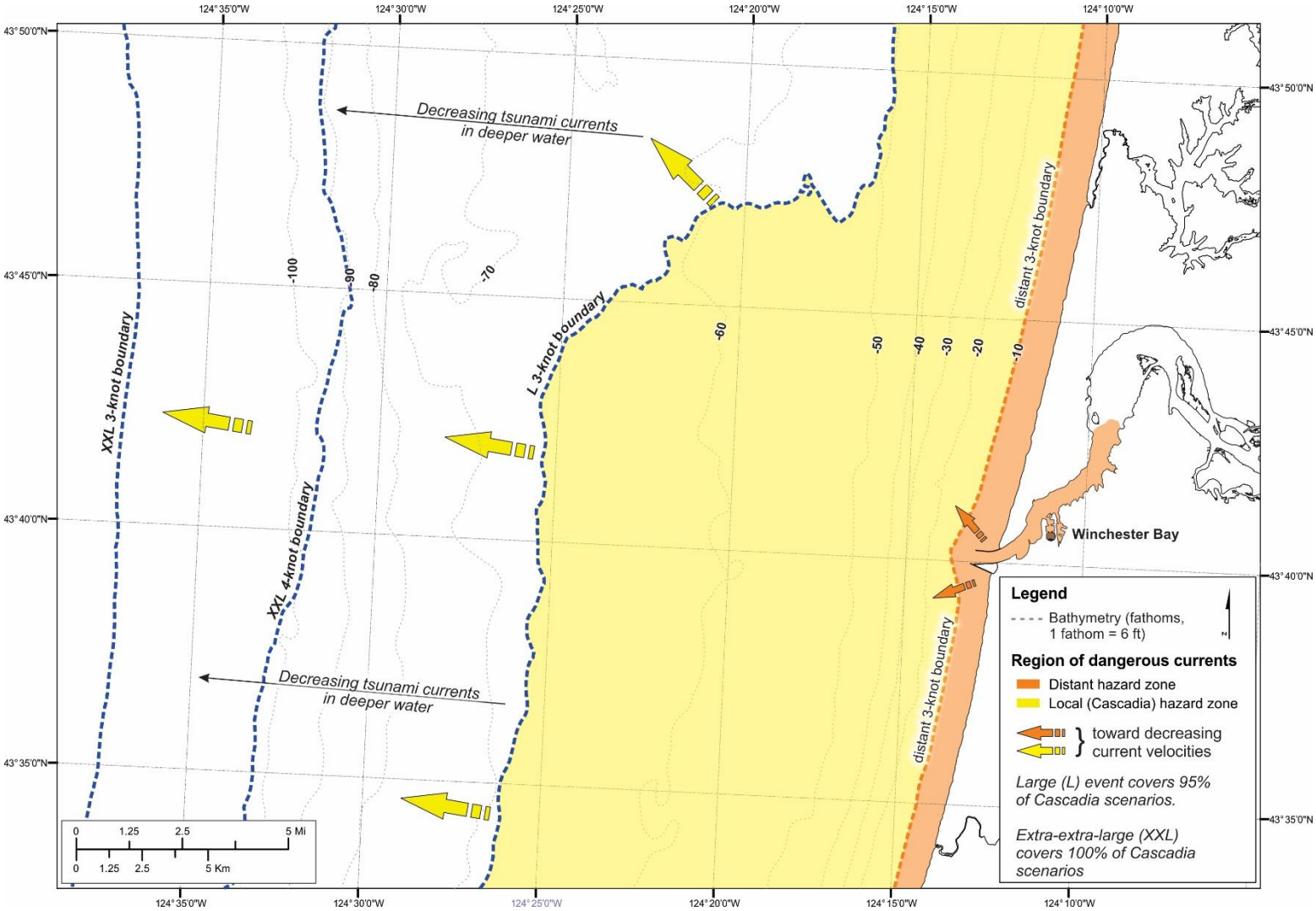

6.2 Maritime Guidance for a Distant Tsunami

For the maximum-considered distant (AKMax) tsunami scenario, our modeling indicates that the tsunami reaches the Umpqua Estuary ~3 hours, 50 minutes after the start of earthquake shaking. For distant events originating in Japan the tsunami will take ~9–10 hours to arrive (Allan and others, 2012). For the AKMax scenario, a tsunami warning will be issued by the U.S. Tsunami Warning Center[8] based out of Palmer, Alaska, as well as via channel 16 from the U.S. Coast Guard (USCG). In this scenario, maritime operators will have time to respond. If vessels are already on the water, we advise operators to check with the USCG before taking any action. If offshore evacuation is advised by USCG, a maritime operator should consider the size of the vessel relative to the prevailing (and forecast) ocean conditions, and the vessel and operator's ability to remain offshore for a potentially extended period of time.

We recommend that vessels seaward of the Umpqua River mouth evacuate to depths greater than 18 m (10 fathoms (60 ft); orange dash line in* Figure 39*). Dangerous currents exceeding 2.6 m/s (>5 knots) are expected to occur at depths shallower than 10 fathoms in this scenario, near the coastline, and especially around and within the estuary mouth (**Figure 34**, *bottom*). Furthermore, within the orange hazard zone, wind generated waves and swell may be greatly amplified by strong opposing tsunami currents making this region especially dangerous. Seaward of the distant maritime evacuation zone (orange dash line in **Figure 39**), the tsunami currents are expected to fall below 1.5 m/s (3 knots) and is located ~1.8 km (1 nm) west of the mouth of the estuary. If conditions do not permit offshore evacuation, maritime operators should dock their vessels and evacuate on foot out of the distant tsunami evacuation zone. The distant evacuation staging area for the Umpqua area occurs at depths that are notably shallower than recommended elsewhere (**Table 4**), such as offshore of the Columbia River (Allan and others, 2018b) and Coos Bay (Allan and others, 2020). This difference is likely due to a combination of factors including:

- differences in the offshore bathymetry (the shelf is generally wider and shallower offshore the Umpqua when compared to the Coos Estuary)
- the absence of any nearby submarine canyons that allow for focusing of the tsunami toward the Umpqua
- sheltering caused by Stonewall Bank located 64 km (40 mi) to the northeast of the Umpqua, which causes the tsunami to be refracted, while also enhancing the dispersion of the tsunami wave energy

For vessels operating within the estuary, the model results indicate that parts of the estuary between RM-1 and RM4 would be affected by strong currents in the 1.5–4.5 m/s (3–9 knot) range (**Figure 34**, *bottom*; **Figure 37**). Currents of this magnitude are likely to cause moderate to severe damage to facilities located within the Winchester Bay marina. For vessels moored in the marina, currents of this magnitude could result in broken mooring lines, collisions with other vessels, and damage to the docks and pilings. Although our simulations indicate little impact from an AKMax distant tsunami event at Reedsport, vessel operators may want to take further steps to safeguard their boats by adding additional mooring lines and/or drag anchors to help stabilize their vessels.

Evacuation upriver toward Reedsport may be feasible for some boats. However, this will depend on how long it takes the vessel to get underway and the speed at which the boat can travel. **Table 5** identifies the time and distance to safety for select areas in the Umpqua Estuary. These times assume an average transit time of 3 m/s (6 knots) and do not account for ocean or riverine conditions that could serve to slow travel times. As an example, the distance from Winchester Bay to Reedsport (where tsunami currents

[8] https://www.tsunami.gov/

fall below 1.5 m/s; 3 knots) is 18 km (9.8 nm; **Table 5**). For a vessel traveling at 3 m/s (6 knots), this equates to ~1 hour, 38 minutes travel time. Offshore evacuation, although possible for vessels moored at Reedsport, is not necessary. For interest, we note that the distance from Reedsport to the distant tsunami staging area (outside of the orange hazard zone, **Figure 39**) offshore of the estuary mouth is 20 km (10.8 nm), and a vessel traveling at 3 m/s (6 knots) would take ~1 hour, 48 minutes to reach the areas of expected low currents. Offshore evacuation assumes that conditions seaward of the estuary mouth are manageable for vessels trying to move out through the mouth into the Pacific Ocean.

Our modeling indicates that the worst conditions generated by a distant tsunami occur within the estuary mouth and Winchester Bay. The height of the tsunami waves decrease to <1 m (<3 ft) upriver of The Point (~RM7), and the simulated tsunami currents are below the 1.5-m/s (3-knot) threshold (**Figure 35** and **Figure 36**). Thus, for vessels operating in the vicinity of The Point, mariners may choose to deploy additional drag anchors to further safeguard their vessels and simply ride out the tsunami or evacuate upriver to Reedsport.

Table 5. Maritime evacuation times to nearest offshore (where currents fall below 3 knots) and upriver staging destinations for a distant tsunami. Evacuation times assume an average vessel speed of 3 m/s (6 knots).

Location	Distance to Offshore Safety (km / NM)	Time to Safety (min)	Distance to Upriver Safety (km / NM)	Time to Safety (min)
Winchester Bay	5 / 2.7	27 min	18 / 9.8	1 hour 38 min
The Point	13.4 / 7.3	1 hour 13 min	6.4 / 3.5	35 min
Reedsport	20 / 10.8	1 hour 48 min	NA	NA

7.0 CONCLUSIONS

Over the past 160 years, 29 distant (far-field) earthquake events have produced transoceanic tsunamis that struck the Oregon coast (Lander and others, 1993; NGDC, 2017). The majority of these have resulted in negligible effects in ports and harbors located on the Oregon coast. Of these, the largest event was the 1964 Alaska tsunami, which generated water levels that ranged from ~2.5 to 3.7 m (8 to 12 ft; Schatz and others, 1964; Zhang and others, 2011), with higher wave heights at the open coast. Unfortunately, Winchester Bay did not have a tide gauge in operation in the marina and hence there are no quantitative measurements of the Alaska 1964 tsunami. Nevertheless, qualitative observations of the tsunami were identified at Winchester Bay with one estimate of a peak water level observation of "plus 4.2 m" at the marina entrance (Wilson and Torum, 1968). Although this number is larger than our own results, we note that the discrepancy could entirely be due to differences in datums and errors in the historic observation. Furthermore, modeling undertaken at Coos Bay (Allan and others, 2020) and in the Columbia River (Allan and others, 2018b), found excellent agreement between simulations of the 1964 event and actual measured water levels from local tide gauges. These similarities give us strong confidence in the SCHISM modeling undertaken in the Umpqua Estuary. The most recent tsunami is the March 11, 2011, event that resulted in significant damage to several ports and harbors (e.g., Depoe Bay, Coos Bay, and Brookings), as well as to recreational and commercial vessels attempting to escape the tsunami (Allan and others, 2018a). Accordingly, even modest distant tsunamis like the one in 2011 pose a major risk within the ports

and harbors of Oregon, as well as to the safety of commercial and recreational mariners that operate offshore the coast.

To address the issue of maritime tsunami preparation and safety on the Oregon coast, this study has evaluated an entirely new suite of tsunami modeling results completed for both distant and local Cascadia tsunamis for the Umpqua Estuary. The goal of this effort has been to examine the interaction of tsunamis with dynamic tides, riverine flows, and friction to better simulate the nonlinear interactions that will probably occur between them in order to provide an improved understanding of tsunami effects offshore the Umpqua mouth and within the estuary. These data are necessary for developing improved maritime guidance for this region. Modeling involved 15 simulations based around two distant earthquake scenarios: the 1964 Anchorage, Alaska (AK64) event and a maximum-considered eastern Aleutian Island (AKMax) earthquake, and two local CSZ scenarios: Large1 (L1) and Extra-extra-large1 (XXL1).

Although the 1964 Alaska event was used to quality control our modeling, results from this event also provide an excellent reference for the effects of the most extreme distant event to strike the northern Oregon coast in historical times. Accordingly, the Alaska 1964 event remains an important benchmark when developing maritime guidance for distant tsunami events. Thus, for the 1964 scenario (coinciding with a spring flood tide) the modeled maximum tsunami water levels reached 2 m (6 ft) above MSL along the north Umpqua Spit, and 1.5 m (5 ft) adjacent to the estuary mouth (**Figure 8**). Within the Winchester Bay marina, our simulation indicates water levels reached 0.9–1.2 m (3–3.9 ft) above MSL. Near Reedsport, differences between the typical river-tide water levels compared with the Alaska 1964 tsunami water levels were found to be negligible. Accordingly, upriver from about Winchester Bay, the tsunami waves rapidly decrease in height. Strongest currents (3 m/s; >6 knots) are observed at the mouth of the Umpqua, between RM-1 and RM1, and within the entrance to the Winchester Bay marina. Elsewhere in the estuary, the tsunami current velocities are generally below the 1.5 m/s (3-knot) current/damage threshold (**Figure 9**). Damage to ports and harbors tends to occur above this threshold.

For the AKMax scenario, our analyses indicate that the initial wave arrival at the Umpqua River occurs ~3 hours, 50 minutes after the start of the earthquake (**Figure 23**) and takes an additional 8 minutes to reach its peak at the mouth. The tsunami reaches the Winchester Bay marina in ~4 hours, The Point in 24 minutes, and the town of Gardiner in ~40 minutes. The total travel time for the Alaska 1964 tsunami to reach Reedsport is 4 hours, 26 minutes. However, the peak tsunami does not occur for another 2.6 hours.

The simulations demonstrated significant along-coast and in-water variability in maximum tsunami water levels and currents (**Figure 34**), because of localized bathymetric effects, as well as interactions between the tsunami, tidal and riverine hydraulics. The effects of the AKMax tsunami within the upper Umpqua Estuary is suppressed when compared to other estuaries (e.g., the Coos estuary; Allan and others, 2020). This is likely due to the morphology of the estuary, it being generally narrower and shallower than the Coos estuary.

From a maritime standpoint, the most dangerous conditions in an Alaska tsunami event will occur between the mouth and ~RM4, located just east of Winchester Bay (**Figure 34**). Strong currents exceeding 3 m/s (6 knots) will dominate this portion of the estuary (**Figure 34**, *bottom*). ***For vessels seaward of the Umpqua River mouth, we recommend proceeding to a staging area greater than 18 m deep (10 fathoms (60 ft); orange dash line in* Figure 39*), located ~1.8 km (one nm) west of the mouth. Dangerous currents (> 2.6 m/s; 5 knots) are expected to occur at depths shallower than 18 m (10 fathoms; 60 ft; orange hazard zone in* Figure 39*)***.

For vessels operating within the Umpqua Estuary and especially Winchester Bay, several options are available to maritime operators in the event of a distant tsunami. Offshore maritime evacuation may be feasible for some vessels operating out of Winchester Bay, or in the navigation channel downstream of

The Point (**Table 5**). Conversely, smaller vessels upriver of The Point may choose to evacuate farther upriver toward Reedsport. Operators of larger vessels located near Reedsport could deploy additional drag anchors or mooring ropes to further safeguard their vessels.

In a real distant tsunami event, local officials will have time to work with NOAA, U.S. Coast Guard (USCG), and Oregon Emergency Management to provide guidance tailored to the size of the expected tsunami. Mariners should follow that guidance, if possible.

A locally generated CSZ event will reach the entrance to the Umpqua Estuary eight minutes after the start of earthquake shaking (**Figure 20**). It will reach Winchester Bay in ~21 minutes (peak wave at 25 minutes) and Reedsport in ~42 minutes. Tsunami water levels and currents along the open coast and offshore the estuary mouth will be catastrophic. Maximum water levels exceeding 14 m (46 ft) are observed at the mouth and at Winchester Bay, decreasing to ~10–12 m (~33–39 ft) in the navigation channel between RM2 and RM3. Upriver of RM3, the tsunami energy is dispersed across a broader valley and becomes strongly influenced by the shallowing estuary. Significant energy is also lost as the tsunami inundates the north Umpqua Spit. Maximum tsunami water levels upriver of The Point (RM7) are generally in the range of 6 to 8 m (20 to 26 ft; MHHW) depending on the tidal stage (**Figure 26** and **Figure 27**). Extreme currents exceeding 6 m/s (12 knots) will be observed across the lower estuary between RM-1 and RM4 (**Figure 29** and **Figure 30**). These currents will be enhanced during ebb tide conditions (**Figure 15**), which could contribute toward localized amplification of tsunami waves at the estuary mouth. Damage to the Winchester Bay marina in this scenario will probably be devastating.

Because the tsunami arrives at the entrance to the Umpqua Estuary in eight minutes, there is insufficient time for vessels moored in Winchester Bay or along the navigation channel to respond to this event other than to evacuate by foot to high ground. Thus, maritime evacuation planning for a locally generated tsunami is largely limited to those vessels already operating out on the open ocean. For these vessels west of the mouth, the most effective strategy is to immediately evacuate toward deeper water and, accordingly, toward decreasing tsunami-generated currents. ***We recommend an Umpqua River maritime evacuation zone for a local tsunami hazard zone beginning at ~118 m depth (~65 fathoms (390 ft) in Figure 39, ~27 km (14.6 nm) west of the river mouth) and extending westward to depths >182 m depth (100 fathoms (600 ft), Figure 39).*** Increasing safety occurs with additional westward travel because tsunami-generated current velocities will continue to decrease with westward travel and thus increasing water depth. The preferred staging area is in depths greater than 182 m (100 fathoms; 600 ft), located ~33 km (18 nm) west of the Umpqua mouth. Under these circumstances, mariners should prepare to remain offshore for potentially days as the estuary mouth is unlikely to be navigable. Hence, vessel operators should develop plans to evacuate to potentially safe ports located to the south of Cape Mendocino on the California coast.

Simulations undertaken as part of this study using dynamic tides and average river flows have yielded some additional useful insights for both local and distant tsunamis, when compared with static models undertaken at MHHW and with no flows. These include:

- Tsunamis arriving with a flood spring tide can be expected to be more damaging (**Figure 21**; XXL; **Figure 24**; AKMax), when compared to other tide levels.
- Under ebb tide conditions (**Figure 24**), our simulations demonstrate that a distant (AKMax) tsunami is strongly suppressed by the outgoing tidal currents, such that the largest tsunami waves and currents are confined to the estuary mouth. Upriver of Winchester Bay, the effects of a distant tsunami become negligible under ebb tide conditions.
- Suppression of the distant tsunami water levels is also apparent under ebb slack and flood slack conditions.

- Later arriving tsunamis may be locally enhanced by different tidal stages, particularly in the upper estuary, producing high water levels many hours after the initial tsunami wave has arrived.
- The predicted maximum velocities exhibit more local extrema along the open coast and within the estuary (between RM-1 and RM4), but especially near the mouth where the interaction is found to be strongest due to powerful currents and shoaling of tsunami waves (**Figure 15** to **Figure 17**).

8.0 ACKNOWLEDGMENTS

This project was funded under award NA20NWS4670064 by NOAA through the National Tsunami Hazard Mitigation Program. We thank Dr. Reed Burgette from DOGAMI for their insightful report reviews and comments, and the staff at Gneiss Editing for their copy-editing. Simulations used in this paper were conducted using the following computational facilities: 1) SciClone at the College of William and Mary, which was provided with assistance from the National Science Foundation, the Virginia Port Authority, Virginia's Commonwealth Technology Research Fund, and the Office of Naval Research; 2) the Extreme Science and Engineering Discovery Environment (XSEDE; grant TG-OCE130032), which is supported by National Science Foundation grant number OCI-1053575; and 3) NASA's Pleiades supercomputer.

9.0 REFERENCES

Allan, J. C., Komar, P. D., Ruggiero, P., and Witter, R. C., 2012, The March 2011 Tōhoku tsunami and its impacts along the U.S. West Coast: Journal of Coastal Research, v. 28, no. 5, p. 1142–1153. https://doi.org/10.2112/JCOASTRES-D-11-00115.1

Allan, J. C., Priest, G. R., Zhang, Y. J., and Gabel, L. L., 2018a, Maritime tsunami evacuation guidelines for the Pacific Northwest coast of Oregon: Natural Hazards, v. 94, no. 1, p. 21–52. https://doi.org/10.1007/s11069-018-3372-2

Allan, J. C., 2020, Maritime Guidance for Distant Source Tsunami Events: Coos Bay, Coos County, Oregon, MTRG-2020-OR-01_Port-of-Coos-Bay.

Allan, J. C., Zhang, J., O'Brien, F., and Gabel, L., 2018b, Columbia River Tsunami Modeling: Towards Improved Maritime Planning Response, Oregon Department of Geology and Mineral Industries Special Paper 51. https://www.oregongeology.org/pubs/sp/p-SP-51.htm

Allan, J. C., Zhang, J., O'Brien, F., and Gabel, L., 2020, Coos Bay tsunami modeling: Toward improved maritime planning response, Oregon Department of Geology and Mineral Industries Open-File Report O-20-08. https://www.oregongeology.org/pubs/ofr/p-O-20-08.htm

Atwater, B. F., Nelson, A. R., Clague, J. J., Carver, G. A., Yamaguchi, D. K., Bobrowsky, P. T., Bourgeois, J., Darienzo, M. E., Grant, W. C., Hemphill-Haley, E., Kelsey, H. M., Jacoby, G. C., Nishenko, S. P., Palmer, S. P., Peterson, C. D., and Reinhart, M. A., 1995, Summary of coastal geologic evidence for past great earthquakes at the Cascadia subduction zone: Earthquake spectra, v. 11, no. 1, p. 1-18.

Atwater, B. F., Satoko, M.-R., Satake, K., Yoshinobu, T., Kazue, U., and Yamaguchi, D. K., 2005, The orphan tsunami of 1700—Japanese clues to a parent earthquake in North America: U.S. Geological Survey Professional Paper 1707, 144 p. https://doi.org/10.3133/pp1707

Borrero, J. C., Lynett, P. J., and Kalligeris, N., 2015, Tsunami currents in ports: Philosophical Transactions of the Royal Society A, v. 373, no. 2053, p. 20140372. https://doi.org/10.1098/rsta.2014.0372

Bunya, S., Dietrich, J. C., Westerink, J., Ebersole, B., Smith, J., Atkinson, J., Jensen, R., Resio, D., Luettich, R., and Dawson, C., 2010, A high-resolution coupled riverine flow, tide, wind, wind wave, and storm surge model for southern Louisiana and Mississippi. Part I: Model development and validation: Monthly weather review, v. 138, no. 2, p. 345-377.

Burla, M., Baptista, A. M., Zhang, Y., and Frolov, S., 2010, Seasonal and interannual variability of the Columbia River plume: A perspective enabled by multiyear simulation databases: Journal of Geophysical Research: Oceans, v. 115, no. C2.

Carignan, K. S., Amante, C., Love, M. R., and Stiller, M., 2021, Digital Elevation Models of Central Oregon: Procedures, Data Sources and Analysis. NOAA, National Centers for Environmental Information (NCEI). 11p.

DOGAMI, 2014, Tsunami! What Oregon boat owners need to know: Oregon Deparment of Geology and Mineral Industries Tsunami Clearing House website: http://www.oregongeology.org/pubs/tsubrochures/TsunamiBrochureMaritime.pdf.

Goldfinger, C., Galer, S., Beeson, J., Hamilton, T., Black, B., Romsos, C., Patton, J., Nelson, C. H., Hausmann, R., and Morey, A., 2017, The importance of site selection, sediment supply, and hydrodynamics: A case study of submarine paleoseismology on the Northern Cascadia margin, Washington USA: Marine Geology, v. 384, p. 4-46.

Goldfinger, C., Nelson, C. H., Morey, A., Johnson, J. E., Gutierrez-Pastor, J., Eriksson, A. T., Karabanov, E., Patton, J., Gracia, E., Enkin, R., Dallimore, A., Dunhill, G., and Vallier, T., 2012, Turbidite event history: Methods and implications for Holocene paleoseismicity of the Cascadia subduction zone, USGS Professional Paper 1661-F. https://doi.org/10.3133/pp1661F

González, F., Geist, E. L., Jaffe, B., Kânoğlu, U., Mofjeld, H., Synolakis, C., Titov, V. V., Arcas, D., Bellomo, D., and Carlton, D., 2009, Probabilistic tsunami hazard assessment at seaside, Oregon, for near-and far-field seismic sources: Journal of Geophysical Research: Oceans, v. 114, no. C11.

Homer, C. G., Dewitz, J. A., Yang, L., Jin, S., Danielson, P., Xian, G., Coulston, J., Herold, N. D., Wickham, J. D., and Megown, K., 2015, Completion of the 2011 National Land Cover Database for the conterminous United States—representing a decade of land cover change information: Photogrammetric Engineering and Remote Sensing, v. 81, no. 5, p. 345–354.

Hyndman, R. D., and Wang, K., 1995, The rupture zone of Cascadia great earthquakes from current deformation and the thermal regime: Journal of Geophysical Research, v. 100, no. B11, p. 22,133–22,154. https://doi.org/10.1029/95JB01970

Johnson, J., Satake, K., Holdahl, S. R., and Sauber, J., 1996, The 1964 Prince William Sound earthquake: joint inversion of tsunami and geodetic data: Journal of Geophysical Research, v. 101, no. B1, p. 523–532. https://doi.org/10.1029/95JB02806

Kelsey, H. M., Nelson, A. R., Hemphill-Haley, E., and Witter, R. C., 2005, Tsunami history of an Oregon coastal lake reveals a 4600 yr record of great earthquakes on the Cascadia subduction zone: Geological Society of America Bulletin, v. 117, no. 7/8, p. 1009–1032. https://doi.org/10.1130/B25452.1

Lander, J. F., Lockridge, P. A., and Kozuch, M. J., 1993, Tsunamis affecting the west coast of the United States, 1806–1992: National Oceanic and Atmospheric Administration, National Geophysical Data Center key to geophysical Records Documentation (KGRD) No. 29, 242 p. ftp://ftp.library.noaa.gov/noaa_documents.lib/NESDIS/NGDC/key_to_geophysical_records_documentation/Kgrd-29.pdf

Lynett, P. J., Borrero, J., Son, S., Wilson, R., and Miller, K., 2014, Assessment of the tsunami-induced current hazard: Geophysical Research Letters, v. 41, no. 6, p. 2048–2055. https://doi.org/10.1002/2013GL058680

Lynett, P. J., Gately, K., Wilson, R., Montoya, L., Arcas, D., Aytore, B., Bai, Y., Bricker, J. D., Castro, M. J., and Cheung, K. F., 2017, Inter-Model Analysis of Tsunami-Induced Coastal Currents: Ocean Modelling, v. 114, p. 14-32. https://doi.org/10.1016/j.ocemod.2017.04.003

McCaffrey, R., Qamar, A., King, R. W., Wells, R. W., Khazaradze, G., Williams, C., Stevens, C., Vollick, J. J., and Zwick, P. C., 2007, Fault locking, block rotation and crustal deformation in the Pacific Northwest: Geophys. J. Int., v. 169, p. 1315–1340.

McCrory, P. A., Blair, J. L., Oppenheimer, D. H., and Walter, S. R., 2004, Depth to the Juan de Fuca slab beneath the Cascadia subduction margin—a 3-D model for sorting earthquakes: U.S. Geological Survey Data Series DS-91. https://pubs.usgs.gov/ds/91

Mitchell, C. E., Vincent, P., Weldon, R. J., II, and Richards, M. A., 1994, Present-day vertical deformation of the Cascadia margin, Pacific Northwest, United States: Journal of Geophysical Research: Solid Earth, v. 99, no. B6, p. 12,257–12,277. https://doi.org/10.1029/94JB00279

Mori, N., and Takahashi, T., 2012, Nationwide post event survey and analysis of the 2011 Tōhoku earthquake tsunami: Coastal Engineering Journal, v. 54, no. 1, 1250001-1–1250001-27. https://doi.org/10.1142/S0578563412500015

Mori, N., Takahashi, T., Yasuda, T., and Yanagisawa, H., 2011, Survey of 2011 Tōhoku earthquake tsunami inundation and run-up: Geophysical Research Letters, v. 38, no. 7. https://doi.org/10.1029/2011GL049210

National Geophysical Data Center/World Data Service (NGDC), NCEI/WDS Global Historical Tsunami Database. NOAA National Centers for Environmental Information. https://doi.org/10.7289/v5pn93h7 [accessed May 2022]

Nelson, A. R., Kelsey, H. M., and Witter, R. C., 2006, Great earthquakes of variable magnitude at the Cascadia subduction zone: Quaternary Research, v. 65, no. 3, p. 354–365. https://doi.org/10.1016/j.yqres.2006.02.009

NTHMP, 2017, Guidance for safe minimum offshore depth for vessel movement for tsunamis: National Tsunami Hazard Mitigation Program. https://nws.weather.gov/nthmp/documents/GuidanceforSafeMinimumOffshoreDepthforVesselMovement.pdf. Accessed July 10, 2017.

O'Connor, J. E., Wallick, J., Sobieszczyk, S., Cannon, C., and Anderson, S. W., 2009, Preliminary assessment of vertical stability and gravel transport along the Umpqua River, southwestern Oregon: U. S. Geological Survey Open-File Report 2009–1010.

Oregon Department of Geology and Mineral Industries (DOGAMI), 2014, Tsunami! What Oregon boat owners need to know. https://www.oregongeology.org/pubs/tsubrochures/TsunamiBrochureMaritime.pdf, 2 p. Accessed August 5, 2017.

Priest, G. R., Goldfinger, C., Wang, K., Witter, R. C., Zhang, Y., and Baptista, A. M., 2009, Tsunami hazard assessment of the northern Oregon coast: A multi-deterministic approach tested at Cannon Beach, Clatsop County, Oregon: Oregon Department of Geology and Mineral Industries Special Paper 41. https://www.oregongeology.org/pubs/sp/SP-41.zip

Priest, G. R., Goldfinger, C., Wang, K., Witter, R. C., Zhang, Y., and Baptista, A. M., 2010, Confidence levels for tsunami-inundation limits in northern Oregon inferred from a 10,000-year history of great earthquakes at the Cascadia subduction zone: Natural Hazards, v. 54, no. 1, p. 27–73. https://doi.org/10.1007/s11069-009-9453-5

Priest, G. R., Witter, R. C., Zhang, Y. J., Wang, K., Goldfinger, C., Stimely, L. L., English, J. T., Pickner, S. G., Hughes, K. L. B., Willie, T. E., and Smith, R. L., 2013, Tsunami inundation scenarios for Oregon: Oregon Department of Geology and Mineral Industries Open-File Report O-13-19. https://www.oregongeology.org/pubs/ofr/p-O-13-19.htm

Satake, K., Wang, K., and Atwater, B. F., 2003, Fault slip and seismic moment of the 1700 Cascadia earthquake inferred from Japanese tsunami descriptions: Journal of Geophysical Research, v. 108, no. B11. https://doi.org/10.1029/2003JB002521

Schatz, C. E., Curl, H., and Burt, W. V., 1964, Tsunamis on the Oregon coast: Ore Bin, v. 26, no. 12, p. 231–232. https://www.oregongeology.org/pubs/og/OBv26n12.pdf

Suppasri, A., Shuto, N., Imamura, F., Koshimura, S., Mas, E., and Yalciner, A. C., 2013, Lessons learned from the 2011 Great East Japan tsunami: performance of tsunami countermeasures, coastal buildings, and tsunami evacuation in Japan: Pure and Applied Geophysics, v. 170, no. 6–8, p. 993–1018. https://doi.org/10.1007/s00024-012-0511-7

Suppasri, A., Nguyen, D., Abe, Y., Yasuda, M., Fukutani, Y., Imamura, F., and Shuto, N., 2015, Offshore evacuation of fishing boats—Lessons from the 2011 great east Japan tsunami and its future challenge: Tsunami Engineering Technical Report, 32, p. 33–45.

Torrence, C., and Compo, G. P., 1998, A practical guide to wavelet analysis: Bulletin of the American Meteorological society, v. 79, no. 1, p. 61–78. https://doi.org/10.1175/1520-0477(1998)079<0061:APGTWA>2.0.CO;2

Tsunami Pilot Study Working Group (TPSWG), 2006, Seaside, Oregon tsunami pilot study—modernization of FEMA flood hazard maps: Seattle, Wash., U.S. National Oceanic and Atmospheric Administration, Office of Oceanic and Atmospheric Research, Pacific Marine Environmental Laboratory, NOAA OAR special report (Contribution No. 2975), 94 p., 7 appendices. https://www.pmel.noaa.gov/pubs/PDF/tsun2975/tsun2975.pdf

U.S. Army Corps of Engineers (USACE), 2008, HEC-RAS River Analysis System, hydraulic reference manual, v. 4.0, March 2008: Davis, Calif., USACE Hydraulic Engineering Center, Computer Program Documentation CPD-69.

Uslu, B., Eble, M., Titov, V. V., and Bernard, E. N., 2010, Distant tsunami threats to the ports of Los Angeles and Long Beach, California; Tsunami Hazard Assessment Special Series, v. 2: National Oceanic and Atmospheric Administration, Office of Oceanic and Atmospheric Research (OAR) Special Report, 100 p. https://nctr.pmel.noaa.gov/hazard_assessment_reports/02_LA_LB_CA_3532_web.pdf

Wilson, B. W., and Torum, A., 1968, The tsunami of the Alaskan earthquake, 1964: Engineering Evaluation: U.S. Army Corps of Engineers, Coastal Engineering Research Center, Technical Memorandum No. 25.

Wilson, R. I., Admire, A. R., Borrero, J. C., Dengler, L. A., Legg, M. R., Lynett, P., McCrink, T. P., Miller, K. M., Ritchie, A., Sterling, K., and Whitmore, P. M., 2013, Observations and impacts from the 2010 Chilean and 2011 Japanese tsunamis in California (USA): Pure and Applied Geophysics, v. 170, no. 6–8, p. 1127–1147. https://doi.org/10.1007/s00024-012-0527-z

Wiśniewski, B., and Wolski, T., 2012, The safety of the shipping and ports in the aspect of the tsunami events: Maritime University of Szczecin Scientific Journals [Zeszyty Naukowe/Akademia Morska w Szczecinie], v. 30, no. 102, p. 150–157.

Witter, R. C., 2008, Prehistoric Cascadia tsunami inundation and runup at Cannon Beach, Clatsop County, Oregon: Oregon Department of Geology and Mineral Industries Open-File Report O-08-12, 36 p., 3 appendices. https://www.oregongeology.org/pubs/ofr/O-08-12.zip

Witter, R. C., Kelsey, H. M., and Hemphill-Haley, E., 2003, Great Cascadia earthquakes and tsunamis of the past 6700 years, Coquille River estuary, southern coastal Oregon: Geological Society of America Bulletin, v. 115, no. 10, p. 1289–1306. https://doi.org/10.1130/B25189.1

Witter, R. C., Zhang, Y., Goldfinger, C., Priest, G. R., and Wang, K., 2010, Validating numerical tsunami simulations in southern Oregon using late Holocene records of great Cascadia earthquakes and tsunamis [abs.], Seismological Society of America 2010 Annual Meeting, Portland, Oreg.: Seismological Research Letters. v. 81, no. 2, p. 290. https://doi.org/10.1785/gssrl.81.2.284

Witter, R. C., Zhang, Y., Wang, K., Priest, G. R., Goldfinger, C., Stimely, L. L., English, J. T., and Ferro, P. A., 2011, Simulating tsunami inundation at Bandon, Coos County, Oregon, using hypothetical Cascadia and Alaska earthquake scenarios: Oregon Department of Geology and Mineral Industries Special Paper 43, 57 p. https://www.oregongeology.org/pubs/sp/p-SP-43.htm

Witter, R. C., Zhang, Y., Wang, K., Goldfinger, C., Priest, G. R., and Allan, J. C., 2012, Coseismic slip on the southern Cascadia megathrust implied by tsunami deposits in an Oregon lake and earthquake-triggered marine turbidites: Journal of Geophysical Research; Solid Earth, v. 117, no. B10. https://doi.org/10.1029/2012JB009404

Witter, R., Zhang, Y. J., Wang, K., Priest, G. R., Goldfinger, C., Stimely, L. L., English, J. T., and Ferro, P. A., 2013, Simulated tsunami inundation for a range of Cascadia megathrust earthquake scenarios at Bandon, Oregon, USA: Geosphere, v. 9, no. 6, p. 1783–1803. https://doi.org/10.1130/GES00899.1

Zhang, Y. J., and Baptista, A. M., 2008, SELFE: A semi-implicit Eulerian-Lagrangian finite-element model for cross-scale ocean circulation: Ocean Modelling, v. 21, no. 3-4, p. 71–96. https://doi.org/10.1016/j.ocemod.2007.11.005

Zhang, Y. J., Witter, R. C., and Priest, G. R., 2011, Tsunami–tide interaction in 1964 Prince William Sound tsunami: Ocean Modelling, v. 40, p. 246–259. https://doi.org/10.1016/j.ocemod.2011.09.005

Zhang, Y. J., Stanev, E. V., and Grashorn, S., 2016a, Seamless cross-scale modelling with SCHISM: Ocean Modelling, v. 102, p. 64–81. https://doi.org/10.1016/j.ocemod.2016.05.002

Zhang, Y. J., Priest, G. R., Allan, J. C., and Gabel, L., 2016b, Benchmarking an unstructured-grid model for tsunami current modeling: Pure and Applied Geophysics, v. 173, no. 12, p. 4075–4087. https://doi.org/10.1007/s00024-016-1328-6